

AD 717817

# FOREIGN TECHNOLOGY DIVISION



NUMERICAL FORECAST AND ANALYSIS OF METEOROLOGICAL FIELDS  
(Selected Articles)



DDC  
RECEIVED  
FEB 12 1971  
REGISTRY  
D

Distribution of this document is unlimited. It may be released to the Clearinghouse, Department of Commerce, for sale to the general public.

Reproduced by  
**NATIONAL TECHNICAL  
INFORMATION SERVICE**  
Springfield, Va. 22151

Best Available Copy

178

## EDITED MACHINE TRANSLATION

NUMERICAL FORECAST AND ANALYSIS OF  
METEOROLOGICAL FIELDS (Selected Articles)

English pages: 108

Source: Gidrometeorologicheskij Nauchno-  
Issledovatel'skiy Tsentri SSSR. Trudy  
(Hydrometeorological Scientific Research  
Center of the USSR. Transactions), No. 19,  
1968, pp. 1-66, 72-84.

This document is a SYSTRAN machine aided translation,  
post-edited for technical accuracy by: K. L. Dion.

UR/3269-68-000-019

THIS TRANSLATION IS A RENDITION OF THE ORIGINAL FOREIGN TEXT WITHOUT ANY ANALYTICAL OR EDITORIAL COMMENT. STATEMENTS OR THEORIES ADVOCATED OR IMPLIED ARE THOSE OF THE SOURCE AND DO NOT NECESSARILY REFLECT THE POSITION OR OPINION OF THE FOREIGN TECHNOLOGY DIVISION.

PREPARED BY:

TRANSLATION DIVISION  
FOREIGN TECHNOLOGY DIVISION  
WP-AFB, OHIO.

TABLE OF CONTENTS

U. S. Board on Geographic Names Transliteration System.....	ii
Designations of the Trigonometric Functions.....	iii
Improvement of the Methodology of Forecasting the Baric Field for Several Days; by S. A. Mashkovich.....	1
Finite-Difference Algorithm of a Solution of the Vorticity Equation for the Middle Troposphere Over the Northern Hemisphere; by N. V. Isayev and M. S. Fuks-Rabinovich.....	10
Numerical Solution of the Balance Equation in the Framework of a Quasi-Solenoidal Forecast Diagram of the Geopotential for the Northern Hemisphere; by I. G. Sitnikov and S. O. Krichak.....	27
The Investigation of Heating in the Stratosphere Using Numerical Experiments; by B. Barg and S. A. Mashkovich.....	40
On the Application of the Filtration Theory of Random Processes to Some Problems of Objective Analysis; by B. V. Ovchinskiy.....	60
On the Filtration of Fields Obtained as a Result of Nonlinear Transformations of the Initial Values of Meteorological Factors; by L. N. Strizhevskiy.....	81
Objective Analysis of the Geopotential Field Using Supplemen- tal Information, by V. D. Sovetova.....	94

U. S. BOARD ON GEOGRAPHIC NAMES TRANSLITERATION SYSTEM

Block	Italic	Transliteration	Block	Italic	Transliteration
А а	<i>А а</i>	A, a	Р р	<i>Р р</i>	R, r
Б б	<i>Б б</i>	B, b	С с	<i>С с</i>	S, s
В в	<i>В в</i>	V, v	Т т	<i>Т т</i>	T, t
Г г	<i>Г г</i>	G, g	У у	<i>У у</i>	U, u
Д д	<i>Д д</i>	D, d	Ф ф	<i>Ф ф</i>	F, f
Е е	<i>Е е</i>	Ye, ye; E, e*	Х х	<i>Х х</i>	Kh, kh
Ж ж	<i>Ж ж</i>	Zh, zh	Ц ц	<i>Ц ц</i>	Ts, ts
З з	<i>З з</i>	Z, z	Ч ч	<i>Ч ч</i>	Ch, ch
И и	<i>И и</i>	I, i	Ш ш	<i>Ш ш</i>	Sh, sh
Й й	<i>Й й</i>	Y, y	Щ щ	<i>Щ щ</i>	Shch, shch
К к	<i>К к</i>	K, k	Ъ ъ	<i>Ъ ъ</i>	"
Л л	<i>Л л</i>	L, l	Ы ы	<i>Ы ы</i>	Y, y
М м	<i>М м</i>	M, m	Ь ь	<i>Ь ь</i>	'
Н н	<i>Н н</i>	N, n	Э э	<i>Э э</i>	E, e
О о	<i>О о</i>	O, o	Ю ю	<i>Ю ю</i>	Yu, yu
П п	<i>П п</i>	P, p	Я я	<i>Я я</i>	Ya, ya

\* ye initially, after vowels, and after ъ, ь; e elsewhere.  
 When written as Ѣ in Russian, transliterate as yĕ or ě.  
 The use of diacritical marks is preferred, but such marks  
 may be omitted when expediency dictates.

FOLLOWING ARE THE CORRESPONDING RUSSIAN AND ENGLISH  
 DESIGNATIONS OF THE TRIGONOMETRIC FUNCTIONS

Russian	English
sin	sin
cos	cos
tg	tan
ctg	cot
sec	sec
cosec	csc
sh	sinh
ch	cosh
th	tanh
cth	coth
sch	sech
csch	csch
arc sin	sin <sup>-1</sup>
arc cos	cos <sup>-1</sup>
arc tg	tan <sup>-1</sup>
arc ctg	cot <sup>-1</sup>
arc sec	sec <sup>-1</sup>
arc cosec	csc <sup>-1</sup>
arc sh	sinh <sup>-1</sup>
arc ch	cosh <sup>-1</sup>
arc th	tanh <sup>-1</sup>
arc cth	coth <sup>-1</sup>
arc sch	sech <sup>-1</sup>
arc csch	csch <sup>-1</sup>
rot	curl
lg	log

This collection includes work with numerical hydrodynamic methods of weather forecasting. A number of articles is dedicated to certain aspects of objective analysis of meteorological fields and to development of methodology of operational forecasting by numerical methods with the aid of electronic computers.

The collection is dedicated to scientific colleagues, engineers, weather forecasters, students of higher courses in hydrometeorologic institutes and universities, interested in the problems of calculating weather ahead of time by hydrodynamic methods.

IMPROVEMENT OF THE METHODOLOGY OF FORECASTING  
THE BARIC FIELD FOR SEVERAL DAYS

S. A. Mashkovich

A generalization is given of an earlier proposed [2] linear three-level forecast model. The effect of horizontal turbulent mixing in the vorticity equation and effects of surface friction are considered additionally. The system is computerized. An evaluation of the forecasts is given.

Works [2], [3] proposed a forecasting system, which is based on a linear three-level model of the atmosphere. The formulation of the problem was based on a method proposed by Ye. N. Blinova. This system is used in the work of the hydrometeorologic center of the USSR for forecasting ground pressure for several days.

The present article is dedicated to the improvement of the mentioned forecasting methodology. Namely, in the vorticity equation a component describing horizontal turbulent perturbation is considered additionally; furthermore, the effect of surface friction is drawn in.

In this instance linearized vorticity equations and heat inflow equations are written respectively in the form:

$$\begin{aligned} \left(\frac{\partial}{\partial t} + \bar{\omega} \frac{\partial}{\partial \lambda}\right) \Delta \psi + 2\bar{\omega} \frac{\partial \psi}{\partial \lambda} &= -\frac{2\omega a_0^2 g \cos \theta}{\rho} \frac{\partial p w}{\partial \zeta} + \frac{k_2}{a_0^2} \Delta \Delta \psi, \\ \left(\frac{\partial}{\partial t} + \bar{\omega} \frac{\partial}{\partial \lambda}\right) \frac{\partial \psi}{\partial \zeta} - \frac{d\bar{\omega}}{d\zeta} \frac{\partial \psi}{\partial \lambda} - \frac{(\gamma_0 - \gamma) R}{2\omega \cos \theta} \frac{w}{\zeta} &= \frac{k_1}{a_0^2} \Delta \frac{\partial \psi}{\partial \zeta}. \end{aligned} \quad (1)$$

Here the following designations are introduced:  $\psi$  - stream function,  $w$  - vertical component of velocity,  $t$  - time,  $\theta, \lambda$  - spherical coordinates,  $\omega$  - angular velocity of earth rotation,  $\alpha$  - index of circulation,  $\zeta = p/P$ ,  $p$  - pressure,  $P = 1000$  mbar,  $a_0$  - radius of earth,  $g$  - acceleration of gravity,  $k_1$  and  $k_2$  - coefficients of turbulent mixing,  $R$  - gas constant,  $\gamma_0$  and  $\gamma$  - dry adiabatic and vertical temperature gradients,  $\Delta$  - Laplacean operator in spherical coordinates.

Let us introduce dimensionless variables according to the formulas

$$\begin{aligned} \psi &= \bar{\psi} \psi', \quad w = \bar{\omega} w', \quad p = \bar{p} p', \\ t &= \frac{t'}{\omega}, \quad \bar{\psi} = \frac{2\omega a_0^2 g \rho \cos \theta}{\rho} \bar{\omega} \end{aligned}$$

and designate

$$\Gamma = \frac{(\gamma_0 - \gamma) R R}{(2\omega a_0 \cos \theta) \bar{\omega} \rho} \frac{1}{\zeta}, \quad \bar{\omega} = \frac{\omega}{\omega}.$$

Then system of equations (1) takes the form (primes on letters have been omitted):

$$\begin{aligned} \frac{\partial \psi}{\partial t \partial \zeta} + \bar{\omega} \frac{\partial \psi}{\partial \lambda \partial \zeta} - \frac{d\bar{\omega}}{d\zeta} \frac{\partial \psi}{\partial \lambda} - \Gamma w &= \frac{k_1}{a_0^2} \Delta \frac{\partial \psi}{\partial \zeta}, \\ \left(\frac{\partial}{\partial t} + \bar{\omega} \frac{\partial}{\partial \lambda}\right) \Delta \psi + 2\bar{\omega} \frac{\partial \psi}{\partial \lambda} &= -\frac{\partial p w}{\partial \zeta} + \frac{k_2}{a_0^2} \Delta \Delta \psi. \end{aligned} \quad (2)$$

We introduce the following designations for the operators:

$$\begin{aligned} Z &= \frac{\partial}{\partial t} + \bar{\omega} \frac{\partial}{\partial \lambda} - \frac{k_1}{a_0^2} \Delta, \\ L &= \left(\frac{\partial}{\partial t} + \bar{\omega} \frac{\partial}{\partial \lambda}\right) \Delta + 2\bar{\omega} \frac{\partial}{\partial \lambda} - \frac{k_2}{a_0^2} \Delta \Delta. \end{aligned} \quad (3)$$

Then equation (2) can be written in the form:

$$\frac{\partial}{\partial \zeta} (Z \psi) - 2 \frac{d\bar{\sigma}}{d\zeta} \frac{\partial \psi}{\partial \zeta} - \Gamma w = 0 \quad (4a)$$

$$L \psi = - \frac{d(\rho w)}{d\zeta} \quad (4b)$$

We consider processes in the lower half of the atmosphere, namely: in the layer located between sea level ( $\zeta = 1$ ) and the isobaric surface of 500 mbar ( $\zeta = 0.5$ ).

As boundary conditions we take:

$$w = k^* \Delta \psi \quad \text{when } \zeta = 1 \quad (k^* = \frac{k}{\sigma_0}) \quad (5a)$$

$$\frac{d(\rho w)}{d\zeta} = 0 \quad \text{when } \zeta = \zeta_c = 0.5 \quad (5b)$$

Condition (5a) speaks about the fact that at the lower boundary of the considered layer of atmosphere exist vertical motions conditioned by the effect of friction in the boundary layer (see [1]). Condition (5b) designates assumption about the quasi-barotropic nature of motions in the middle part of the atmosphere. It allows writing equation (4b) at a level  $\zeta = \zeta_c$  in the form

$$L \psi = 0 \quad \text{when } \zeta = \zeta_c \quad (6)$$

Consequently, the stream function at a level  $\zeta = \zeta_c$  can be found from equation (6) independently of the solution of system (4). The solution of the equations (6) is written in the form

$$\psi_c = \text{Re} \sum_{n,m} B_{n,m}^* e^{i(m\lambda - \tau_c^* t)} P_n^m(\theta) \quad (7)$$

where

$$s = \frac{2m}{y} - \tau_c^* + i\gamma \bar{\sigma};$$

$$y = n(n+1), \quad \bar{\sigma} = \frac{h}{\sigma_0}$$

$P_n^m(\theta)$  - associated Legendre polynomial.

Let us break the considered area of the atmosphere into two layers (see Fig. 1). We will consider a three-level model of the atmosphere including sea level ( $\zeta = 1$ ), 500 mbar ( $\zeta = \zeta_c$ ) and a certain intermediate level  $\zeta = \zeta_n$ .

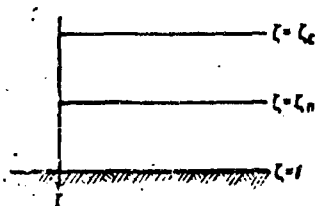


Fig. 1.

Integrate each of equations (4) over the vertical coordinate within limits: 1) from  $\zeta = 1$  to  $\zeta = \zeta_n$ , 2) from  $\zeta = \zeta_n$  to  $\zeta = \zeta_c$ . Here indices 1, n, c, mean that the quantity is referred respectively to sea level, intermediate and mean levels. When the integrals are not calculated analytically, we will approximate them by method of trapeziums. Then system (4) with allowance for boundary conditions (5) can be written in the form:

$$\begin{aligned} Z_1 \psi_1 - Z_n \psi_n - 2\bar{A}_1 a_1 \frac{\partial}{\partial \lambda} \frac{\psi_1 - \psi_n}{2} - \frac{\Gamma_n \omega_n + \Gamma_1 k \Delta \psi_1}{2} a_1 &= 0, \\ Z_n \psi_n - Z_c \psi_c - 2\bar{A}_2 a_2 \frac{\partial}{\partial \lambda} \frac{\psi_n - \psi_c}{2} - \frac{\Gamma_n \omega_n + \Gamma_c \omega_c}{2} a_2 &= 0, \\ \frac{a_1}{2} (L_1 \psi_1 + L_n \psi_n) + \rho_1 k \Delta \psi_1 - \rho_n \omega_n &= 0, \\ \frac{a_2}{2} L_n \psi_n + \rho_n \omega_n - \rho_c \omega_c &= 0, \end{aligned} \quad (8)$$

where

$$\begin{aligned} \bar{A}_1 &= \frac{1}{a_1} (\bar{a}_1 - \bar{a}_n), \quad \bar{A}_2 = \frac{1}{a_2} (\bar{a}_n - \bar{a}_c), \\ a_1 &= 1 - \zeta_n, \quad a_2 = \zeta_n - \zeta_c. \end{aligned}$$

System of equations (8) is heterogeneous and contains a known right side of type (7).

Let us find the general solution of uniform equations, which correspond to system (8). We look for this solution in the form:

$$\begin{aligned} \varphi_j &= \operatorname{Re} \sum_{n=1}^{\infty} B_j^n e^{i(m\lambda + \frac{a_n}{2} t)} P_n^m(\theta); \\ \omega_j &= \operatorname{Re} \sum_{n=1}^{\infty} A_j^n e^{i(m\lambda + \frac{a_n}{2} t)} P_n^m(\theta). \end{aligned} \quad (9)$$

( $j=1, n, c$ ).

To reduce the writing let us drop subsequently the indices  $n$  and  $m$ . We introduce the designations:

$$\begin{aligned} \varphi &= \frac{k_1}{a_0^2}, \quad \bar{Z}_j = \varphi y + i(\sigma + a_j m), \\ \bar{L}_j &= -iy(\sigma + i a_j m) + 2im - y^2 \varphi. \end{aligned}$$

Substitute (9) in the system of uniform equations. After simple transformations we go to the following equations:

$$\begin{aligned} B_1^* [\bar{Z}_1 - a_1 \bar{A}_1 m i + \frac{a_1}{2} \Gamma_1 k y] - B_n^* (\bar{Z}_n + a_1 \bar{A}_1 m i) - \frac{a_1}{2} \Gamma_n A_n^* &= 0; \\ B_n^* (\bar{Z}_n - a_2 \bar{A}_2 m i) - A_n^* \frac{a_2}{2} \Gamma_n - A_c^* \frac{a_2 \Gamma_c}{2} - b_c^* (\bar{z}_c + a_2 \bar{A}_2 m i); \\ B_1 (\frac{a_1}{2} L_1 - \varphi k y) + B_n \frac{a_1}{2} \bar{L}_n - \rho_n A_n^* &= 0; \\ B_n \frac{a_2}{2} \bar{L}_n + \rho_n A_n^* - \rho_c A_c^* &= 0. \end{aligned} \quad (10)$$

Equate to zero the determinant of system (10)

$$\begin{vmatrix} \bar{Z}_1 - iC_4 + C_{10} & -\bar{Z}_n - iC_4 & -C_5 & 0 \\ 0 & \bar{Z}_n - iC_6 & -C_8 & -C_9 \\ C_2 \bar{L}_1 + C_{11} & C_2 \bar{L}_n & C_3 & 0 \\ 0 & C_2 \bar{L}_n & -C_3 & C_1 \end{vmatrix} = 0. \quad (11)$$

Here:

$$\begin{aligned} C_1 &= -\rho_c; \quad C_2 = \frac{a_1}{2}; \quad C_3 = -\rho_n; \quad C_4 = a_1 \bar{A}_1 m; \quad C_5 = \frac{a_1 \Gamma_n}{2}; \\ C_6 &= a_2 \bar{A}_2 m; \quad C_7 = \frac{a_2}{2}; \quad C_8 = -\frac{a_2 \Gamma_n}{2}; \quad C_9 = \frac{a_2 \Gamma_c}{2}; \\ C_{10} &= \frac{a_1}{2} \Gamma_1 k y; \quad C_{11} = -\rho_1 k y. \end{aligned}$$

Condition (11) gives us the characteristic equation for determination of  $\sigma$ , which can be written in the form

$$a\sigma^2 + (b + ic)\sigma + d + if = 0, \quad (12)$$

where

$$\begin{aligned} a &= -\beta_{0,1}y^2 + (\beta_{7,1} + \beta_{0,1})y - \beta_{0,1}; \\ b &= -y^2 m \beta_{0,1}(\bar{x}_1 + \bar{x}_n) + ym[(\beta_{7,1} + \beta_{0,1})(\bar{x}_1 + \bar{x}_n) + \beta_{1,2} + \beta_{2,2} + \\ &\quad + 4\beta_{3,1}] - m[2(\beta_{7,1} + \beta_{0,1}) + \beta_{1,2} + \beta_{3,2} + \beta_{0,1}(\bar{x}_1 + \bar{x}_n)]; \\ c &= 2\beta_{0,1}\bar{\varphi}y^2 - y^2(\bar{\varphi} + \bar{\varphi})(\beta_{7,1} + \beta_{0,1}) - y(\beta_{2,1} - 2\beta_{0,1}\bar{\varphi}) + \beta_{0,1}; \\ d &= \bar{\varphi}^2 \beta_{0,1}y^4 - \bar{\varphi}(\beta_{7,1} + \beta_{0,1})\bar{\varphi}y^3 + y^2[\beta_{0,1}\bar{\varphi}^2 - \beta_{0,1}m\bar{x}_1\bar{x}_n - \beta_{2,1}\bar{\varphi}] + \\ &\quad + y[m^2[\bar{x}_1\beta_{1,2} + \bar{x}_n\beta_{2,2} + 2\beta_{0,1}(\bar{x}_1 + \bar{x}_n) + \bar{x}_1\bar{x}_n(\beta_{7,1} + \beta_{0,1})] + \bar{\varphi}\beta_{0,1}] + \\ &\quad + m^2[\beta_{0,1} - 2(\beta_{1,2}^2 + \beta_{2,2}^2) - 4\beta_{3,1} - (\bar{x}_1\beta_{4,2} + \bar{x}_n\beta_{5,2}) - \\ &\quad - \bar{x}_1\bar{x}_n\beta_{0,1} - 2(\bar{x}_n\beta_{7,1} + \bar{x}_1\beta_{0,1})]; \\ \beta_{1,2} &= C_2C_3C_4C_5 - C_1C_2C_3C_6 + C_1C_2C_4C_8; \\ \beta_{2,1} &= C_3C_7C_9C_{10} + C_3C_7C_9C_{11} + C_2C_3C_9C_{10} + C_1C_2C_9C_{10}; \\ \beta_{2,2} &= -C_3C_4C_7C_9 - C_2C_2C_4C_9 - C_1C_2C_4C_8; \\ \beta_{3,1} &= C_2C_3C_7C_9; \quad \beta_{4,2} = -C_1C_3C_8; \\ \beta_{5,1} &= C_3C_9C_{11} + C_1C_3C_{10} + C_1C_3C_{11} + C_1C_3C_{11}; \\ \beta_{7,2} &= -C_1C_3C_3; \quad \beta_{0,1} = C_1C_3; \quad \beta_{7,1} = C_2C_3C_9 + C_1C_2C_3 + C_1C_2C_8; \\ \beta_{0,1} &= C_3C_7C_9 + C_2C_3C_9 + C_1C_2C_8; \quad \beta_{9,1} = -C_1C_2C_4C_8; \\ \beta_{9,2} &= -C_1C_2C_9C_{10} + C_{11}(C_2C_4C_9 - C_1C_3C_8 + C_1C_4C_8); \\ \beta_{k,j} &= m\beta_{k,j}. \end{aligned}$$

Characteristic equation (12) has two roots  $\sigma_1$  and  $\sigma_2$ . Accordingly, the general solution of the uniform system of equations we write in the form:

$$\begin{aligned} \vartheta_n^0 &= \operatorname{Re} \sum_{r=1}^2 \sum_{m,n} B_r e^{i(m\lambda - \tau_r t)} P_n^m(\theta), \\ \vartheta_1^0 &= \operatorname{Re} \sum_{r=1}^2 \sum_{m,n} \bar{K}_r B_r e^{i(m\lambda + \tau_r t)} P_n^m(\theta), \\ \bar{K}_r &= \frac{\mu_4 \bar{z}_n - \mu_3 \bar{L}_n - \mu_2}{\mu_4 \bar{z}_1 - \mu_3 \bar{L}_1 + \mu_2} \Big|_{s=\sigma_r}, \\ \mu_3 &= -iC_1C_3C_4, \quad \mu_4 = C_1C_3, \quad \mu_5 = C_1C_2C_5, \\ \mu_3^* &= \mu_3 + C_1C_3C_{10} + C_1C_3C_{11}. \end{aligned} \quad (13)$$

Expressions of analogous type are written for  $w_j$ . The particular solution of heterogeneous system of equations (8) we look for in the form:

$$\begin{aligned}\psi_j^H &= \operatorname{Re} \sum_{m,n} B_j^* e^{i(m\lambda + \sigma_c^j)} P_n^m(\theta), \\ w_j^H &= \operatorname{Re} \sum_{m,n} A_j^* e^{i(m\lambda + \sigma_c^j)} P_n^m(\theta)\end{aligned}\quad (14)$$

( $j = 1, n$ ).

Having substituted (14) and (7) in (8), we obtain a system of heterogeneous algebraic equations from which can be found expressions for coefficients  $A^*$  and  $B^*$  through coefficients  $B_c$ . As a result we obtain the following formulas:

$$\begin{aligned}\psi_n^H &= \operatorname{Re} \sum_{m,n} \Pi_n B_c e^{i(m\lambda + \sigma_c^j)} P_n^m(\theta), \\ \psi_1^H &= \operatorname{Re} \sum_{m,n} \bar{K}_c \Pi_n B_c e^{i(m\lambda + \sigma_c^j)} P_n^m(\theta), \\ \Pi_n &= \frac{\Lambda^{**}}{\Lambda^*}, \\ \Lambda^* &= a\sigma_c^2 + (b + ct)\sigma_c + d + fi, \\ \Lambda^{**} &= (\bar{L}_1 \mu_1 + \bar{Z}_1 \mu_2 + \bar{Z}_c \mu_3 + \bar{Z}_1 \bar{Z}_c \mu_4 + L_1 \bar{Z}_c \mu_5 + \mu_6)_{\dots \sigma_c}, \\ \mu_1 &= C_1 C_2 C_3 C_4, \quad \mu_2 = iC_1 C_3 C_6, \\ \mu_3 &= C_1 C_2 C_1 C_c + iC_1 C_d (C_3 C_{10} + C_2 C_{11}).\end{aligned}\quad (15)$$

The expression for  $\bar{K}_c$  is obtained from the above formula for  $\bar{k}_r$  with the substitution  $\sigma = \sigma_c$ .

Thus, the general solution for stream function  $\psi$  is written in the form:

$$\begin{aligned}\psi_n &= \operatorname{Re} \sum_{m,n} [B_1 e^{i(m\lambda + \sigma_c^j)} + B_2 e^{i(m\lambda + \sigma_c^j)} + \Pi_n B_c e^{i(m\lambda + \sigma_c^j)}] P_n^m, \\ \psi_1 &= \operatorname{Re} \sum_{m,n} [\bar{K}_1 B_1 e^{i(m\lambda + \sigma_c^j)} + \bar{K}_2 B_2 e^{i(m\lambda + \sigma_c^j)} + \bar{K}_c \Pi_n B_c e^{i(m\lambda + \sigma_c^j)}] P_n^m.\end{aligned}\quad (16)$$

Analogously it is possible to give the solution for  $w$ . Arbitrary constants  $B_1, B_2$  are determined according to initial conditions.

The process of their determination coincides completely with that given in works [2] and [3] and we will not repeat here the corresponding conclusion.

The forecasting scheme described above was computerized. During calculations values of coefficients were taken as  $k_2 = 5 \cdot 10^5 \text{ m}^2/\text{s}$ ,  $k = 140 \text{ m}$ , and the remaining parameters were the same as in [2]. Forecasts by this scheme were compared with forecasts according to the scheme given in [2]. As a quantitative estimate of the quality of the forecasts we used the relative forecast error (ratio of mean absolute error of forecast to mean absolute variability). Forecasts of pressure at sea level for the North Atlantic were analyzed (zone between  $80^\circ$  west longitude and  $10^\circ$  east longitude and between  $20^\circ$  and  $80^\circ$  north latitude).

Table 1.

Original date	$\delta$		$E$	
	1	2	1	2
3 III 1966	10.1	7.7	1.24	0.96
17 III	9.4	7.8	1.28	1.08
22 III	10.6	8.2	1.32	1.04
27 III	9.2	7.8	1.23	0.92
15 IV	10.2	7.8	1.44	1.09
18 IV	11.8	11.2	1.13	1.07
22 IV	13.3	11.0	1.61	1.33
27 IV	10.6	7.4	1.40	0.98
29 IV	7.9	5.4	0.96	0.67
6 V	11.1	8.3	1.23	0.92
13 V	8.3	7.2	0.83	0.72
18 V	8.3	6.8	1.32	1.09
20 V	9.5	7.5	1.12	0.88
23 V	8.2	7.7	0.97	0.91
25 V	9.9	7.7	1.46	1.16
30 V	9.5	7.6	1.27	1.03
1 VI	8.8	6.9	1.22	0.94
Average.....	9.8	7.9	1.25	1.03

Table 1 gives estimates of the quality of forecasts for four days ahead:  $\delta$  - mean absolute error of forecast (decameter) in the considered area,  $E$  - relative error. The magnitudes of the estimate are given according to the system in [2] (column 1) as well as

according to the given system (column 2). During analysis of the data of Table 1 one ought to consider that the estimate was made for regions badly illustrated by the data of observations.

The data of Table 1, and also immediate comparison of forecast maps composed by both systems testify to a systematic increase in the quality of forecast using the new system. From July 1966, ground pressure has been forecasted using the system described above.

#### Bibliography

1. Kibel' I. A. Vvedeniye v gidrodinamicheskiye metody kratkosrochnogo prognoza pogody (Introduction to hydrodynamic methods of short-range weather forecasting). GTTL, M., 1957.
2. Mashkovich S. A., Kheyfets Ya. M. K teorii dolgosrochnogo prognoza s uchetom vertikal'noy stratifikatsii atmosfery i turbulentnogo peremeshivaniya (Theory of long-range forecasting with allowance for vertical stratification of the atmosphere and turbulent mixing). Tr. TsIP, vyp. 93, 1960.
3. Mashkovich S. A., Kheyfets Ya. M. Opyt chislennogo prognoza nazemnogo davleniya na neskol'ko dney vpered (Experience in numerical forecasting of ground pressure for several days in advance). Tr. TsIP, vyp. 126, 1963.

FINITE-DIFFERENCE ALGORITHM OF A SOLUTION OF THE VORTICITY  
EQUATION FOR THE MIDDLE TROPOSPHERE OVER THE  
NORTHERN HEMISPHERE

N. V. Isayev and M. S. Fuks-Rabinovich

A system for forecasting the geopotential at the middle troposphere using a space (in coordinates  $x, y$ ) finite-difference approximation, which provided conservation of the quadratic integral features is considered (i.e., vorticity, its square and kinetic energy); integration in time follows the method of Adams. Charts of the change in average kinetic energy of forecast fields  $H_{500}$  in time are constructed. Results are given for the calculation of long-range forecasting of a brief length of time before forecast phenomenon occurrence according to the given system.

Introduction

With the numerical solution of forecast equations one of the greatest difficulties is selecting an algorithm which would provide stability of multistage calculation. In view of the complexity of forecast equations and the large volumes of original and intermediate information, it was impossible to show earlier a method of solving the forecast problem which was optimum in the sense of resistance and economy. The selection of such a solution can be made only on the basis of numerical experiments with the forecast model being investigated.

In writing a finite-difference model of linear terms one must take into account that a source of instability can be inaccuracy in the approximations of both the space and time derivatives. In a number of works [8, 13] it was shown that a certain improvement of the quality of the solution can be obtained by using a higher approximation (third order) of the first and second space derivatives. In this case, however, the source of the instability, connected with nonlinear terms, is not removed. This type of instability, called nonlinear instability, is shown in the work of Phillips [12]. The system, having linear stability (i.e., stability investigated on the basis of linearized equations), was far from always suitable for solving nonlinear tasks, for which nonlinear instability can prevail.

#### Approximation of Nonlinear Terms of the Barotropic Vorticity Equation

An attempt to remove instability connected with nonlinear terms was undertaken in [5]. It was proposed to use a finite-difference system of calculating the Jacobian, which provided the conservation of the first integrals of the barotropic vorticity equation.

Let us remember that for the barotropic atmosphere the absolute vorticity of velocity  $\Omega$  is the retained quantity and the vorticity equation can be written in the form

$$\frac{d\Omega}{dt} = 0. \quad (1)$$

where  $\Omega = \frac{\partial v}{\partial x} - \frac{\partial u}{\partial y} + l$ ,  $u$  and  $v$  - horizontal components of velocities,  $l$  - Coriolis parameter,

$$\frac{d}{dt} = \frac{\partial}{\partial t} + u \frac{\partial}{\partial x} + v \frac{\partial}{\partial y}.$$

On the other hand, the general kinetic field energy

$$E = \iint \frac{u^2 + v^2}{2} d\sigma. \quad (2)$$

does not change with time under the condition of invariability of values of the stream function on the boundary of the range of integration  $\sigma$ . In integral form conditions of conservation can be written in the form:

$$\bar{E} = \int \int E(x, y, t) d\sigma = \text{const.} \quad (3)$$

$$\bar{\Omega} = \int \int \Omega(x, y, t) d\sigma = \text{const.} \quad (4)$$

moreover, the constants in the right side of these relationships are a function of time.

It is obvious that during the transition to a finite-difference type of forecast equations it is advisable that relationships (3) and (4) be executed with the highest possible degree of accuracy. However, the majority of existing difference schemes provides retention of only part of the integral features of the original equations (for example, only vorticity velocity  $\bar{\Omega}$  is retained). Therefore there is great interest in the work of Arakawa [5], which proposes a finite-difference model of nonlinear terms of the vorticity equation, which provided an integral retention of the vorticity velocity  $\bar{\Omega}$ , square of the vorticity velocity  $\bar{\Omega}^2 = \int \int \Omega^2(x, y, t) d\sigma$  and kinetic energy  $\bar{E}$ , i.e., all integral features simultaneously.

In the work of Lilly [8] on simplified test models it is shown that using the Arakawa system various sources of nonlinear instability are mutually compensated and nonlinear instability is exhausted.

A number of authors [3, 9, 14] expresses the opinion that for purposes of short-range forecasting it is compulsory not to use finite-difference systems in which the integral features of the original equations are accurately retained, but it is possible to use a system where retention of integral features is provided only approximately. But for long-range forecasting even of a brief length of time before forecast phenomenon occurrence, already it is extremely advisable to use systems which provide accurate retention (at least within the framework of the test model) of integral

features of type (3), (4) and free from nonlinear instability, because during multistage calculation in long-range forecasting nonlinear instability is considerably stronger than in short-range forecasting.

In the present work nonlinear members of the vorticity equation were represented in finite-difference form according to the Arakawa system. Following [8], let us describe briefly this algorithm.

Let us examine the vorticity equation in the solenoid approach for the barotropic atmosphere (at  $l = \text{const}$ )

$$\frac{\partial \zeta}{\partial t} + J(\zeta, \psi) = \frac{\partial \zeta}{\partial x} \frac{\partial \psi}{\partial y} - \frac{\partial \zeta}{\partial y} \frac{\partial \psi}{\partial x}. \quad (5)$$

where  $\zeta = \Delta \psi$ ,  $\psi$  - stream function,  $J(\zeta, \psi)$  - Jacobian,  $\Delta$  - two-dimensional Laplacean operator.

We introduce the designations:

$$\begin{aligned} \delta_x F(x) &= \frac{1}{\Delta x} \left[ F\left(x + \frac{\Delta x}{2}\right) - F\left(x - \frac{\Delta x}{2}\right) \right], \\ \overline{F(x)} &= \frac{1}{2} \left[ F\left(x + \frac{\Delta x}{2}\right) + F\left(x - \frac{\Delta x}{2}\right) \right], \\ \overline{\delta_x F(x)} &= \delta_x \overline{F(x)} = \frac{1}{2\Delta x} [F(x + \Delta x) - F(x - \Delta x)], \end{aligned} \quad (6)$$

where  $F(x)$  is any of the considered functions.

In (6) let us write down three such difference expressions for Jacobian  $J$ :

$$\begin{aligned} J_1 &= \delta_x \overline{(\zeta \delta_y \psi)} - \delta_y \overline{(\zeta \delta_x \psi)}, \\ J_2 &= \delta_x (\overline{\psi \delta_y \zeta}) - \delta_y (\overline{\psi \delta_x \zeta}), \\ J_3 &= -\delta_x (\overline{\zeta \delta_y \psi}) + \delta_y (\overline{\zeta \delta_x \psi}). \end{aligned} \quad (7)$$

According to [8], each of these relationships provides vorticity retention, the vorticity square and kinetic energy respectively.

If, however, we put together

$$J_A = \frac{1}{3}(J_1 + J_2 + J_3). \quad (8)$$

then this finite-difference model will guarantee retention of all three shown features simultaneously.

Being limited in the approximation of nonlinear terms to the second order of accuracy, we have the following working formulas for determination of  $J_A$  (see Fig. 1):

$$J_A = \frac{1}{12h^2} \{ (\psi_1 - \psi_2)(\psi_2 - \psi_3) - (\psi_2 - \psi_1)(\psi_1 - \psi_3) + (\psi_3 - \psi_1) - (\psi_3 - \psi_2) - (\psi_2 - \psi_1) + (\psi_1 - \psi_2) + (\psi_2 - \psi_1) - (\psi_1 - \psi_2) - (\psi_2 - \psi_1) + (\psi_3 - \psi_2) - (\psi_3 - \psi_1) \}. \quad (9)$$

where  $h$  - grid interval.

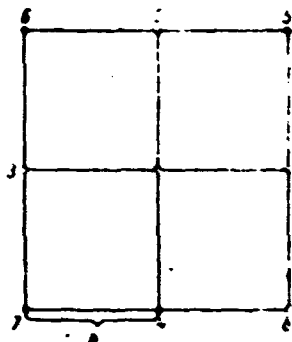


Fig. 1. Grid-template for calculating non-linear terms ( $h$  - grid interval).

#### Approximation of Derivative in Time

In forecasting systems and in models of the overall circulation are applied various methods of approximating the derivative in time. Along with the method of central differences, various authors use the systems of Lax-Wendroff [7], Miyakoda [11], Matsuno [10], Hoyne [6], and others. According to test calculations in a work of Lilly [8] a good index of stability goes with the method of Adams [1]. For integration in time this work tested the system of Adams,

Miyakoda, Hoyne, Matsuno and the method of central differences. The results which were best and very close in quality were obtained with the system of Adams and Miyakoda.

In Table 1 are estimates of various methods of integration in time. Along with the change in kinetic energy for the various systems the mean relative forecast errors by these systems are given. Averaging took in 75 points. Furthermore, the amounts of divergence between the different systems are given. The best results were with the systems of Adams and Miyakoda (however, the divergences between them are small). Both these systems are more accurate than the method of central differences (and the methods of Matsuno and Hoyne).

Table 1. Comparison of certain methods of integration in time.

Method	Formula	T=1			T=2			T=3		
		W	$\epsilon_{cp}$	$ a _{cp}$	W	$\epsilon_{cp}$	$ a _{cp}$	W	$\epsilon_{cp}$	$ a _{cp}$
Miyakoda	$\left(3 - \frac{1}{2}\right) x^{n+1} - 3x^n +$ $+ \left(\frac{1}{2} - 3\beta\right) x^{n-1} -$ $- 3x^{n-2} + f^n \Delta t; \beta > 0$	1.1	0.71	7.3	2.5	0.81	9.8	3.7	0.90	12.9
Adams	$x^{n+1} = x^n + \left[\frac{3}{2} f^n -$ $- \frac{1}{2} f^{n-1}\right] \Delta t$ $x^{(n+1)p} = x^n + f^n \Delta t$	1.1	0.72	7.2	2.6	0.83	10.1	3.9	0.92	13.4
Hoyne	$x^{n+1} = x^n + \frac{1}{2} (f^n +$ $+ f^{n-1}) \Delta t$	1.9	0.83	8.2	5.1	0.96	12.2	10	1.08	14.9
Central difference	$x^{n+1} = x^{n-1} + 2f^n \Delta t$	2.1	0.9	9.4	6.8	1.02	14.2	20	1.20	16.4

Note.  $x^n$  - value of geopotential on the  $n$ -th time interval  $f^n = \left(\frac{dx}{dt}\right)_n$  - value of derivative in time from geopotential on the  $n$ -th interval;  $|W|$  - absolute deviation in the kinetic energy in percent,  $\epsilon_{cp}$  - mean relative forecast error;  $|a|_{cp}$  - mean absolute error of forecast in decimeters;  $\Delta t$  - time interval;  $T$  - number of days;  $\beta$  - parameter in system of Miyakoda.

In using the methods of Adams and Miyakoda kinetic energy is retained to a greater extent in the course of calculation than otherwise. The method of Adams is distinguished also by its simplicity, it is handy for using on a computer and requires keeping only one additional field (as the method of central differences). In view of the greatest effectiveness and economy we stayed with the method of Adams and used it in this work for approximation of the derivative in time.

We will give the derivation of the Adams extrapolation formula, limiting ourselves to an approximation of the second order of accuracy.

Decompose functions  $\psi_{n+1}$  and  $\psi_n$  (values of stream function on the  $n + 1$  and  $n$  time interval respectively) in a Taylor series in  $\Delta t$  and  $2\Delta t$

$$\begin{aligned}\psi_{n+1} &= \psi_n + \psi'_n \Delta t + \psi''_n \frac{(\Delta t)^2}{2} + O(\Delta t^3); \\ \psi_{n-1} &= \psi_{n-1} + \psi'_{n-1} (2\Delta t) + \psi''_{n-1} \frac{(2\Delta t)^2}{2} + O(\Delta t^3); \\ \psi_n &= \psi_{n-1} + \psi'_{n-1} \Delta t + \psi''_{n-1} \frac{(\Delta t)^2}{2} + O(\Delta t^3).\end{aligned}\tag{10}$$

We multiply the first and second relationships from (10) by certain real numbers  $\alpha$  and  $\beta$  respectively and combine the results

$$\begin{aligned}(\alpha + \beta)\psi_{n-1} &= \alpha\psi_n + \beta\psi_{n-1} + (\alpha\psi'_n + 2\beta\psi'_{n-1})\Delta t + \\ &+ (\alpha\psi''_n + 4\beta\psi''_{n-1})\frac{(\Delta t)^2}{2} + O(\Delta t^3).\end{aligned}\tag{11}$$

Considering the third relationship from (10), let us rewrite formula (11) in the form:

$$\begin{aligned}(\alpha + \beta)\psi_{n+1} &= (\alpha + \beta)\psi_n + (\alpha\psi'_n + \beta\psi'_{n-1})\Delta t + \\ &+ (\alpha\psi''_n + 3\beta\psi''_{n-1})\frac{(\Delta t)^2}{2} + O(\Delta t^3).\end{aligned}\tag{11'}$$

In order to obtain an approximation of the second order of accuracy, the term of relationship (11') containing  $\Delta t^2$  must be equivalent to zero. For this condition it is necessary that

$$\alpha = -3\beta,$$

whence

$$\alpha + \beta = -2\beta.$$

Substituting these values into expression (11'), we obtain the Adams formula

$$\psi_{n+1} = \psi_n + \left( \frac{3}{2} \psi'_n - \frac{1}{2} \psi'_{n-1} \right) \Delta t + O(\Delta t^3). \quad (12)$$

### Parameters of the Forecast System

On the basis of the algorithm given in previous sections a system was constructed to forecast the geopotential for  $H_{500}$  over almost all the northern hemisphere (Fig. 2). As in [4] the barotropic vorticity equation in the quasi-geostrophic approach is written in the following form:

$$\Delta \frac{\partial H}{\partial t} = \left( \frac{m^2}{f} \Delta H + l, H \right), \quad (13)$$

where  $H$  - geopotential,  $l = l(\phi)$  - Coriolis parameter;  $m = m(\phi)$  - parameter of the increase in stereographic projection;  $\phi$  - geographical latitude,

$$(a, b) = \frac{\partial a}{\partial x} \frac{\partial b}{\partial y} - \frac{\partial a}{\partial y} \frac{\partial b}{\partial x}. \quad (14)$$

The original geopotential field  $H$  is given in 2181 mesh points (Fig. 2), having the form of an octagon (51 points in the longest columns and lines of the octagon and 23 points in the shortest) with the center of symmetry at the north pole. Nonlinear terms were approximated according to the Arakawa system, and the derivative in time by the method of Adams. Equation (13) relative to  $\partial H / \partial t$  was solved by the extrapolation method of Liebmann. In this case at the edge of the octagonal area a condition of invariability of

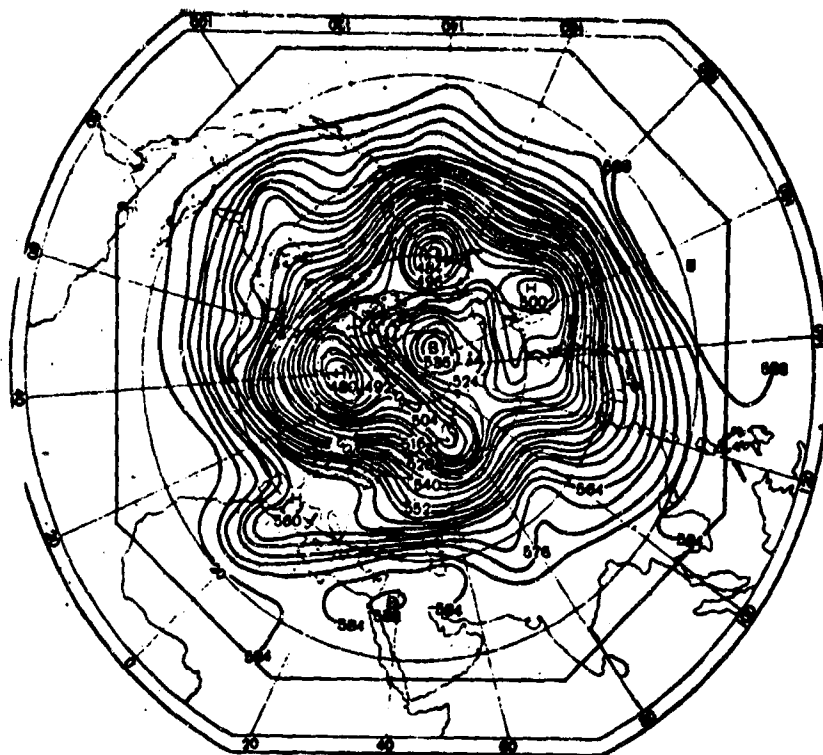


Fig. 2.  $AT_{500}$  forecast map for 0300, 24 December 1963 according to data for 0300, 22 December 1963. The solid line outlines the octagon along which the forecast was resolved.

geopotential with time was assumed. During the calculation no smoothing operators were applied. The interval in coordinates was 390 km at a latitude  $\phi = 60^\circ$ , the time interval  $\Delta t = 3$  hours. This system resolved forecasts of the  $H_{500}$  fields for periods of 24, 48 and 72 hours. Analysis of the forecast fields will be conducted below.

#### Calculation and Adjustment of the Energy of Forecast Fields

Retention of the integral features provided by the Arakawa system nevertheless is distorted during the calculation of a forecast for a long period. The reason for this is not only the errors of extrapolation in time, but a whole series of circumstances. It is widely known that basic factors limiting the earliness of

the forecast model are first of all the simplifications accepted in the derivation of forecast equations (such as, for example, adiabaticity, quasi-geostrophicity, and others), and also inaccuracies in the initial information and boundary conditions. (In forecasting for the hemisphere or sphere specific difficulties appear during the examination of phenomena in the equatorial range. Furthermore, limited computer capabilities force us to resort to economical storage of intermediate information during the calculation, which leads to a rounding of the intermediate values and limits the accuracy of calculations because of the accretion of rounding errors.)

Here we will describe a numerical experiment conducted to determine the interval of earliness of forecast of the given system. Basic criteria for determination of forecast successes were of course synoptic analysis and quantitative estimation; however, in addition the following was done.

On every interval in time during the calculation of the forecast the quantity

$$W = \left( \frac{\bar{E}_n}{\bar{E}_0} - 1 \right) 100\%, \quad (15)$$

was figured, where  $\bar{E}_n$ ,  $\bar{E}_0$  are values of the kinetic energy fields calculated by formula (4) on the  $n$ -th and zero time intervals. The quantity  $W$  shows how much (in percent) the kinetic energy of the field on the  $n$ -th time interval changed in comparison with the initial.

In vorticity equation (13) a term considering horizontal turbulent exchange was introduced, whereupon this equation took the form

$$\Delta \frac{\partial H}{\partial t} = \left( \frac{\partial}{\partial t} \Delta H + l, H \right) + \nu \nabla^2 H, \quad (16)$$

where  $\nabla = \bar{i} \frac{\partial}{\partial x} + \bar{j} \frac{\partial}{\partial y}$  is a plane of Hamiltonian operator;  $\bar{i}$ ,  $\bar{j}$  - unique vectors.

With the aid of parameter  $\nu$  the kinetic energy of the forecast fields was adjusted, namely, in the process of calculating the forecast the quantity  $\nu$  was selected such that the deviations in energy  $W$  would be located within certain limits

$$|W| \leq \delta, \quad (17)$$

where  $\delta$  was assigned as 0.5%.

Until inequality (17) was disturbed, during the calculation of the forecast the value  $\nu = 0$  was used. When inequality (17) was disturbed,  $\nu$  was determined from the relationship

$$\nu_k = \nu_{k-1} + \kappa W_k; \quad \nu_k \geq 0, \quad (18)$$

where  $\kappa$  - an empirically selected coefficient,  $k$  - number of interval on which occurred the disturbance of (17). If on subsequent intervals (17) held, then  $\nu$  did not change. Such intermittent inclusion into calculation of control parameter  $\nu$  allows regulating the kinetic energy of the obtained fields and achieve its change within the limits of 2% (for a lower value of  $\delta$  in (18) it is possible to lower this limit somewhat) with a practically unlimited number of time intervals. The change calculated by actual data for three days likewise is located within the limits of several percent.

The authors calculated the geopotential field  $H_{500}$  for 20 days; the chart of the change  $W(t)$  in time, obtained as a result of numerical experiments using control parameter  $\nu$ , which was determined by formula (18) upon disturbance of condition (17), is given in Fig. 3b.

Changes in values of  $\nu$  during the numerical experiment are shown in Fig. 3a. We see that up to five days the forecast is resolved at very small values  $0 \leq W \leq 2 \cdot 10^4 \text{ m}^2/\text{s}$ , and in the subsequent period the utilized values of  $\nu$  fluctuate from zero and approximately to  $5 \cdot 10^5 \text{ m}^2/\text{s}$ , which agrees well with the values of  $\nu$  used usually in calculations (see for example, [2]).

The most interesting feature of the chart of  $W(t)$  (Fig. 3b) is the fact that after five days the quantity  $|W|$  somewhat increases

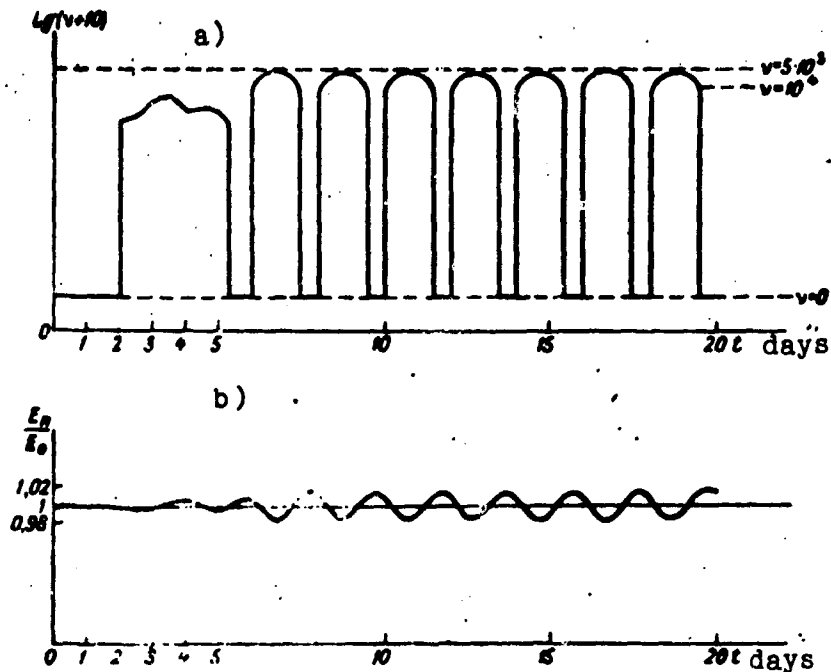


Fig. 3. Charts of the change in parameter  $\lg(\gamma + 10)$  in time (a) and the quantity  $E_n/E_0$  in time (b).  $E_n$  - field energy on the  $n$ -th time interval.  $E_0$  - energy of initial field.

and the change of  $W(t)$  becomes periodic. This periodicity indicates that at approximately the fifth day a large role begins to be played by the balance of purely stray perturbations and damping factors, realizable with the help of control parameter  $v$ . Visual and quantitative estimation of forecast fields likewise shows that four to five days is the limit period for good justification of a forecast based on this system.

Such a mechanism of estimating the earliness of forecast apparently may be applied to other forecasting systems.

#### Analysis and Estimation of Prediction Fields

As already was indicated above, the calculation of forecasts was conducted for  $v = 0$  (in contrast with numerical experiments on determining the interval of earliness of forecast, examined in the previous section).

During the calculation of forecasts simultaneously by formula (14) the quantity  $W(t)$  was calculated in order to be able to observe the degree of retention of kinetic energy in the fields being forecasted. For a period of two to three days the quantity  $W(t)$  was within limits of 2-3.5%, which indicates good retention of the integral features for such a period of calculation. As a comparison let us say that when using the algorithm of forecast calculation given in [4], the quantity  $W(t)$  changed after three days by 15-20%, which indicates nonretention of the integral features as well as a large degree of smoothing of the forecast fields.

As an example let us give the results of forecasting  $H_{500}$  for 48 hours, calculated according to original data for 0300, 22 December 1963 (Fig. 4). The actual and forecast maps for 0300, 24 December 1963 are given in Figs. 2 and 5. (Let us note that we selected the most difficult example during the period of the two-year test in a system based on limited territory.)

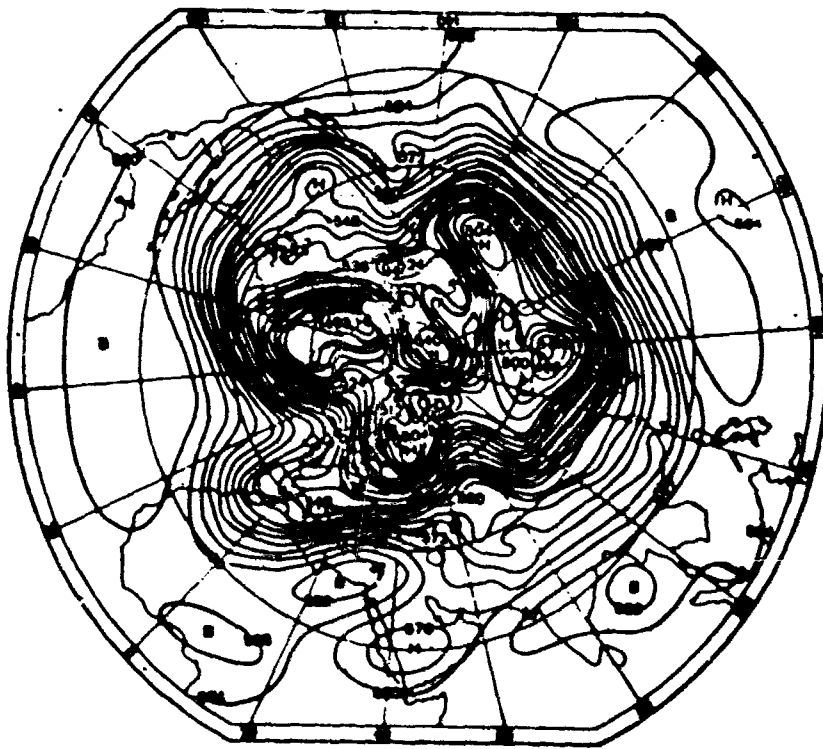


Fig. 4.  $AT_{500}$  original field at 0300  
22 December 1963.



Fig. 5.  $AT_{500}$  actual map for 0300, 24 December 1963.

We see that values of the geopotential in centers were predicted rather well, although a certain lag from their actual movement is observed. Cyclogenesis over the Pyrenees and the formation of a ridge over western Germany (where there is a trough on the original map) were reflected in the forecast. The absence of smoothing and retention of integral features guarantees that the forecast maps will have pressure gradients close to the actual ones.

Quantitative estimates of the example are given in Table 2. Over the illustrated regions relative error  $\epsilon = 0.83$  (over Europe  $\epsilon = 0.72$ ), whereas forecast estimates calculated by the simpler system described in [4] are noticeably worse:  $\epsilon = 1.2-1.4$ . (In Table 2 estimates were resolved over all points of the field.)

An estimate of calculation results for a series of forecasting examples from this system are given in Table 3. The estimate was

Table 2. Estimate of forecast success for 48 hours according to original data for 0300, 22 December 1963 (I - finite-difference model in work [4]; II - in this work).

Regions	No. of points	$ a _{cp}$		$\sum_{i=1}^N  a_i $	$ a _{cp}$	$\delta$	
		I	II			I	II
Whole range used when evaluating.....	1377	13.2	9.5	13081	9.5	1.20	1.00
Europe.....	137	18.6	9.6	1679	12.9	1.44	0.72
North America.....	188	3.1	10.6	2381	12.7	1.08	0.83
Asia.....	348	14.1	11.9	4277	12.3	1.15	0.96
Dark regions (Pacific, Atlantic and North Arctic oceans.....)	716	11.8	8.0	4794	6.8	1.75	1.18

Note.  $|a|_{cp}$ ,  $|\delta|_{cp}$  - mean absolute values of error and variability (for 48 hours) respectively;  $\delta_i$  - variability (for 48 hours) at point of regular mesh;  $N$  - number of points of regular mesh in a given region;  $\epsilon = \frac{|a|_{cp}}{|a|_{cp}}$  - relative error.

Table 3. Estimates of forecasts for 24, 48 and 72 hours.

Raw data		t=1			t=2			t=3		
		$\epsilon_{cp}$	$\epsilon_{oce}$	$\epsilon_g$	$\epsilon_{cp}$	$\epsilon_{oce}$	$\epsilon_g$	$\epsilon_{cp}$	$\epsilon_{oce}$	$\epsilon_g$
1500	16 XII 1965	—	—	—	0.82	0.73	—	0.85	0.65	0.80
1500	17 XII 1965	—	—	—	—	—	—	1.02	0.95	0.98
1500	18 XII 1965	—	—	—	—	—	—	1.11	0.94	1.14
1500	19 XII 1965	—	—	—	—	—	0.72	0.90	0.90	0.83
0300	14 VIII 1966	—	—	—	0.71	0.63	0.49	0.80	—	—
0300	15 VIII 1966	0.68	0.65	0.51	0.73	0.71	0.74	0.78	0.79	0.88
0300	16 VIII 1966	0.65	0.60	0.63	0.75	0.77	0.82	0.71	0.70	0.76
0300	15 IX 1966	—	—	—	0.76	0.72	0.78	0.82	0.78	0.80
0300	8 X 1961	—	—	—	0.88	—	—	—	—	—
0300	7 VII 1963	—	—	—	0.85	—	—	—	—	—
0300	22 XII 1963	—	—	—	1.00	0.83	—	—	—	—
0300	24 XII 1963	—	—	—	0.95	0.87	—	—	—	—
Mean.....		0.67	0.63	0.57	0.83	0.75	0.67	0.87	0.82	0.87

Note.  $\epsilon_{cp}$  - the estimate took in 75 points,  $\epsilon_{oce}$  - points in dark regions,  $\epsilon_g$  - 12 points in the North Atlantic and Europe ( $\epsilon = \frac{|a|_{cp}}{|a|_{cp}}$  - relative error).

over 75 points ( $\epsilon_{cp}$ ), as far as possible evenly distributed through the forecast range, and also through 12 points ( $\epsilon_g$ ), located in the North Atlantic and on the European territory of the USSR.

One ought to note that the examples of forecasts using raw data for 0300 15-19 December 1965 were specially selected for the purpose of testing the system on complex synoptic situations.

Analysis of a series of examples of forecasting (12 cases), calculated by this system, allows us to make the following qualitative conclusions. First of all one ought to note that such important phenomena in reconstruction of fields as cyclo- and anti-cyclogenesis frequently are provided in forecasts (cases of cyclo- and anticyclogenesis, conditioned basically by dynamic factors). Furthermore, the change in pressure in the centers of the baric formations, and also values of gradients in the pressure field are correctly predicted. At the same time, a certain (of the order of 20%) error in predicting movements of the centers of the baric formations is observed. (The last drawback can be in some measure removed by increasing the order of approximation of the nonlinear terms.)

In conclusion let us note that this finite-difference algorithm can be applied even to baroclinic forecast systems.

#### Bibliography

1. Berezin I. S. and Zhidkov N. P. *Metody vychisleniy* (Methods of calculations), t. 2, GIFML, M., 1959.
2. Mashkovich S. A., Kheyfets Ya. M. *K teorii dolgosrochnogo prognoza s uchetom vertikal'noy stratifikatsii atmosfery i turbulentnogo peremeshivaniya* (Theory of long-range forecasting considering vertical stratification of the atmosphere and turbulent mixing). Tr. TsIP. vyp. 93. 1960.
3. Pressman D. Ya. *Raznostnaya skhema kratkosronnogo prognoza pogody po polnym uravneniyam (prostranstvennaya model')* (Difference systems for short-range weather forecasting based on complete equations (spatial model)). Tr. MMTs, vyp. 14, 1966.

4. Sitnikov I. G., Fuks-Rabinovich M. S. O vospolnenii nedostayushchey informatsii v pole geopotentsiala dlya obshirnykh maloosveshchennykh rayonov severnogo polushariya (Supplementing insufficient information in the geopotential field for extensive badly illustrated regions of the northern hemisphere). Tr MMTs, vyp. 10, 1965.
5. Arakawa A. Computational Design for Long-Term Numerical Integration of the Equations of Fluid Motion: Two-Dimensional Incompressible Flow. Part I. Journal of Computational Physics, Vol. 1, No. 1, 1966.
6. Lorenz E. N. Deterministic Non-periodic Flow. J. Atm. Sci., Vol. 20, No. 2, Mar, 1963.
7. Lax P. D. and Wendroff B. Systems of the Conservation Laws. Communications of Pure and Applied Mathematics, Vol. 13, 1960.
8. Lilly D. K. On the Computational Stability of Numerical Solutions of Time-Dependent Non-Linear Geophysical Fluid Dynamics Problems. Monthly Weather Review. Vol. 93, No. 1, Jan. 1963.
9. Lilly D. K. Numerical Solutions for the Shape-Preserving Two-Dimensional Thermal Convection Element. J. Atm. Sci., Vol. 21, No. 1, Jan. 1964.
10. Mintz Y. Very Long-Term Global Integration of the Primitive Equations of Atmospheric Motion. WMO-JUGG Symposium of Research and Development Aspects of Long-Range Forecasting, Technical Note, No. 66, Boulder, Colorado, 1964.
11. Miyakoda K. Contribution to the Numerical Weather Prediction Computation with Finite Difference. Jap. J. Geophys., Vol. 3, 1962.
12. Phillips N. A. An Example of Non-Linear Computational Instability. The Atmosphere and the Sea in Motion, pp. 501-504. Rockefeller Institute Press in Association with Oxford University Press, New York, 1959.
13. Shuman F. G. and Vanderman L. W. Truncation Errors in Numerical Weather Prediction, Paper Presented at 45th Annual Meeting, American Geophysical Union, Washington, D. C., Apr. 1964.
14. Shuman F. G. and Stackpole I. D. A Note on the Formulation a Map Scale Factor. (Lektsii po chislennym kratkosrochnym prognozam pogody (Mezhdunarodnyy uchebnyy seminar) (Lectures on numerical short-range forecasts (international educational seminar)). M., 1967.

NUMERICAL SOLUTION OF THE BALANCE EQUATION  
IN THE FRAMEWORK OF A QUASI-SOLENOIDAL  
FORECAST DIAGRAM OF THE GEOPOTENTIAL  
FOR THE NORTHERN HEMISPHERE

I. G. Sitnikov and S. O. Krichak

A finite-difference system of solving the balance equation for the northern hemisphere is given. A series of characteristic features found with the solution of this equation for a belt of low latitudes is shown. The obtained values of the stream function are used to forecast the geopotential field at the middle level of the troposphere for 72 hours. An example of the forecast is presented.

Various questions connected with the technology of numerical solution of the balance equations have been illustrated in a number of works (for example, [1, 3, 5, 6, 7, 8, 9]). Most frequently in this case the problem is solved for a comparatively small area. Of the mentioned works only in [8] is a method stated for solving this equation relative to the northern hemisphere. This work establishes a number of characteristic features found with the solution of the balance equation within the framework of a quasi-solenoidal system of forecasting the geopotential on the northern hemisphere.

1. The balance equation recorded in a local isobaric system of coordinates  $(x, y, p)$  for a polar stereographic projection has the form [9]

$$m^2 \Delta \psi - \frac{2m^4}{l} \left[ \left( \frac{\partial^2 \psi}{\partial x \partial y} \right)^2 - \frac{\partial^2 \psi}{\partial x^2} \frac{\partial^2 \psi}{\partial y^2} \right] + \frac{m^2}{l} \left( \frac{\partial \psi}{\partial x} \frac{\partial l}{\partial x} + \frac{\partial \psi}{\partial y} \frac{\partial l}{\partial y} \right) = \frac{m^2 g}{l} \Delta H.$$

Here  $\psi$  - stream function,  $H$  - height of isobaric surface,  $m$  - "parameter of distortion" of stereographic projection,  $l$  - Coriolis parameter,  $g$  - acceleration of gravity.

It is known that equation (1), considered as the equation for determination of values of  $\psi$ , will belong to the family of Monge-Ampere equations referring either to elliptical or hyperbolic type depending on the relationship of coefficients [4]. A number of authors [8, 9], making use of the so-called Petersen conversion, reduce equation (1) to the form

$$m^2 \Delta \psi = l + \sqrt{l^2 + 2g \Delta H + m^4 \left( -\frac{\partial^2 \psi}{\partial x^2} - \frac{\partial^2 \psi}{\partial y^2} \right)^2} + \dots \rightarrow$$

$$\left[ + 4m^4 \left( \frac{\partial^2 \psi}{\partial x \partial y} \right)^2 - 2m^2 \left( \frac{\partial \psi}{\partial x} \frac{\partial l}{\partial x} + \frac{\partial \psi}{\partial y} \frac{\partial l}{\partial y} \right) \right]. \quad (2)$$

To solve equation (2) usually the method of series approximations is used. In this case equation (2) is considered as a Poisson equation relative to  $\psi$ , considering that values of  $\psi$  in the right side are known and are determined, for example, from the previous approximation.

We will use as the initial approximation for the solution of equation (2) the relationship

$$\psi_0 = \frac{g}{l} H. \quad (3)$$

where  $\bar{l}$  - the value of  $l$  on any fixed latitude  $\phi_0$  (we took  $\phi_0 = 45^\circ$ ). Then, substituting (3) in equation (2), we can after solving (2) determine according to  $\psi_0$  a new approximation  $\psi_1$ ; substituting it in the right side of (2), we obtain  $\psi_2$ , etc.

As a boundary condition, following Miyakoda [8], we take relationship  $\psi|_{rp} = \frac{g}{l} H|_{rp}$ , where again  $\bar{l} = l(\phi_0)$ ,  $\phi_0 = 45^\circ$ .

The obtained field  $\psi$  was used as the initial field for the quasi-solenoidal forecast in terms of a barotropic model on the northern hemisphere (system proposed in [2]).

The forecasts of  $\psi$  were for 24, 48 and 72 hours. At the end of each period the  $H_{500}$  field was located by means of so-called "inversion" of the balance equation, i.e., of the solution relative to  $H$  for known distribution of  $\psi$ .

2. For a solution of equation (1) we must require that this equation be elliptical in all points of the grid. As experiment shows, the criterion of ellipticity of equation (1) having the form

$$\Gamma = 2gm^2\Delta H + F - 2\left(\frac{\partial\psi}{\partial x}\frac{\partial l}{\partial x} + \frac{\partial\psi}{\partial y}\frac{\partial l}{\partial y}\right) > 0, \quad (4)$$

is observed for synoptic objects, at least for moderate latitude, and with a grid interval of no less than 250 km [4].

Usually the last term of (4) in absolute value is considerably less than the first two terms, therefore frequently (see, for example, [8, 9]) a simpler criterion of ellipticity is used.

$$\Gamma = 2gm^2\Delta H + F \geq 0. \quad (5)$$

This work assumed criterion (5). On Fig. 1 is shown the distribution over the northern hemisphere of points with  $\Gamma < 0$  for one of the analyzed examples. The same figure represents the  $H$  field. During the calculation of  $\Gamma$  values of Laplacian  $\Delta H$  were taken with  $\delta s = 390$  km at a latitude of  $60^\circ$  (at a latitude of  $10^\circ$ , to which the extreme grid points reached, the grid interval was about 200 km). The number of grid points in which equation (1) is hyperbolic attains here 400, i.e., 18% of all grid points. In this case the overwhelming majority of these points falls in low latitudes,  $\phi < 30^\circ$ . For the belt of latitudes  $\phi > 45^\circ$  the number of points of the hyperbolicity of equation (1) is 25.

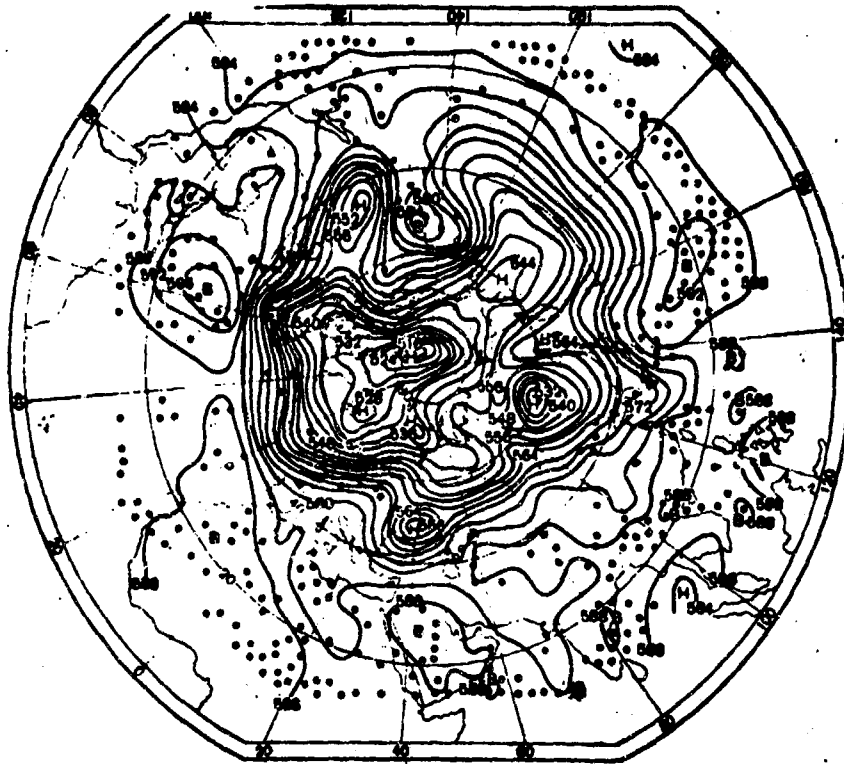


Fig. 1. Distribution of points of hyperbolicity of equation (1) for the northern hemisphere for a square grid with an interval  $\delta s = 390$  km at latitude  $\phi = 60^\circ$  and  $H_{500}$  field at 0300 17 September 1965.

As one would expect, a considerable number of points for which  $\Gamma < 0$  is connected with the central ranges of deep anticyclones (mainly, subtropical), where  $\Delta H$  Laplacians take large negative values.

It is possible to fulfill the criterion of ellipticity of (5) for all grid points by correcting the values of  $\Delta H$  in those areas where  $\Gamma < 0$ . This was done in the following manner. Assume that at point 0 (Fig. 2)  $\Gamma = \Gamma_0 < 0$ . Write criterion of ellipticity (5) in finite-difference form

$$\Gamma = 2g \frac{m^2 H}{(\delta s)^2} + P > 0 \quad (6)$$

(here  $\delta H$ , for example, at point 0 is expressed as  $(\delta H)_0 = H_1 + H_2 + H_3 + H_4 - 4H_0$ ).

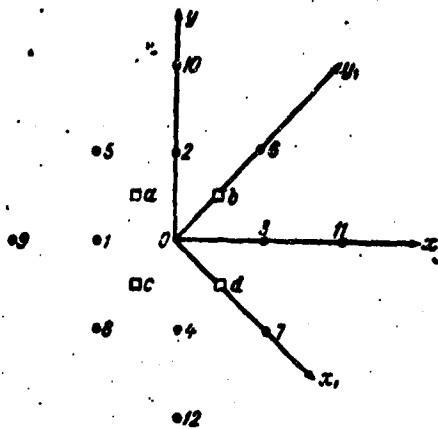


Fig. 2. Finite-difference approximation of first and second derivatives in neighborhood of point 0.

Divide both sides of (6) by  $m^2/(\delta s)^2$ . We obtain

$$\gamma = \frac{\Gamma(\delta s)^2}{m^2} - 2g\delta H + \frac{(\delta s)^2 L}{m^2} = 2g\delta H + L > 0. \quad (6a)$$

Let now  $\tilde{\gamma}_0 = 0$  be the new value of  $\gamma$  at point 0. Add to each of the values of  $\gamma_i$  ( $i = 1; 2; 3; 4$ ) the quantity  $\gamma_0/4$  and determine new values of  $\gamma_i$  at points 1-4 as  $\gamma_i = \gamma_i + (\gamma_0/4)$ . This means that the mean value of  $\gamma$  in nearest neighborhood of point 0 becomes constant.

We consider now that the values of field  $H$  at points 0, 1, 2, 3, 4 are unknown (designate them  $\tilde{H}_0$ , etc.), and determine them from the following system (see Fig. 2):

$$\left. \begin{aligned} \tilde{H}_1 + \tilde{H}_2 + \tilde{H}_3 + \tilde{H}_4 - 4\tilde{H}_0 &= \frac{1}{2g}(\tilde{\gamma}_0 - L_0) = -\frac{1}{2g}L_0; \\ \tilde{H}_0 + H_9 + H_8 + H_5 - 4\tilde{H}_1 &= \frac{1}{2g}(\tilde{\gamma}_1 - L_1); \\ \tilde{H}_0 + H_9 + H_{10} + H_6 - 4\tilde{H}_2 &= \frac{1}{2g}(\tilde{\gamma}_2 - L_2); \\ \tilde{H}_0 + H_6 + H_{11} + H_7 - 4\tilde{H}_3 &= \frac{1}{2g}(\tilde{\gamma}_3 - L_3); \\ \tilde{H}_0 + H_6 + H_7 + H_4 - 4\tilde{H}_4 &= \frac{1}{2g}(\tilde{\gamma}_4 - L_4). \end{aligned} \right\} \quad (7)$$

Solving system (7), we find new values of  $\tilde{H}_0, \tilde{H}_1, \dots, \tilde{H}_4$  such that the value of  $\gamma$  at the investigated point (point 0) is equal to zero. The described method is close to the method used by Shuman [9].

We agree to call numerical values of  $\gamma_i$  in (6a) the "hyperbolicity" at an arbitrary field point  $i$ . Experiment showed that by the examined means it is possible to blur the hyperbolicity at the given point over the nearest neighborhoods of this point. Having applied the described procedure to all points of the grid where  $\gamma_i < 0$  (except the boundary), we decrease the absolute value of both maximum hyperbolicity  $\gamma_{\text{макс}}$  and average hyperbolicity  $\gamma_{\text{ср}}$  over the whole field ( $\gamma_{\text{ср}} = \frac{\sum \gamma}{N}$ , where the summing is over all  $N$  inside field points in which  $\gamma < 0$ ) because of the more precise determination of values of  $H$  at points where earlier it was  $\gamma \geq 0$ . For a further decrease in the values of  $\gamma_{\text{макс}}$  and  $\gamma_{\text{ср}}$  it is necessary to make several circuits of the entire map.

We considered the task completed if  $|\gamma_{\text{макс}}| < 0.25$ . Note that after the first circuit of the map the quantity  $|\gamma_{\text{макс}}|$  was usually 10.0-30.0. For field  $H$  shown in Fig. 1 after the first circuit  $\gamma_{\text{макс}} = -20.3$ ,  $\gamma_{\text{ср}} = -2.75$ ; after the tenth circuit  $\gamma_{\text{макс}} = -0.23$ ;  $\gamma_{\text{ср}} = -0.02$ . In this case the maximum difference between the values of original and corrected field  $H$  did not exceed 3 decameters in even one point. The greatest corrections were necessary on low latitudes, and regions with weak meteorological treatment.

The modified field  $H$  was used as the initial field for solving the balance equation relative to  $\psi$ .

3. Let us write equation (2) in finite differences for point 0 (Fig. 2), having multiplied the left and right sides by  $(\delta s)^2/m_0^2$  ( $m_0$  - value of "distortion parameter"  $m$  at point 0). We have

$$\begin{aligned} \psi_1 + \psi_2 + \psi_3 + \psi_4 - 4\psi_0 = & -\frac{(\Delta s)^2}{m_0^2} l_0 + \sqrt{\left[\frac{(\Delta s)^2}{m_0^2} l_0\right]^2 + \dots} \\ & + \frac{(\Delta s)^2}{m_0^2} (H_1 + H_2 + H_3 + H_4 - 4H_0) + \frac{1}{4} (\psi_1 + \psi_2 - \psi_3 - \psi_4)^2 + \\ & + (\psi_1 + \psi_2 - \psi_3 - \psi_4)^2 - \frac{(\Delta s)^2}{2m_0^2} [(\psi_1 - \psi_2)(l_3 - l_1) + (\psi_1 - \psi_3)(l_1 - l_2)] \end{aligned} \quad (8)$$

(here  $\Delta s$  - value of step of grid in decameters:  $\Delta s = (\delta s) \cdot 10^2$ , where  $\delta s = 390$  km;  $l_0$  - value of Coriolis parameter at point 0). During the calculation of finite-difference models of the second derivatives  $\frac{\partial^2 \psi}{\partial x^2}$ ,  $\frac{\partial^2 \psi}{\partial y^2}$ ,  $\frac{\partial^2 \psi}{\partial x \partial y}$  first differences were used with an interval  $\sqrt{2}\delta s$  over the grid  $(x_1, y_1)$ , rotated  $45^\circ$  in comparison with the original. Thus, at point 0 we have (Fig. 2):

$$\begin{aligned} \frac{\partial^2 \psi}{\partial x_1^2} &= \frac{\partial}{\partial x_1} \frac{\psi_d - \psi_a}{\sqrt{2}\delta s} = \frac{\psi_b + \psi_c - 2\psi_0}{2(\delta s)^2}, \\ \frac{\partial^2 \psi}{\partial y_1^2} &= \frac{\partial}{\partial y_1} \frac{\psi_e - \psi_c}{\sqrt{2}\delta s} = \frac{\psi_1 + \psi_2 - 2\psi_0}{2(\delta s)^2}, \\ \frac{\partial^2 \psi}{\partial x_1 \partial y_1} &= \frac{\partial}{\partial x_1} \frac{\psi_b - \psi_c}{\sqrt{2}\delta s} = \frac{\psi_3 - \psi_4 - \psi_5 + \psi_6}{2(\delta s)^2}. \end{aligned} \quad (9)$$

Such a recording of the second derivatives is close to "method C" analyzed in [8]. It is the finite-difference expressions of first derivatives of type  $\frac{\partial \psi}{\partial x}$ ,  $\frac{\partial \psi}{\partial y}$  ( $q = x, y$ ) taken with an interval of  $2\delta s$ , Laplacian  $\Delta H$  with an interval of  $\sqrt{2}\delta s$ , Laplacian  $\Delta \psi$  in the left side of (8) with an interval of  $\delta s$ .

For calculations from formula (8), furthermore, it was convenient to multiply both sides of the equation by  $10^{-4}$ , considering new function  $\psi^* = \psi \cdot 10^{-4}$ . The value of function  $\psi^*$  in  $\text{dam/s}^2$ , as is simple to see, for example, from expression  $\psi^* = \frac{\tilde{\kappa} \cdot 10^{-4}}{l} H$  ( $\tilde{\kappa} = 0.98 \text{ dam/s}^2$ ), has the same order of magnitude as the values of  $H$  in decameters.

To solve system of equations (8) in all inside points of the grid the extrapolated Liebmann method was applied, modified in the following manner. Namely, the series approximations  $\psi^1$ ,  $\psi^2$ ,  $\psi^3$ , etc., developing in the solution process, were substituted in the right sides of equations (8), not every time, but only after the fulfillment of some fixed number of iterations  $N$ . We took  $N = 10$ . Thus new fields  $F$  were formed after the 10, 20, 30th, etc., iteration, and the entire process of calculation consisted of two

cycles "imbedded" in one another. Calculations were conducted up to the achievement of the final accuracy of  $\delta$ , in other words,

it was necessary that  $\left| \frac{1}{\delta} (\psi^{(k+1)} - \psi^{(k)}) \right| < \delta$ .

This technology of solving system of equations (8) is close to the "accelerated" method (fast method), given in work [8, 9]. For an accuracy of  $\delta = i$  dam it was necessary, as a rule, to have 80-100 iterations (the field of right sides was calculated only 8-10 times). This calculation occupied about 30 minutes of machine time.

In the course of a solution in all grid points where the subradical expression in formulas (8) is less than zero (observance of criterion (5) leaves this possibility), it is equated to zero. It was clarified that the number of points in which it is necessary to produce this correction is, as a rule, 150-200 (7-9% of all grid points), moreover these points are distributed mainly on belt of low latitudes. This effect can be connected with the fact that in low latitudes the term  $2m^2 \left( \frac{\partial^2}{\partial x^2} \frac{\partial l}{\partial x} - \frac{\partial^2}{\partial y^2} \frac{\partial l}{\partial y} \right)$  in the subradical expression in the right side of equation (2) sometimes acquires large positive values. It is possible that a correction of field  $H$  in accordance with criterion of ellipticity (4), instead of (5), would bring down the number of points in which an artificial change in the size of the subradical expression is required.

We must note one circumstance leading to a reduction of the rate of convergence during calculation for low latitudes. As experiment showed, the calculated values of  $\psi^*$ , numerically equal in the geostrophic approach to values  $H$  dam, in the quasi-solenoidal approach seem, as a rule, more than  $H$ . This one can be seen well in Fig. 3. In moderate and high latitudes  $\psi^*$  gradients are less than  $H$  gradients, but in low latitudes, under condition (3), fixing values of  $\psi^*$  on the boundary,  $\psi^*$  gradients grow in comparison with  $H$  gradients. Such a configuration of field  $\psi^*$  in low latitudes leads to a drop in the rates of convergence of the iteration process (in comparison with the initial, geostrophic, approach).

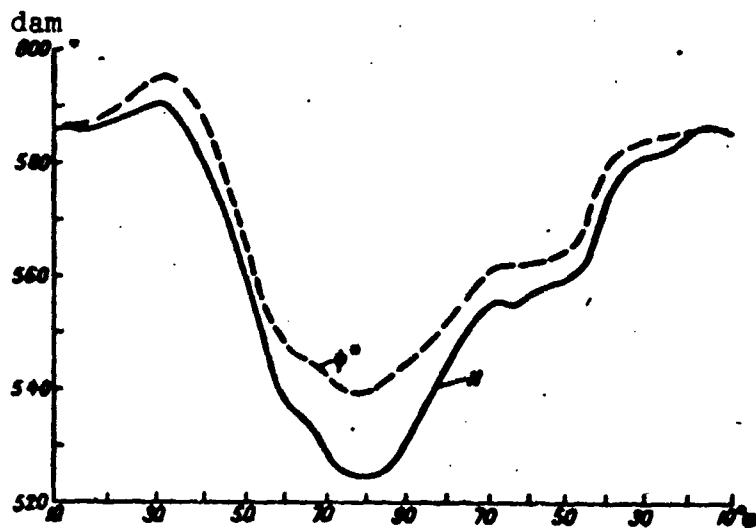


Fig. 3. Cut along 45° west longitude and 135° east longitude for the  $H_{500}$  field at 0300 17 September 1965 and the  $\psi^*$  field, obtained by solving the balance equation.

4. Let us stop at the question about the inversion of the balance equation. Inasmuch as equation (1) relative to function  $H$  is Poisson equation, its numerical solution does not represent difficulty. Multiply equation (1) by  $l/m^2g$ , exchange the left and right sides and write it in finite-difference form (see Fig. 2)

$$\begin{aligned}
 H_1 + H_2 + H_3 + H_4 - 4H_0 &= \frac{\tilde{l}}{2\pi} (\psi_1^2 + \psi_2^2 + \psi_3^2 + \psi_4^2 - 4\psi_0^2) - \\
 - \frac{m^2}{2g(\Delta x)^2} &[(\psi_1^2 + \psi_2^2 - \psi_3^2 - \psi_4^2)^2 - (\psi_1^2 + \psi_2^2 - 2\psi_0^2)(\psi_3^2 + \psi_4^2 - 2\psi_0^2)] + \\
 + \frac{1}{4\tilde{g}} &[(\psi_1^2 - \psi_2^2)(\tilde{l}_1 - \tilde{l}_2) + (\psi_3^2 - \psi_4^2)(\tilde{l}_1 - \tilde{l}_2)]. \quad (10)
 \end{aligned}$$

Here  $\tilde{l} = l \cdot 10^4$ ;  $\tilde{g} = 0.98 \text{ dam/s}^2$ ;  $\psi^* = \psi \cdot 10^{-4}$ ; expressions  $\frac{\partial^2}{\partial x^2}$ ,  $\frac{\partial^2}{\partial y^2}$ ,  $\frac{\partial^2}{\partial x \partial y}$  are solved according to formulas (9). A system of equations of form (10) we solve by the extrapolated Liebmann method. To achieve an accuracy of  $\delta_0 = 0.5 \text{ dam}$ , as a rule about 10 iterations are necessary. Inversion of the balance equation after a forecast for 24, 48 and 72 hours occupies in overall complexity about 10 minutes of machine time.

Inversion of the balance equation was used also in the next experiment. A system of equations of form (8) was solved relative to  $\psi^*$ , and in terms of the found values the inversion immediately was executed according to formulas (10). The inverted field must, generally speaking, completely repeat the original field  $H$  (except those points in which either the criterion of ellipticity (5) was not executed, or subradical expressions in (8) were equated to zero). The absence of iteration indicates either deficiencies of the finite-difference recording of (8) or (10), or inaccuracy in the direct or inverse solution of the balance equation.

Comparison of the profiles of original and inverted  $H$  fields shows that the agreement is entirely satisfactory.

5. A finite-difference system of barotropic prediction of the geopotential on the northern hemisphere in the quasi-geostrophic approach is described in [2]. This system was used by the authors to forecast the values of stream function  $\psi^*$ , obtained as a result of solving the balance equation. The balance equation was inverted following formula (10). In Fig. 4 are given the contours of the area for which the forecasts were made by the system (grid interval  $\delta s = 390$  km at latitude  $60^\circ$ ), and the  $H_{500}$  forecast field for 1500 hours, 10 October 1961, calculated 48 hours in advance by original data from 1500 hours, 8 October 1961. For comparison Fig. 5 shows the  $H_{500}$  field forecast on a quasi-geostrophic model, and in Fig. 6 the actual  $H_{500}$  field in the same period.

The amount of mean relative error was calculated for 19 points evenly distributed over European territory of the USSR: for the quasi-geostrophic forecast for the given period  $\epsilon = 0.75$ , and for the quasi-solenoidal -  $\epsilon = 0.68$ .

Comparison of quasi-geostrophic and quasi-solenoidal forecasts calculated on a barotropic model for the northern hemisphere allows hoping that during tests of quasi-solenoidal forecasts under operative conditions satisfactory results will be achieved.

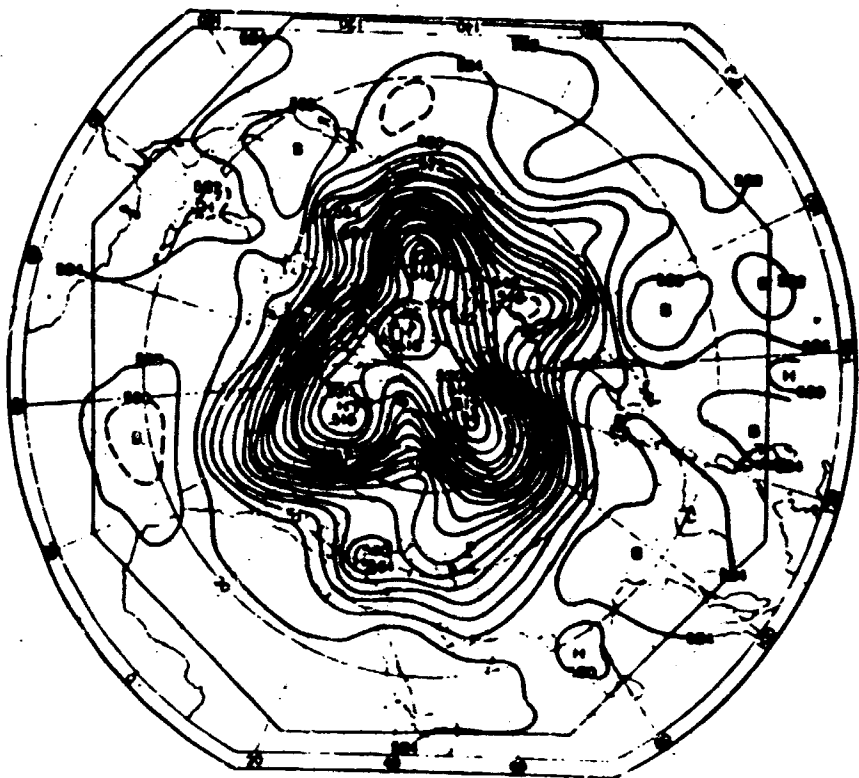


Fig. 4.  $H_{500}$  forecast map for 1500 hours, 10 October 1961 based on original data for 1500 hours, 8 October 1961, calculated according to a quasi-solenoidal model. A continuous line shows the contours of the area for which the forecast was made.

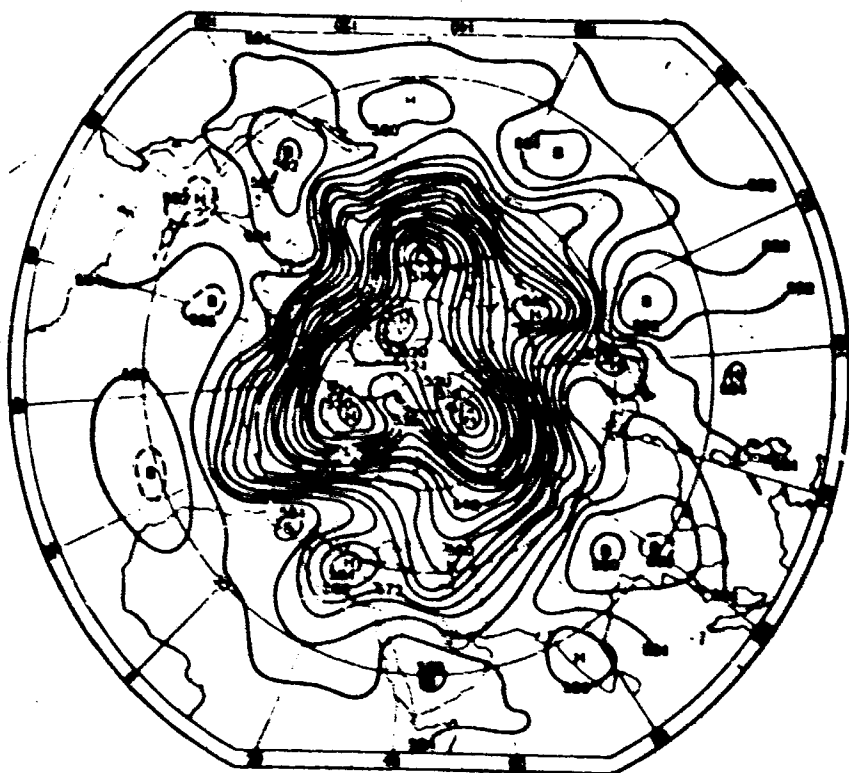


Fig. 5.  $H_{500}$  forecast map for 1500 hours, 10 October 1961 according to original data from 1500 hours, 8 October 1961, calculated according to a quasi-geostrophic model.



Fig. 6. Actual  $H_{500}$  map for 1500 hours,  
10 October 1961.

#### Bibliography

1. Dzhabar-Zade R. M. Ob odnom metode prognoza meteoelementov pri gipoteze kvazisoloidal'nosti (One method of forecasting meteorological elements using the hypothesis of quasi-solenoidality). Tr. TsIP, vyp. 106, 1960.
2. Sitnikov I. G., Fuks-Rabinovich M. S. O vospolnenii nedostayushchey informatsii v pole geopotentsiala dlya obshirnykh maloosveshchennykh rayonov severnogo polushariya (Supplementing insufficient information in the geopotential field for extensive badly treated areas of the northern hemisphere). Tr. MMTs, vyp. 10, 1965.
3. Turyanskaya N. G. Ispol'zovaniye solenoidal'noy sostavlyayushchey vetra v prognosticheskikh skhemakh diya prognoza geopotentsiala (Utilization of the solenoid component of wind in forecast systems for forecasting the geopotential). Tr. TsIP, vyp. 146, 1965.
4. Yudin M. I. Novyye metody i problemy kratkosrochnogo prognoza pogody (New methods and problems in short-range weather forecasting). Gidrometeoizdat, L., 1963.

5. Yudin M. I. and Vulis I. L. Primeneniye statisticheskikh metodov k issledovaniyu konechno-raznostnoy struktury uravneniya balansa (Applying statistical methods to the investigation of the finite-difference structure of the balance equation). Izv. AN USSR, ser. geofiz., No. 1, 1964.

6. Bolin B. An Improved Barotropic Model and Some Aspects of Using the Balance Equation for Three-dimensional Flow. Tellus, Vol. 8, No. 1, 1956.

7. Bring A. and Charasch E. An Experiment in Numerical Prediction with Two Non-geostrophic Models. Tellus, Vol. 10, No. 1, 1958.

8. Miyakoda K. Numerical Solution of Balance Equation. Collected Meteorological Papers, Vol. 10. No. 1-2, Tokyo, 1960.

9. Shuman F. G. Numerical Methods in Weather Prediction: I. The Balance Equation. Monthly Weather Review, Vol. 85, No. 10, 1957.

THE INVESTIGATION OF HEATING IN THE STRATOSPHERE  
USING NUMERICAL EXPERIMENTS<sup>1</sup>

B. Barg and S. A. Mashkovich

The evolution of temperature perturbation in the stratosphere is studied. The initial equations were proposed by A. S. Dubov [1] for forecasting in the stratosphere. The question about the original temperature perturbation is considered. A finite-difference approximation of equations is stated, a numerical method of solving the problem is formulated, and its calculating stability is investigated. Results of calculations for different variants of the initial temperature perturbation are presented.

From literature it is known that at the end of winter as well as in the beginning of spring in the stratosphere there can be sudden warming trends. This phenomenon, discovered by Sgherhag [10] and known by the name "Berlin phenomenon," was then confirmed by further observations and became the object of numerous investigations (see, for example, [6, 9]).

The majority of investigations were in first place to establish possible reasons for these warming trends. This work does not consider these questions and primary attention is given an attempt

---

<sup>1</sup>The present article is the result of the joint work of the Institute for the Study of Large-Scale Weather of the GDR Weather Service and Hydrometeorologic Center of the USSR.

to study the evolution of the warming trend and its values. In other words, it assumes that temperature perturbation in the stratosphere is suitably described by a priore methods, and its further development requires the use of hydrodynamic equations. Outwardly such an investigation is similar with the work of Khinkel'man [4], Berkovskiy and Shapiro [7].

However, in contrast with the investigations in [7] we limit ourselves to an examination of processes in the stratosphere. Therefore we can use the work of Dubov [1], in which approximate forecast equations for layers of the atmosphere with a high statistical stability are obtained, i.e., equations which are suitable for dynamic examination of stratospheric processes. One ought likewise to show that results obtained in [1] allow sufficiently accurate passing from equations in a three-dimensional space to equations for a two-dimensional case. This circumstance from a mathematical point of view is essential, since it noticeably facilitates calculations.

According to Dubov [1], we will begin from the following equations:

$$\Delta \frac{\partial z}{\partial t} = -\frac{g}{l}(z, \Delta z) - \beta \frac{\partial z}{\partial x} - \frac{g l}{R T_{10}}(T, z) \quad (1)$$

$$\Delta \frac{\partial T}{\partial t} = -\frac{g}{l} \left[ (T, \Delta z) + (z, \Delta T) + \frac{l \beta}{g} \frac{\partial T}{\partial x} \right] \quad (2)$$

Here and subsequently we accept the designations:  $z$  - height of considered isobaric surface,  $T$  - temperature on this surface,  $g$  - acceleration of gravity,  $l$  - Coriolis parameter,  $\beta$  - Rossby parameter,  $\Delta$  - Laplace operator,  $(e, d)$  - Jacoby operator,  $\gamma_a$  - dry adiabatic gradient,  $\alpha$  - radius of earth.

#### Initial Conditions

If equations (1), (2) are used to solve the model problem, then it is hardly expedient to use as initial conditions the data of observations for practical synoptic situations. It is more useful

to use a problem which gives the initial fields of meteorological elements in the simplest form. How must the basic fields, and consequently, the initial conditions look?

A good correspondence to actual conditions would hardly be achieved if mean maps, for example mean monthly maps, would be used as these fields. It is known that in averaging important parts of a field are lost, such as the intensity of stratospheric polar eddy. It is possible to approximate more the practical relationships in the atmosphere if we suitably stylize the determined observable typical states.

To do this the chart shows profiles of the geopotential and temperatures for 50 mbar along a definite meridian at 0000 hours Greenwich time for 5, 16 and 17 January 1958 (Fig. 1).

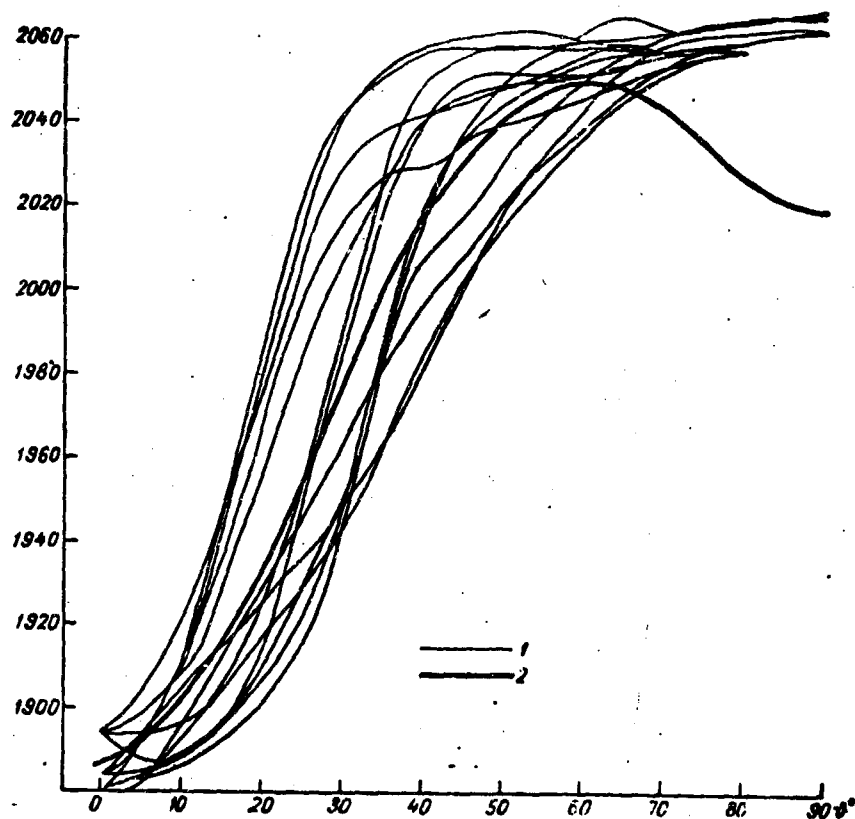


Fig. 1. Approximation of  $H_{50}$  meridian profile with the aid of formula (6). 1 - meridian distribution by data of observations; 2 - distribution calculated by formula (6).

Let us present now the observed profiles using an analytic expression. If we do not require that the approximation be the best, then there are definite degrees of freedom which one could use.

From observations which must generally describe the polar vortex, it is possible to borrow the following facts:

- a. At the pole wind velocity is zero.
- b. Wind velocity turns into zero between the equator and 30° north latitude.
- c. Maximum wind velocity is between 60 and 75° north latitude (in our formulas it will be accepted that the maximum lies at 60° north latitude).
- d. Undisturbed wind velocity has only zonal component  $u$ .

These assumptions, and also the assumption that the initial undisturbed field depends on longitude  $\lambda$ , allow selecting for wind velocity a parabolic profile

$$u = c(\theta - \theta_1)(\theta - \theta_2), \quad (3)$$

where  $u$  is the zonal wind velocity,  $\theta$  - polar angle,  $\theta_1 = 0^\circ$ ;  $\theta_2 = 60^\circ = 2\theta_{\text{max}}$ ;  $\theta_{\text{max}} = 30^\circ$ .

From expression (3) follows

$$u = c_1\theta^2 + c_2\theta; \quad c_1 = -\frac{u_{\text{max}}}{\theta_{\text{max}}^2}; \quad c_2 = \frac{2u_{\text{max}}}{\theta_{\text{max}}}. \quad (4)$$

Applying the formula for geostrophic wind

$$u = \frac{g}{f} \frac{1}{a} \frac{\partial z}{\partial \theta}, \quad (5)$$

we obtain from (4) the expression for the height of the 50 mbar isobaric surface

$$z = \frac{a}{g} 2\omega c_1 |(\theta^2 - 2)\sin \theta + 2\theta \cos \theta| + c_2 [\theta \sin \theta - \cos \theta] + z_0 \quad (6)$$

( $z$  is expressed in decameters,  $z_0 = 820$  dam).

In Fig. 1 it is evident that the selected parabolical meridian wind profile will give a distribution of  $H_{50}$  which agrees well with the data of observations. Such means can also obtain the expression for approximation of temperature. From examination of the field it is evident that the investigation must embrace the range from the pole to  $\theta = 60^\circ$ . Accordingly the temperature field we will approximate also in the zone between  $\theta = 0^\circ$  and  $\theta = 60^\circ$ ; in this case the formula for temperature distribution has the form

$$T = t_0 + A \cos 3,5\theta + 273^\circ. \quad (7)$$

where  $t_0 = -70^\circ$ ,  $A = 12^\circ$ . As can be seen from Fig. 2, this approximation is sufficiently accurate.

These expressions approximate undisturbed basic fields. In accordance with our original thesis we assume that local temperature perturbation can be arbitrary. From systematical considerations before we describe how this perturbation is assigned, we will give certain information from the technology of a numerical solution. On a map of the northern hemisphere in stereographic projection (with the section covering  $60^\circ$  north latitude) is imposed a regular grid with  $42 \times 42$  points (Fig. 3). The pole does not coincide with the grid point, but is in the central point of the grid. Grid interval  $s$  is 330 km at  $60^\circ$  north latitude. This regular grid is used as the system of coordinates. In this instance temperature perturbation  $T^*$  can be given by the formula

$$T^* = A^* \cos\left(B^* \frac{2\pi}{36} r^*\right) + K^*, \quad r^* = \sqrt{(x - x_s)^2 + (y - y_s)^2}. \quad (8)$$

Here  $x_s, y_s$  - coordinates of the center of the temperature perturbation, expressed in units of length equal to the grid interval;  $A^*, B^*, K^*$  - arbitrary constants,  $r^*$  - radius of temperature perturbation, likewise expressed in grid intervals.

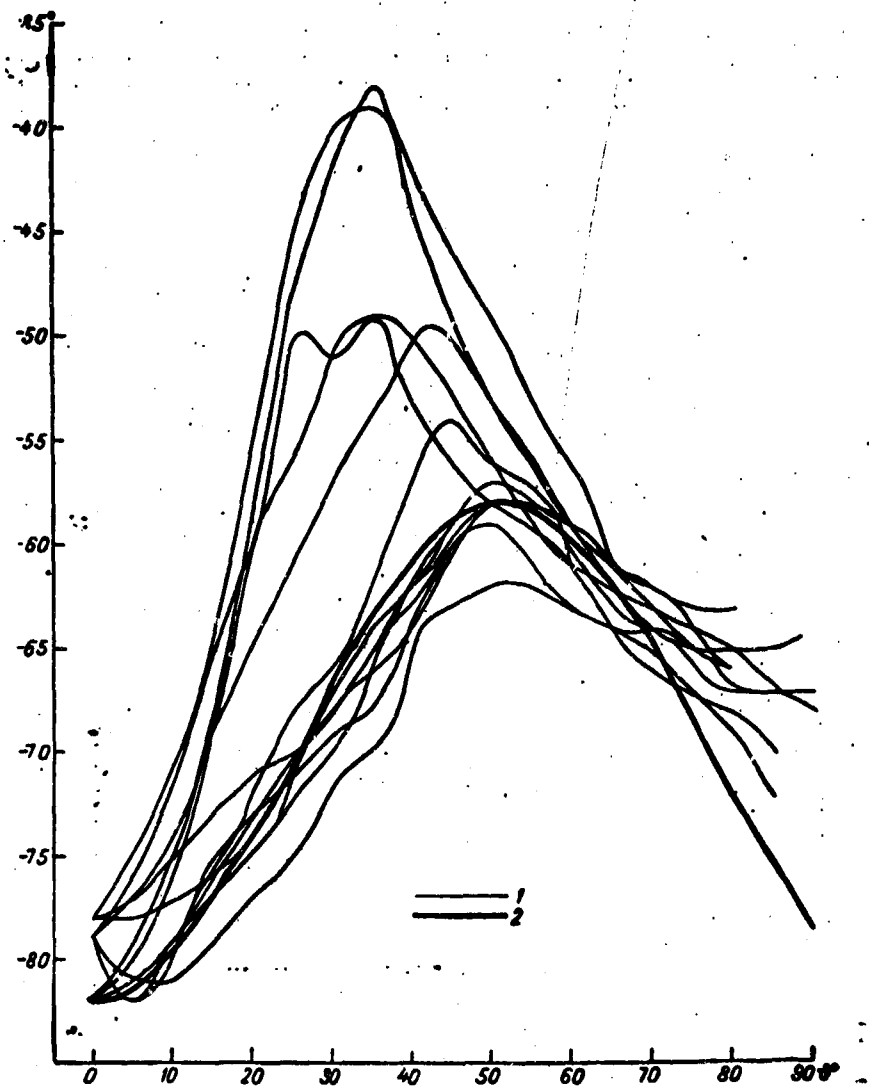


Fig. 2. Approximation of meridian of temperature profile on 50 mbar isobaric surface. 1 - temperature profile from the data of observations; 2 - profile calculated by formula (7).

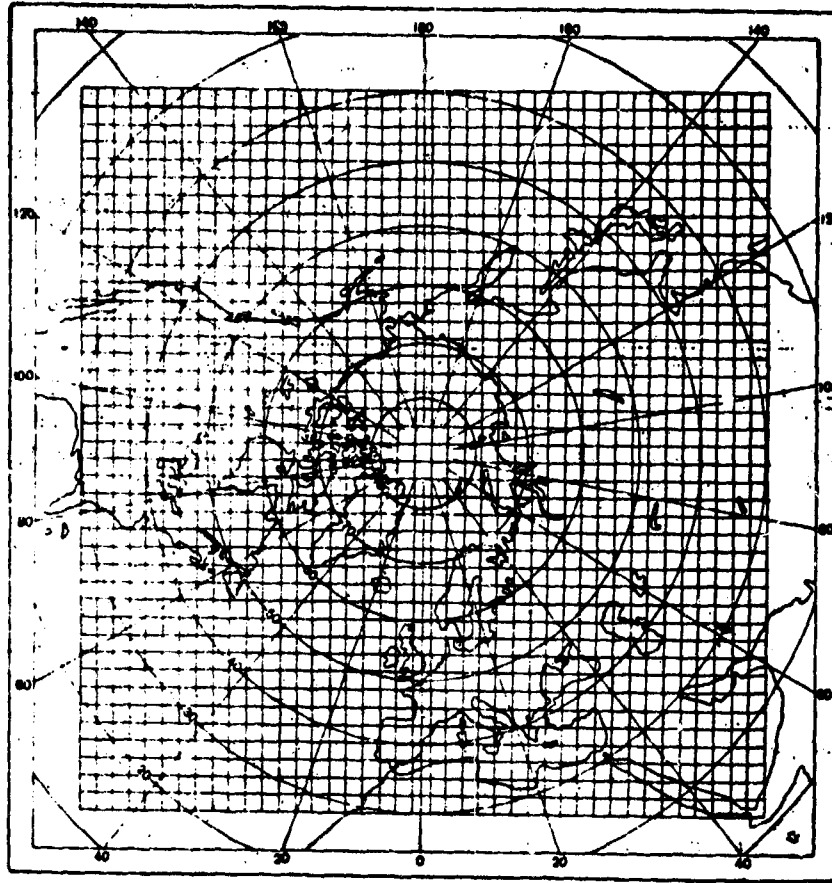


Fig. 3. Regular grid used for calculations.

From formula (8) it is evident that perturbation has a circular formula relative to a regular grid (on the spherical earth it acquired a pear shape). The perturbation lies so that it would be as far as possible from the edges of the considered area on which artificial boundary conditions are assigned ( $\partial z/\partial t$  or  $\partial T/\partial t$  equal to zero).

Approximation of Derivatives in Time.  
Stability Analysis of Solution

When selecting a numerical method for solving the problem at hand, an important question is the finite-difference approximation of derivatives in time. Therefore it is useful to estimate the accuracy of the solution with different means of approximation of these derivatives. Such estimates can be obtained by comparing

an accurate solution with the numerical. For the above problem it is possible to find an accurate solution in the case of initial conditions of a special form. Below is stated the means of obtaining the accurate solution and this accurate solution is compared with the numerical with different variants of approximation of the derivative in time.

We will consider quasi-solenoidal motion and assume that stream function  $\psi$  is connected to geopotential  $z$  by the following approximate relationship:

$$\psi \approx \frac{1}{2} z. \quad (9)$$

Then the system of equations of our problem in spherical coordinates is written in the form

$$\begin{aligned} \frac{\partial \Delta T^*}{\partial t} &= - \frac{1}{a^2 \sin^2 \theta} [(T^*, \Delta \psi) + (\psi, \Delta T^*)] - 2\omega \frac{\partial T^*}{\partial \lambda}; \\ \frac{\partial \Delta \psi}{\partial t} + \frac{1}{a^2 \sin^2 \theta} (\psi, \Delta \psi) + 2\omega \frac{\partial \psi}{\partial \lambda} &= \frac{4g}{(\gamma_0 - \gamma) R^2 \sin^2 \theta} (\psi, T^*), \end{aligned} \quad (10)$$

where  $T = 2T^*$ .

We assume that the stream function and temperature function can be presented as the sum of two components: zonal (not depending upon geographical longitude and time) and nonzonal. Then we write that

$$\begin{aligned} \psi(\theta, \lambda, \zeta, t) &= \bar{\psi}(\theta, \zeta) + \psi'(\theta, \lambda, \zeta, t); \\ T^* &= \bar{T}^*(\theta, \zeta) + T^{*'}(\theta, \lambda, \zeta, t). \end{aligned} \quad (11)$$

Zonal component  $\bar{\psi}$  we represent by the formula

$$\bar{\psi} = \psi_0(\zeta) - \alpha(\zeta) a^2 \cos \theta, \quad (12)$$

where  $\alpha$  - index of circulation. Then from the equation of statics and of relationships (9) we obtain the following expression for the zonal component of temperature:

$$\bar{T}^* = - \frac{\zeta}{R} \left( \frac{d\psi_0}{d\zeta} - a^2 \cos \theta \frac{d\alpha}{d\zeta} \right). \quad (13)$$

Writing  $T^*$  for the level ( $\zeta = \zeta_1$ ) of interest, we obtain

$$T^*|_{k-\zeta} = c_1 - c_2 \cos \theta, \quad (14)$$

where

$$c_1 = -\frac{\zeta_1}{R} \left( \frac{d\psi_0}{dt} \right)_{k-\zeta}; \quad c_2 = -\frac{\zeta_1}{R} a^2 \left( \frac{d\psi_0}{dt} \right)_{k-\zeta}.$$

Let us substitute now relationships (11), (12), (14) in equations (10):

$$\begin{aligned} \frac{\partial \Delta T^*}{\partial t} &= -\frac{c_2}{a^2} (2 + \lambda) \frac{\partial \psi'}{\partial \lambda} - 2(\alpha + \omega) \frac{\partial T^*}{\partial \lambda} - 2 \frac{\partial \Delta T^*}{\partial \lambda} - \\ &\quad - \frac{1}{a^2 \sin \theta} [(T^*, \Delta \psi') + (\psi', \Delta T^*)]; \\ \frac{\partial \Delta \psi'}{\partial t} + 2 \frac{\partial \Delta \psi'}{\partial \lambda} + k_1 \frac{\partial \psi'}{\partial \lambda} + \frac{1}{a^2 \sin \theta} (\psi', \Delta \phi') &= \\ = k_2 \frac{\partial T^*}{\partial \lambda} + \frac{Fg}{(\gamma_0 - \gamma) R T_1 \sin \theta} (\psi', T^*), \end{aligned} \quad (15)$$

where

$$\begin{aligned} k_1 &= 2(\alpha + \omega) + \frac{(k_2 - 2\omega T^*) Fg}{(\gamma_0 - \gamma) R T_1}, \\ k_2 &= \frac{(\omega) Fg}{(\gamma_0 - \gamma) R T_1}. \end{aligned}$$

We accept subsequently that  $k_1$  and  $k_2$  can be approximately considered constants.

We assume that in initial moment  $t = 0$  the nonzonal parts of stream function  $\psi'$  and temperature  $T^*$  are represented by the formulas:

$$\begin{aligned} \psi'|_{k-\zeta} &= \operatorname{Re} A_n e^{im\lambda} P_n^m(\theta), \\ T^*|_{k-\zeta} &= \operatorname{Re} B_n e^{im\lambda} P_n^m(\theta), \end{aligned} \quad (16)$$

where  $P_n^m$  is an adjoint Legendre polynomial.

Accordingly look for the solution of system (15) in the form:

$$\begin{aligned}\psi &= \operatorname{Re} A(t)e^{i\omega t} P_n^{(0)}(\theta), \\ T' &= \operatorname{Re} B(t)e^{i\omega t} P_n^{(0)}(\theta).\end{aligned}\quad (17)$$

Having substituted (17) and (15), we obtain the usual linear differential equations in time:

$$\begin{aligned}y \frac{dA}{dt} + (\alpha y - k_1) A - i m k_2 B &= 0, \\ y \frac{dB}{dt} - \frac{c_2}{\sigma^2} (2 - y) A + [2(\alpha + \omega) - \alpha y] B, \\ y &= n(n + 1).\end{aligned}\quad (18)$$

It is easy to see that the solution of system (18) can be obtained in analytical form. Namely, let:

$$A = A_1 e^{i\sigma t}, \quad B = B_1 e^{i\sigma t}.\quad (19)$$

Substitution of (19) into (18) gives:

$$\begin{aligned}\frac{c_2}{\sigma^2} (2 - y) A_1 - [y\sigma - 2(\alpha + \omega) + \alpha y] B_1, \\ (k_1 + \alpha y - y\sigma) A_1 - k_2 B_1.\end{aligned}\quad (20)$$

Equating to zero the determinant of system (20), we obtain the characteristic equation for determination of  $\sigma$

$$\sigma^2 - p\sigma + q = 0,\quad (21)$$

where

$$\begin{aligned}p &= \frac{1}{y} (\alpha + 2\omega + \alpha y + k_1), \\ q &= \frac{k_2 c_2}{(\alpha y)^2} (2 - y) + \frac{(\alpha y + k_1)(y - 2(\alpha + \omega))}{y}.\end{aligned}$$

Consequently, the solution of equations (15) is written in the form:

$$\begin{aligned}\psi &= \operatorname{Re} (\tilde{A} e^{i\omega t + i\sigma^{(1)} t} + \tilde{A} e^{i\omega t + i\sigma^{(2)} t}) P_n^{(0)}(\theta), \\ T' &= \operatorname{Re} (\tilde{k} \tilde{A} e^{i\omega t + i\sigma^{(1)} t} + \tilde{k} \tilde{A} e^{i\omega t + i\sigma^{(2)} t}) P_n^{(0)}(\theta),\end{aligned}\quad (22)$$

where  $\tilde{k} = \frac{1}{k_2} [k_1 - y(\alpha - \sigma)]$ ;  $\sigma^{(1)}$  and  $\sigma^{(2)}$  - roots of the characteristic equation;  $\sigma^{(j)} = \sigma_1^{(j)} + i\alpha_2^{(j)}$ .

Let us go now to the solution of system (18) by the numerical method. Namely, let us examine two variants of approximation: 1) *explicit* scheme with replacement of derivatives in time by "forward" differences, 2) *implicit* scheme.

In the first variant derivatives in time are represented in the form:

$$\frac{dA}{dt} = \frac{A^{t+\Delta t} - A^t}{\Delta t}; \quad \frac{dB}{dt} = \frac{B^{t+\Delta t} - B^t}{\Delta t}, \quad (23)$$

and all remaining terms in equations (18) are written for preceding instant  $t$ . We set

$$A = A_2 e^{i\omega t}; \quad B = B_2 e^{i\omega t}. \quad (24)$$

Then considering expressions (23) and (24) equations (18) will take the form:

$$\begin{aligned} y(e^{i\omega\Delta t} - 1)A_2 &= -im\Delta t[k_2 B_2 - (k_1 - ay)A_2]; \\ y(e^{i\omega\Delta t} - 1)B_2 &= -im\Delta t \left\{ -\frac{z_2}{\sigma^2} (2 - y)A_2 + [zy - 2(a + \omega)]B_2 \right\}. \end{aligned} \quad (25)$$

From (25) can be obtained the following equation for determination of  $B_2/A_2$ :

$$\left(\frac{B_2}{A_2}\right)^2 - \frac{k_1 - 2z_2 - \omega}{k_2} \frac{B_2}{A_2} + \frac{z_2}{k_2 \sigma^2} (2 - y) = 0. \quad (26)$$

The quantity  $B_2/A_2$  can be both real and complex. Let us write down the expression for  $B_2/A_2$  in the form

$$\left(\frac{B_2}{A_2}\right) = \overset{\circ}{f}_1 = f_1 i; \quad f_1 > 0. \quad (27)$$

while

$$\overset{\circ}{f}_1 = f_1 \quad \text{when} \quad f_1 \neq 0.$$

Substituting (27) in (25) and separating real and imaginary parts, we obtain after simple transformations:

$$e^{-\frac{U}{v_2} \delta t} = \left(1 \pm \frac{m \delta t k_2 f_2}{y}\right)^2 + \frac{(m \delta t)^2 (k_2 f_2 - k_1 + \alpha y)^2}{y^2}; \quad (28)$$

$$\operatorname{tg} v_2 \delta t = - \frac{m \delta t (k_2 f_2 - k_1 + \alpha y)}{y \pm m \delta t k_2 f_2}; \quad (29)$$

$$v = v_1 + \delta v_2. \quad (30)$$

It is obvious that when

$$e^{-\frac{U}{v_2} \delta t} = \left(1 + \frac{m \delta t k_2 f_2}{y}\right)^2 + \frac{(m \delta t)^2 (k_2 f_2 - k_1 + \alpha y)^2}{y^2},$$

we have  $\frac{U}{v_2} < 0$  and, consequently, in accordance with (29), (30) amplitude grows in time.

Let us examine now the solution in the case of the implicit scheme. In this variant derivatives in time also are approximated by the formula (23), however all remaining terms of (18) are written for the subsequent moment of time  $t + \delta t$ . Using (23) and (24), we can write system (18) in the form:

$$\begin{aligned} [y - im(k_1 - \alpha y) \delta t] A_2 + im k_2 \delta t B_2 &= y A_2 e^{-i \delta t}; \\ [y + im \delta t (\alpha y - 2(\alpha + \omega))] B_2 - \frac{\epsilon_2}{\alpha^2} (2 - y) m \delta t A_2 &= y B_2 e^{-i \delta t}. \end{aligned} \quad (31)$$

From (31) we obtain the equation for the determination of  $B_2/A_2$ , completely coinciding with (26). Making use of expression (27), after simple transformations

$$e^{-\frac{U}{v_2} \delta t} = \left(1 \pm \frac{m \delta t k_2 f_2}{y}\right)^2 + \frac{(m \delta t)^2 (k_2 f_2 - \alpha y - k_1 f_1)^2}{y^2}. \quad (32)$$

Obtained formulas allow evaluating the accuracy of the numerical solution. For this let us compare results of calculation for accurate solution of (17) and (19) with calculations from formulas (28) and (32).

Calculations were produced for the following values of parameters:  $\delta t = 1$  hour,  $T_{cp}^* = 200^\circ$ ,  $\bar{T}_1 = 250^\circ$ ,  $\gamma = 0$ ,  $m = 1$ ,  $n = 2, 5, 10$ . Very important is the selection of the values of circulation index and its derivative in the vertical coordinate. The last

quantity is substantially different in different seasons. Inasmuch as sudden warming trends in the stratosphere are observed predominantly at the end of winter and beginning of spring, the value  $da/dz$  referred to this time of year was taken, namely

$$\frac{da}{dz} = -a.$$

Results of calculations are presented in Table 1. The table shows quantities characterizing the change in wave amplitude in the time interval  $\delta t = 1$  hour. In the case of an accurate solution there exist only real roots of characteristic equation (21), i.e.,  $\frac{\omega}{\sigma_2} = 0$ , therefore wave amplitude does not change in time. With the numerical solution method there appear changes of amplitude in time. These changes seem greatest for small values of  $n$ , so for  $n = 2$  in the hourly interval amplitude changes by 0.3% of the initial amount. Using "forward" differences there is a growth of amplitude; this variant of solution seems unstable in calculations. In the case of the implicit scheme, stable in calculations, a decrease of amplitude in time is noted.

Table 1.

n	Accurate solution		"Forward" difference		Implicit scheme	
	(1) $\exp(-\gamma_2 \delta t)$	(2) $\exp(-\gamma_2 \delta t)$	(1) $\exp(-\gamma_2 \delta t)$	(2) $\exp(-\gamma_2 \delta t)$	(1) $\exp(-\gamma_2 \delta t)$	(2) $\exp(-\gamma_2 \delta t)$
2	1.0	1.0	1.0030	1.0014	0.9970	0.9986
5	1.0	1.0	1.0008	1.0000	0.9992	1.0000
10	1.0	1.0	1.0001	1.0000	0.9999	1.0000

#### Calculation System

Passage to a Cartesian system of coordinates is carried out. A scale factor is introduced by the formula

$$m = \frac{\alpha(1 + \rho^2)}{2\alpha}. \quad (33)$$

where  $c = a(1 + \sin \varphi_0)$ ;  $\rho = \frac{r}{c}$ ;  $\varphi$  - geographical latitude on which the plane of projection lies;  $r$  - distance of considered point from the pole in the plane of projection.

The Laplace operator in the right sides of (1) and (2) is approximated by the expression

$$\Delta z \approx \frac{1}{2s^2} [z_1 + z_2 + z_3 + z_4 + \frac{1}{2}(z_5 + z_6 + z_7 + z_8) - 6z_0]. \quad (34)$$

The arrangement of points is shown in Fig. 4. Terms in the Jacobian are represented in the form

$$\frac{\partial \alpha}{\partial x} \frac{\partial \beta}{\partial y} \approx \frac{1}{8s} [a_0 - a_1 + 2(a_2 - a_3) + a_4 - a_5] \frac{1}{8s} [\beta_0 - \beta_1 + \dots]. \quad (35)$$

We introduce the designations:

$$\Delta z = \frac{1}{2s^2} \overline{\Delta z}; \quad (\alpha, \beta) = \frac{1}{(8s)^2} = \overline{(\alpha, \beta)}. \quad (36)$$

The expression of the Laplace operator in the left sides of (1) and (2) we approximate by the formulas:

$$\begin{aligned} \Delta \frac{\partial z}{\partial t} &\approx \frac{1}{s^2} \frac{1}{\delta t} (\delta z_1 + \delta z_2 + \delta z_3 + \delta z_4 - 4\delta z_0) = \frac{1}{s^2 \delta t} \overline{\Delta \delta z}, \\ \Delta \frac{\partial T}{\partial t} &\approx \frac{1}{s^2 \delta t} \overline{\Delta \delta T}, \end{aligned} \quad (37)$$

while

$$\frac{\partial z}{\partial t} \approx \frac{\delta z}{\delta t}, \quad \frac{\partial T}{\partial t} \approx \frac{\delta T}{\delta t}.$$

We will use the MTS system for all quantities except geopotential  $z$ ; we will express it in decameters. Designate  $l = l_0 \lambda$ , then equations (1) and (2) can be represented in the form:

$$\begin{aligned} \overline{\Delta \delta z} &= -\delta t s^2 \left[ \frac{1}{(8s)^2} \frac{10g}{l_0} \frac{1}{2s^2} \left( z, \frac{m^2}{\lambda} \overline{\Delta z} + \frac{l_0^2}{10g} 2s^2 \lambda \right) + \right. \\ &\quad \left. + \frac{1}{(8s)^2} \frac{g}{RT_{10}} l_0 \lambda (T, z) \right]; \end{aligned} \quad (38)$$

$$\Delta \delta T = -\delta t s^2 \left[ \frac{1}{(\delta s)^2} \frac{10g}{6} \frac{1}{2s^2} \left( T, \frac{m^2}{\lambda} \Delta z + \frac{6}{10g} 2s^2 \lambda \right) + \frac{1}{(\delta s)^2} \frac{10g}{6} \frac{1}{2s^2} \left( z, \frac{m^2}{\lambda} \Delta T \right) \right] \quad (39)$$

where  $\delta t = \frac{86400}{n}$ ,  $n$  - number of time intervals in a twenty-four hour period.

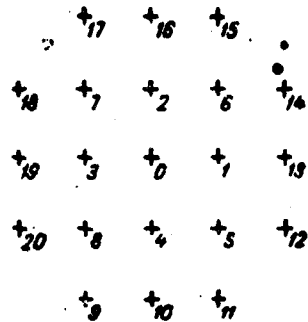


Fig. 4. Arrangement of points in the calculation of Laplace and Jacoby operators.

The solution of equations proceeds as follows:

- a. The right sides of equation (38) are resolved.
- b. Determine  $\delta z$  in decameters by solving the Poisson equations and calculate  $z$  for  $t_0 + \delta t$ . As boundary conditions with the solution of the Poisson equation we take  $\delta z|_{np} = 0$  (first boundary problem or Dirichlet problem).
- c. Calculate the right side of equation (39) using  $z|_{t-t_0}$ .
- d. By means of the solutions of the Poisson equation with boundary condition  $\delta T|_{np} = 0$  determine  $\delta T$  and find  $T|_{t_0+\delta t}$  (then everything is repeated).

#### Solution of Poisson Equations

It is known that in solving forecasting problems which are close to ours the use of the Poisson equation gives results which are physically insufficiently satisfactory. In order to understand the difficulties it is necessary to take into account that in the considered case it is necessary to solve an elliptical equation

with a known right side. In this instance the effect of perturbation is extended with an infinitely high rate and each point of the field instantly feels the effect. From the viewpoint of meteorology this leads to unrealistic results. In order to avoid these effects, the Poisson equation is replaced by the Helmholtz equation. The basis of such a replacement is different arguments, which bear partially a physical character, partially a mathematical. A survey of these questions can be found in [5].

In a more or less arbitrary passage to the Helmholtz equation, written in the form

$$[\Delta - (sk)^2] \phi = F \quad (40)$$

( $\Delta$  in dimensionless variables), the question arises about determination of  $(sk)^2$ . There are no definite rules on this and the question can be solved only experimentally. However, it is not clear what the results obtained using the solution of the Helmholtz equation (40) with an assigned value of  $(sk)^2$  should be compared with.

To solve equation (40) we use a method proposed by S. V. Nemchinov [3] for the case of a right-angled grid. The advantages of this method are obvious: on one hand, because of the use of recurrent formulas a minimum number of memory cells is necessary, on the other a relatively small number requires arithmetical operations. To this one ought to add that the solution has a high degree of accuracy, which when using iteration methods can be achieved only with great difficulty, and that the calculating process is stable with respect to rounding error. The solution with a change in  $k$  does not require a change in the program (in the case of  $k = 0$  the solution of the Poisson equation is automatically obtained).

In the practice numerical forecasts are satisfied by attempts to obtain an optimum forecast and in this manner determine  $(sk)^2$ . In order to use this experiment in this case a special investigation would be necessary. Therefore we used another way.

Several years ago S. L. Belousov [2] proposed a means of solving the Poisson equation, which since then has been successfully used. The formulas are best of all called a local solution; we will use this term subsequently.

The solution of the Poisson equation

$$\Delta\psi = \frac{\partial^2\psi}{\partial x^2} + \frac{\partial^2\psi}{\partial y^2} = F \quad (41)$$

at known boundary values can be presented in the form

$$\psi_0 = -\frac{1}{2\pi} \int_0^{2\pi} \int_0^R F \ln \frac{R}{r} r dr d\varphi + \frac{1}{2\pi R} \oint \psi ds, \quad (42)$$

where  $\psi_0$  - desired magnitude of the function in the center of a circle of radius  $R$ .

For calculations according to formula (42) Belousov used the method of series approximations. As a first approximation he assumes that the contour integral in (42) is absent, and to calculate the first integral in (42) he used the formula<sup>1</sup>

$$\psi_0^{(1)} = -s^2 \left\{ \frac{3}{8} F_0 + \frac{1}{8} (F_1 + F_2 + F_3 + F_4) + \frac{1}{16} (F_5 + \dots + F_n) \right\}. \quad (43)$$

Since the quantity  $\psi_0^1$  is found in all points, the approximate value of the contour integral in (42) is calculated. In the contour integral the value of  $\psi_0^1$  is substituted; the second approximation is calculated by the formula

$$\psi_0^{(2)} = \psi_0^{(1)} + \frac{1}{12} \sum_{i=1}^n \psi_i^{(1)}. \quad (44)$$

<sup>1</sup>If we consider a relatively small neighborhood of point 0, then the approximate value of the integral can be obtained by approximating the Laplace operator by the formula

$$\Delta\psi_0 \approx \frac{1}{s^2} (\psi_1 + \psi_2 + \psi_3 + \psi_4 - 4\psi_0).$$

In this case the Laplace operator was written for 9 points (from zero to 8th), and the values of  $\psi$  at points from the 9th to the 20th are taken as zero. The solution of the obtained system of algebraic equations leads to formula (43).

We used this means of solving the Poisson equation. Not stopping here on questions connected with the use of this, we refer the reader to [5, 8].

It is possible to compare results for two variants of the solution of system (38), (39): 1) using the Helmholtz equation for various values of  $(sk)^2$ ; 2) using the local solution considering two approximations. It is established that results will well agree if in the first case we take  $(sk)^2 = 0.4$ . This value already has been widely used in actual numerical forecasts. Thus the local solution can be successfully used.

#### Preliminary Results

Solving the problem by computer, initially a finite-difference approximation of derivatives in time with the aid of "forward" differences was used. However, the calculations showed that despite a decrease in the time interval to 30 minutes, the system is unstable. At  $t = t_0 + 48$  hours stray waves show up and intensify, thus hampering the interpretation of results. This agrees with theoretical estimates obtained above. Therefore in basic variants of the calculations an implicit scheme was used. The time interval in this case could be taken as 3 hours.

Calculations were carried out for the following values of parameters, determining temperature perturbation:  $A^* = K^* = 6^\circ$ ;  $B = 3.6$ ;  $r^* \leq 5$ . In this case cases were considered when  $x_s = y_s = -7$  and  $x_s = y_s = -11.9$ . The basic field of flows was given by the values of parameters:

$$1) c_1 = -\frac{108}{\pi^2}; c_2 = \frac{36}{\pi}; u_{max} = 30 \text{ m/s};$$

$$2) c_1 = -\frac{36}{\pi^2}; c_2 = \frac{12}{\pi}; u_{max} = 10 \text{ m/s}.$$

On the basis of results of calculation the following preliminary conclusions can be made.

1. A temperature perturbation of a shown intensity can substantially influence circulation in the stratosphere. It does not lead therefore to a breakdown of the polar vortex.

2. As a result of temperature perturbation a perturbation in the geopotential field is developed, the amplitude of which grows during the considered time interval, while the amplitude of the temperature perturbation diminishes.

3. The maximum of the geopotential perturbation remains during the first 48 hours at the same latitude on which was the temperature perturbation. Then in all cases the geopotential perturbation shifts to the north, which agrees with the data of observations. However, the temperature perturbation remains at the original latitude. The last result strongly differs from processes observed in nature. This difference is partially conditioned by simplifications of the model, and partially by neglecting effects connected with the ozone.

4. The shift of the geopotential perturbation to the north is expressed stronger the better the polar vortex is developed, i.e., the greater the meridional wind shift.

#### Bibliography

1. Dubov A. S. Vliyaniye staticheskoy ustoychivosti na protsessy izmeneniya davleniya i prognosticheskiye uravneniya dlya inzhney stratosfery (Effect of statical resistance on processes of pressure change and forecasting equations for the lower stratosphere). Tr. GGO, vyp. 124, 1962.

2. Kibel' I. A. Vvedeniye v gidrodinamicheskiye metody kratkosrochnogo prognoza pogody (Introduction to hydrodynamic methods of short-range weather forecasting). GTTI, M., 1957.

3. Nemchinov S. V. O reshenii metodom setok krayevykh zadach dlya uravneniy v chastnykh proizvodnykh vtorogo poryadka ellipticheskogo tipa (Using the method of grids to solve boundary problems for equations in partial derivatives of the second (elliptical type) order). Zh. vychislit. matematiki i matemat. fiziki, t. 2, No. 3, 1962.

4. Khinkel'man K. K chislennomu prognozu pogody s pomoshch'yu relaksatsionnogo metoda pri uchete baroklinnykh effektov (Numerical

weather forecasting using the relaxation method and considering baroclinic effects). "Chislennyye metody prognoza pogody" (Collection of translated articles, edited by A. S. Dubov and L. S. Gandin). Gidrometeoizdat, L., 1960.

5. Yudin. M. I. Novyye metody i problemy kratkosrochnogo prognoza pogody (New methods and problems in short-range weather forecasting). Gidrometeoizdat, L., 1963.

6. Behr K. Über markante Erwärmungen in der Stratosphäre. Met. Abhandlungen der Inst. für Meteorologie und Geophysik der Fr. Univ. Berlin, Bd 9, Nr 2, 1960.
7. Berkofsky L., Shapiro R. Some numerical results of a model investigation of the atmospheric response to upper-level heating. Planetary and Space Science, vol. 12, 1964.
8. Koo Chen Chao. On the Simple Approximate Solutions for Finite-Difference Poisson Equation. Acta Met. Sinica, v. 29, N 4, 1958.
9. Proceedings of the International Symposium on Stratospheric and Mesospheric Circulation, 20 to 31 August 1962, Berlin, Germany, Met. Abhandl. d. Inst. Meteor. und Geophysik d. F. Univ. Berlin, Bd 36, 1963.
10. Scherhag R. Die Explosionsartigen stratosphären Erwärmungen des Spätwinters 1951/1952. Berichte des Deutschen Wetterdienstes in der US Zone, Nr 38, 1962.

ON THE APPLICATION OF THE FILTRATION THEORY OF RANDOM  
PROCESSES TO SOME PROBLEMS OF OBJECTIVE ANALYSIS

B. V. Ovchinskiy

Formulas for calculating weighting functions of optimum interpolation and smoothing meteorological elements if correlation functions of the "true" quantity (signal) and errors of observations (noise) are known.

I. Formulating the Problem. Derivation  
of Basic Equations

As is known the data of observations contain random errors. During optimum interpolation it is necessary to consider this and treat the meteorological element at an interpolated point free from these random errors.

Even when the field of meteorological elements is presented rather fully, for further analysis it is useful to remove from the field unsystematic errors, i.e., smooth the field.

As has been accepted in objective analysis, a field of meteorological elements is given at discrete points  $\tilde{\chi}_1, \tilde{\chi}_2, \dots, \tilde{\chi}_N$ . Each of the quantities  $\tilde{\chi}_i$ , except the true value  $g_i$ , still has errors  $\epsilon_i$ , so that

$$\tilde{\chi}_i = g_i + \epsilon_i. \quad (1)$$

Concerning errors  $\epsilon_i$ , they can in the simplest case be either purely random, or contain small-scale fluctuations, of the "noise" type, as happens in radiophysics.

In objective analysis errors were taken as purely random and satisfied the following conditions [2]:

1) mathematical expectation (mean) error  $\epsilon_i$  is equal to zero, i.e.,  $E(\epsilon_i) = 0$ ;

2) errors  $\epsilon_i$  are not correlated with true value of the meteorological element  $E(\epsilon_i g_i) = 0$ ;

3) errors  $\epsilon_i$  do not correlate with each other, i.e.,  $E(\epsilon_i \epsilon_j) = 0$  when  $i \neq j$ .

If we treat more broadly the quantities  $\epsilon_i$  and include here small-scale fluctuations, then we must reject the assumption about the noncorrelatability of the  $\epsilon_i$ . In meteorology this circumstance was studied by Thompson [8], using the apparatus of the theory of filtration of random processes for optimum smoothing of meteorological fields.

Thus we assume that  $g_i$  and  $\epsilon_i$  are stationary random quantities, which obey conditions 1) and 2). The correlation functions of  $g_i$  and  $\epsilon_i$  will be:

$$\begin{aligned} E(g_i g_j) &= R_g(\tau_{ij}), \\ E(\epsilon_i \epsilon_j) &= R_\epsilon(\tau_{ij}). \end{aligned}$$

where  $\tau_{ij}$  - distance between  $i$ -th and  $j$ -th stations.

In relationship to correlation functions  $R_g(\tau_{ij})$  and  $R_\epsilon(\tau_{ij})$  let us note that radius correlation  $\epsilon_i$  is considerably less than the radius of correlation of the  $g_i$ . This means that the connection between the  $\epsilon_i$  weakens much faster with distance (or with time), than the connection between the  $g_i$ .

In accordance with the theory of optimum interpolation we put together the expression

$$g_0 \approx \sum_{i=1}^N \tilde{X}_i P_i = \sum_{i=1}^N (g_i + \epsilon_i) P_i \quad (2)$$

and select weights  $P_i$  such that dispersion

$$J = E \left[ g_0 - \sum_{i=1}^N (g_i + \epsilon_i) P_i \right]^2 \quad (3)$$

is minimum. After this the interpolated value of the meteorological element will not contain "noise," and thus is a smoothed quantity.

Let us suppose, as usual, that  $\tilde{\chi}_i$  are standard deviations and, according to the first condition relative to errors  $\epsilon_i$ , we have

$$E(\tilde{\chi}_i) = E(\epsilon_i) = E(g_i) = 0.$$

After this formula (3) can be brought to the form:

$$J = E(g_0^2) - 2 \sum_{i=1}^N R_g(\tau_{0i}) P_i + \sum_{i=1}^N \sum_{j=1}^N R_g(\tau_{ij}) P_i P_j + \sum_{i=1}^N \sum_{j=1}^N R_\epsilon(\tau_{ij}) P_i P_j. \quad (4)$$

We divide both sides of equality (4) by  $\sigma_g^2$  and turn to standardized correlation functions  $\mu_{ij}$  for the signal ("true quantity") and  $\nu_{ij}$  for errors  $\epsilon_i$  ("noise"), then formula (4) can be rewritten

$$\frac{J}{\sigma_g^2} = J_1^2 = 1 - 2 \sum_{i=1}^N \mu_{0i} P_i + \sum_{i=1}^N \sum_{j=1}^N \mu_{ij} P_i P_j + \frac{\sigma_\epsilon^2}{\sigma_g^2} \sum_{i=1}^N \sum_{j=1}^N \nu_{ij} P_i P_j. \quad (4')$$

The quantity  $\sigma_\epsilon^2 / \sigma_g^2$  in radiophysics is called the signal-to-noise ratio. Subsequently we will designate it by  $\lambda$ . For minimum  $J_1^2$  it is necessary that  $\partial J_1^2 / \partial P_i = 0$ . Hence we obtain a system of linear equations for determination of weights

$$\sum_{j=1}^N (\mu_{ij} + \lambda \nu_{ij}) P_j = \mu_{0i}, \quad i = 1, 2, \dots, N. \quad (5)$$

Assuming that errors  $\epsilon_i$  do not correlate among themselves, i.e., they are purely random, then function  $v_{ij}$  can be represented as:

$$v_{ij} = \begin{cases} 1, & \text{if } i=j; \\ 0, & \text{if } i \neq j. \end{cases} \quad (6)$$

This case corresponds to the fact that in radiophysics it is accepted to say "white noise" [6]. For white noise equation (5) can be rewritten in the form:

$$\sum_{j=1}^N P_j P_{ij} + \lambda P_i = P_w. \quad (5')$$

Formula (5') coincides with the usual equation used in objective analysis [2], because  $\eta = \lambda = \sigma_\epsilon^2 / \sigma_g^2$ . A work of Thompson [9] expresses certain considerations about  $\lambda$ . The signal-to-noise ratio fluctuates from  $\lambda = 0.1$  to  $\lambda = 0.33$ .

If weights  $P_i$  are determined according to formula (5), then interpolation error, according to (4'), can be found by the formula

$$s^2 = 1 - \sum_{i=1}^N P_i P_w. \quad (7)$$

Let us note that formula (7) contains the correlation function of noise  $v_{ij}$ . In order to explain in general terms the effect of the noise part of the field on interpolation error, we set  $\lambda = 1$  and  $\mu_{ij} = v_{ij}$ . Then from equation (5) we obtain

$$\sum_{j=1}^N P_j P_{ij} = \frac{P_w}{2}.$$

i.e., weights  $P_j$  will be half as large as in the same "noiseless" field, and from formula (7) it follows that interpolation error increases and will be  $s^2 = \frac{1}{2} \sum_{i=1}^N P_i P_w$ . This increase in interpolation error for such a noise field can be explained by the fact that there are two identical superimposed fields here.

Let us turn again to system of equations (5) for determination of weights of optimum interpolation. Let us write this system for the case when the data of observations have been taken through equal intervals in space.<sup>1</sup> This simplified scheme will help us to investigate in more detail the structure and features of the weighting function, which is the basic task of this work. Below we will examine the case when observations of the quantities in meteorological elements are continuous. Thus let us assume that the quantities in meteorological elements  $\chi_1, \chi_2, \chi_N$  are given through identical distances from one another, and for simplicity let us take these distances as one. Then the correlation function can be written:

$$\begin{aligned} E(g_i g_j) &= R_r(|i-j|), \\ E(e_i e_j) &= R_e(|i-j|). \end{aligned}$$

For standardized correlation functions let us introduce new designations:

$$\begin{aligned} r_{ij} &= r_r(|i-j|), \\ v_{ij} &= r_e(|i-j|). \end{aligned}$$

After this system (5) for determination of weights of optimum interpolation can be replaced by other system of equations

$$\sum_{j=1}^N [r_r(k-j) + \lambda r_e(k-j)] P_j = r_r(k), \quad k=1, 2, 2, \dots, N. \quad (8)$$

Equation (8) in statistical dynamics of pulse systems [5] is called a discrete analog the Wiener-Hopf equation.

Let us assume that as a result of observations all possible values of  $\chi_i$  have been obtained including  $\chi_0$ . Our problem as before is the determination of  $g_0$  on the basis of the observations. In

---

<sup>1</sup>Of course, we need not hold strictly the selection of observation points through equal intervals. Deviations are possible in such quantities which will not substantially affect the value of the correlation function.

this instance we say that we smooth  $\tilde{\chi}_0$ . Formula (2) will have the form:

$$k_0 = \sum_{i=0}^N P_i \tilde{\chi}_i = \sum_{i=0}^N P_i (\chi_i + \epsilon_i). \quad (9)$$

The distinction from formula (2) is that the summing begins from  $i = 0$ .

System of equations (5) for determination of weights  $P_i$  remains as before with the difference that the summing must begin with  $i = 0$ ;  $j = 0$ . M. I. Yudin proposed two formulas for smoothing meteorological fields, which in form correspond to expression (9) and are written thus [10]:

$$\bar{H} = \frac{1}{2} H_0 + \frac{1}{12} \sum_{i=1}^6 H_i$$

$$\bar{H} = 0,36 H_0 + 0,08 \sum_{i=1}^6 H_i + 0,08 (H_8 + H_{11}).$$

The stations with the numbers 1-6 lay along the circumference with center  $H_0$ ; and stations 8, 11 were outside the circumference symmetrical to the origin of coordinates.

Let us examine the problem of smoothing meteorological elements  $\tilde{u}(x)$ , when  $x$  takes continuous values. Of course, for discrete values of  $x$  the quantity  $\tilde{u}(x)$  must coincide with the observed quantities  $\tilde{\chi}_1, \tilde{\chi}_2, \dots, \tilde{\chi}_N$ , i.e.,  $\tilde{u}[0] = \tilde{\chi}_0, \dots, \tilde{u}[1] = \tilde{\chi}_1, \dots, \tilde{u}[N] = \tilde{\chi}_N$ .

Just as earlier we assume  $\tilde{u}(x)$ , except the true value (signal)  $g(x)$ , still contains random error (noise)  $\epsilon(x)$ . Furthermore,

$$\tilde{u}(x) = g(x) + \epsilon(x).$$

The smoothed out value of  $\tilde{u}(0)$  must not contain noise and its

approximate magnitude by analogy with (8) will be<sup>1</sup>

$$g_0 \approx \int_0^{\infty} \tilde{u}(x) f(x) dx. \quad (10)$$

Let us find such weight function  $f(x)$  that the mean quadratic error of approximate equality (10) is minimum [11]

$$J(f) = E \left\{ g_0 - \int_0^{\infty} [g(x) + \varepsilon(x)] f(x) dx \right\}^2 \quad (11)$$

We transform preliminarily formula (11), making use of the fact that  $g(x)$  and  $\varepsilon(x)$  are stationary random functions, not correlated with one another, i.e.,  $E[\varepsilon(x) g(x)] = 0$ . As a result we obtain

$$J(f) = R_g(0) - 2 \int_0^{\infty} R_g(x) f(x) dx + \int_0^{\infty} \int_0^{\infty} [R_g(x-y) + R_g(x+y)] f(x) f(y) dx dy. \quad (12)$$

In order to find the minimum functional  $J^2(f)$ , it is necessary in formula (12) instead of  $f(x)$  to substitute  $f(x) + \gamma \phi(x)$ . The necessary condition of extreme of the functional will be [3]

$$\left[ \frac{\partial J(f + \gamma \phi)}{\partial \gamma} \right]_{\gamma=0} = 0.$$

Having completed the calculations, we pass to the integral equation for determination of  $f(x)$

$$\int_0^{\infty} [R_g(x-y) + R_g(x+y)] f(y) dy = R_g(x). \quad (13)$$

It is possible to show a sufficiency of condition (13), in other words, if  $f(x)$  satisfies integral equation (13), then  $J^2(f)$  will be minimum [7]. Equation (13) is widely used in the solution of problems of automatic control and is called the Wiener-Hopf

<sup>1</sup>The upper limit of the integral is equal to infinity, which is not obligatory. However, in the beginning we take this for the sake of simplicity of further formulas.

integral equation. Because usually it is more convenient to deal with normalized correlation functions, equation (13) we rewrite in the following form:

$$\int [r_g(x-y) + \lambda r_r(x-y)] f(y) dy = r_g(x). \quad (14)$$

Equation (14) is the original for determination of weight functions of smoothing.

## II. Weight Functions of Optimum Interpolation and Smoothing

Let us pass now to the solution of system (8)

$$\sum_{j=1}^N [r_g(k-j) + \lambda r_r(k-j)] P_j = r_g(k), \quad k = 1, 2, 3, \dots, N.$$

The means of solving equation (8), which is presented later, was used in statistical dynamics of pulse systems [5] as well as in problems of automatic control [1, 7].

By approximating the correlation function by the sum of model functions  $R(\tau) = \sum_{i=1}^n A_i e^{-\alpha_i |\tau|}$ , we can find the  $P_i$  solutions by the method of indeterminate coefficients. Subsequently we will limit ourselves to approximating the correlation function with only the first term of the sum, i.e., we set

$$r_g(\tau) = e^{-\alpha|\tau|}, \quad (15)$$

where  $\alpha$  is determined according to empirical correlation function.

So for the two meteorological elements by which we will conduct the calculation (wind and dew point), the distinctions of the approximated curve from the observed correlation coefficients (Figs. 1 and 2) we consider as entirely permissible. Therefore we assume that the correlation function for the dew point will be

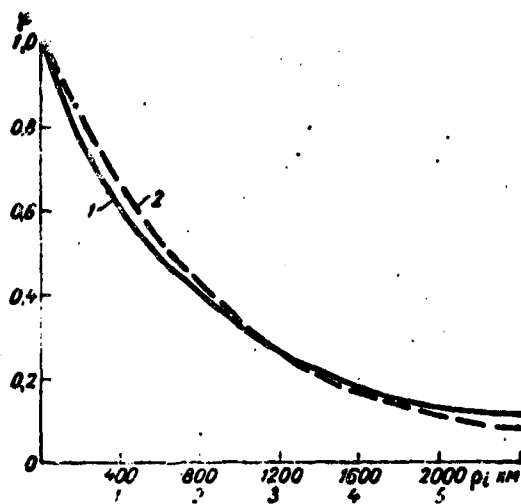


Fig. 1. Autocorrelation position function of the dew point (spring) [2]. 1 - observed, 2 - according to the formula.

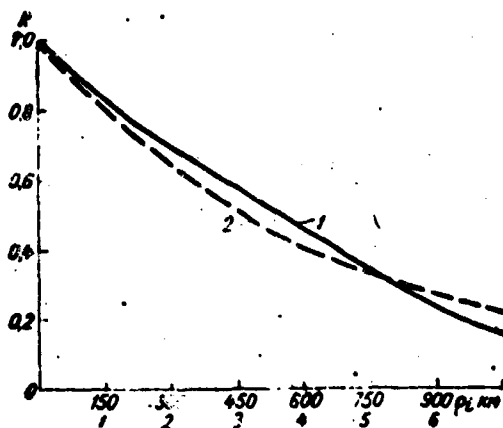


Fig. 2. Autocorrelation function of wind [4]. 1 - observed, 2 - according to the formula.

$r_{\rho}(\rho) = e^{-0.432\rho}$ , and for wind<sup>1</sup>  $r_{\rho}(\rho) = e^{-0.32\rho}$ , where distance  $\rho$  is expressed in arbitrary units, shown in Figs. 1 and 2. Let us examine from the beginning the case when the interference is white noise. The correlation function for errors [see formula (6)] can be written:

<sup>1</sup>During calculations it was accepted  $r_{\rho}(\rho) = e^{-0.32\rho}$ .

$$r_s(k-j) = \begin{cases} 1, & \text{if } k=j; \\ 0, & \text{if } k \neq j. \end{cases}$$

Systems of equations for determination of weights during optimum interpolation and smoothing can be represented in the form:

$$\sum_{j=1}^N r_s(k-j)P_j + \lambda P_k = r_s(k), \quad k=1, 2, \dots, N. \quad (16)$$

$$\sum_{j=0}^N r_s(k-j)\bar{P}_j + \lambda \bar{P}_k = r_s(k), \quad k=0, 1, 2, \dots, N. \quad (17)$$

Let us examine from the beginning system (16). Its solution we look for in the form<sup>1</sup>

$$P_j = Ae^{-\gamma j} + Be^{\gamma j}. \quad (18)$$

Coefficients  $A$ ,  $B$ ,  $\gamma$  will be determined. Let us substitute expressions (15) and (18) in original system (16), then we obtain

$$\sum_{j=1}^k [Ae^{-\gamma j} + Be^{\gamma j}]e^{-\gamma(k-j)} + \sum_{j=k+1}^N (Ae^{-\gamma j} + Be^{\gamma j})e^{-\gamma(j-k)} +$$

$$+ \lambda(Ae^{-\gamma k} + Be^{\gamma k}) = e^{-\gamma k}$$

or

$$Ae^{-\gamma k} \sum_{j=1}^k e^{-(\gamma-k)j} + Be^{-\gamma k} \sum_{j=1}^k e^{(\gamma+k)j} + Ae^{\gamma k} \sum_{j=k+1}^N e^{-(\gamma+k)j} +$$

$$+ Be^{\gamma k} \sum_{j=k+1}^N e^{(\gamma-k)j} + \lambda Ae^{-\gamma k} + \lambda Be^{\gamma k} = e^{-\gamma k}, \quad k=1, 2, \dots, N.$$

Having completed the summation and equating coefficients in the right and left sides at  $e^{-\gamma k}$  ( $e^{\gamma k}$ ),  $e^{-\gamma k}$ ,  $e^{\gamma k}$  we arrive at the equations for determination of  $\gamma$ ,  $A$ ,  $B$ :

$$\frac{e^{-\gamma} - e^{\gamma}}{(e^{\gamma} - e^{-\gamma})(e^{\gamma} - e^{-\gamma})} + \lambda e^{-\gamma} = 0, \quad (19)$$

$$\frac{Ae^{\gamma}}{e^{\gamma} - e^{-\gamma}} + \frac{Be^{-\gamma}}{e^{-\gamma} - e^{\gamma}} = 1, \quad \frac{Ae^{-\gamma N}}{e^{\gamma} - e^{-\gamma}} + \frac{Be^{\gamma N}}{e^{-\gamma} - e^{\gamma}} = 0. \quad (20)$$

<sup>1</sup>Selection of the form of the solution will be clarified at the end of the article.

The order of solution of the system is: from equation (19) we determine  $\gamma$ , and then from system (20) we find  $A$  and  $B$ . For the calculation of  $\gamma$ ,  $A$  and  $B$  it is possible to make use of the following formulas

$$e^{\gamma} = \frac{[\lambda(1+p^2) + p^2 - 1] + \sqrt{p^2 - 1 + \lambda(1+p^2) - 4\lambda^2 p^2}}{2\lambda p}, \quad (21)$$

where

$$p = e^{\alpha},$$

$$A = \frac{(e^{\gamma+\alpha} - 1)(e^{\gamma} - e^{\alpha})}{e^{\alpha} [(e^{\alpha+1} - 1)^2 - e^{-2N\gamma}(e^{\gamma} - e^{\alpha})^2]}, \quad (22)$$

$$B = \frac{(e^{\gamma} - e^{\alpha})(e^{\gamma+\alpha} - 1)}{[(e^{\alpha+1} - 1)^2 e^{2N\gamma} + (e^{\gamma} - e^{\alpha})^2] e^{\alpha+1}}. \quad (23)$$

From formula (21) it follows that  $\gamma$  depends on  $N$  (quantity of stations). The second root of equation (19) gives a negative value of  $\gamma$ , which does not have physical meaning. Figure 3 shows  $\gamma$  as a function of  $\lambda$ .

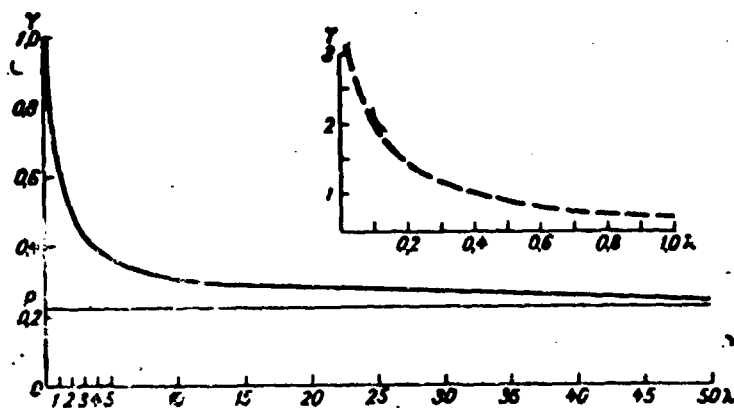


Fig. 3.  $\gamma$  as a function of  $\lambda$ .

As it appears in the graph, an increase of  $\lambda$  decreases values  $\gamma$  as they asymptotically approach  $\alpha$ . However, this asymptotic behavior is achieved for  $\lambda$  of the order of 40-50, which is unrealistic. Therefore it is possible to assume that always  $\gamma$  is more than  $\alpha$ . In other words, the index of weight function  $\gamma$  is much more than the same index for the correlation function.

The turn now to determination of the weight functions of optimum smoothing. For this we must solve system of equations (17).

The weight functions we look for (as earlier) in the following form:

$$\tilde{P}_j = A_1 e^{-\gamma j} + B_1 e^{\gamma j}.$$

The solution of system (17) follows exactly system (16).

As a result of this solution we obtain  $\gamma = \gamma_1$ , i.e., the index of damping of the weight function for optimum  $\gamma$  interpolation coincides with the same index  $\gamma_1$  for smoothing and is determined by formula (21). Coefficients  $A_1$  and  $B_1$  can be found by the formula:

$$A_1 = \frac{(e^{\gamma_1} - 1)^2 (e^{\gamma_1} - e^{\gamma_1})}{e^{\gamma_1} (e^{\gamma_1} - 1)^2 - e^{-\gamma_1 (2N+1)} (e^{\gamma_1} - e^{\gamma_1}) (1 - e^{-\gamma_1 (1-2N)})}, \quad (24)$$

$$B_1 = \frac{(e^{\gamma_1} - e^{\gamma_1}) (e^{\gamma_1} - 1)}{(e^{\gamma_1} - 1)^2 e^{\gamma_1 (N+1)} - (e^{\gamma_1} - e^{\gamma_1})}. \quad (25)$$

Finally let us examine the case when  $N$  (number of stations) increases without limit ( $N \rightarrow \infty$ ). Then from formulas (23) and (25) it is evident that

$$B \rightarrow 0 \text{ and } B_1 \rightarrow 0.$$

The weight functions for optimum  $P_j$  interpolation and smoothing have the form:

$$P_j = (e^{\gamma_1} - 1) e^{-\gamma_1 j}, \quad j = 1, 2, \dots;$$

$$\tilde{P}_j = (1 - e^{-\gamma_1}) e^{-\gamma_1 j}, \quad j = 0, 1, 2, \dots$$

The change in weight function depending on  $\lambda$  for optimum interpolation  $P_j = A e^{-\gamma j}$  and smoothing  $\tilde{P}_j = A_1 e^{-\gamma j}$  is shown in Fig. 4. On the graphs are values of weights only for  $P_1, \tilde{P}_0$ . By these data it is possible to establish that weight  $\tilde{P}_0$  is more than weight  $P_1$  for all  $\lambda$ .

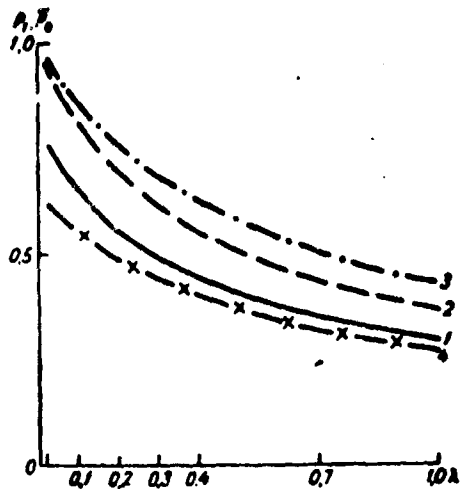


Fig. 4. Change in weight function depending on  $\lambda$  for smoothing wind (1) and dew points (3) for optimum interpolation of wind (2) and dew points (4).

Let us turn now to the more general case when errors  $\epsilon_j$  are connected between one another and the correlation function is assigned by formula

$$r_d(\tau) = e^{-\lambda|\tau|}.$$

Furthermore, we assume the upper limit of summation  $N$  is infinite; then system (8) can be written

$$\sum_{j=1}^{\infty} [r_d(k-j) + r_d(k+j)] P_j = r_d(k), \quad k = 1, 2, 3, \dots \quad (8')$$

The solution of system (8') we look for in the form:

$$P_j = Ce^{-dj} + D\sigma[j-1], \quad j = 1, 2, \dots \quad (26)$$

Quantities  $d$ ,  $C$ ,  $D$  will be determined;  $\sigma[j]$  is the pulse single function which is assigned

$$\sigma[j] = \begin{cases} 1, & \text{if } j=0 \\ 0, & \text{if } j \neq 0. \end{cases}$$

Let us substitute in both sides of equation (8') instead of  $r_g(\tau)$ ,  $r_\epsilon(\tau)$  and  $P_j$  their expressions, then we arrive at

$$\sum_{j=1}^k [e^{-\alpha k - j} + \lambda e^{-\lambda k - j}] [C e^{-d j} + D(j-1)] + \sum_{j=k+1}^{\infty} [e^{-\alpha(j-k)} + \lambda e^{-\lambda(j-k)}] C e^{-d j} = e^{-\alpha k}, \quad k=1, 2, \dots$$

Summing up and equating coefficients in the right and left sides at  $e^{-dk}$ ,  $e^{-\alpha k}$ ,  $e^{-\beta k}$ , we arrive at equations for determination of  $d$ ,  $C$  and  $D$ :

$$\frac{e^{\alpha} - e^{-\alpha}}{(e^d - e^{-d})(e^{\alpha} - e^{-\alpha})} + \lambda \frac{e^{\beta} - e^{-\beta}}{(e^d - e^{-d})(e^{\beta} - e^{-\beta})} = 0. \quad (27)$$

$$\left. \begin{aligned} \frac{C}{e^d - e^{-d}} + D &= e^{-\alpha}, \\ \frac{C}{e^d - e^{-d}} + D &= 0. \end{aligned} \right\} \quad (28)$$

If we must smooth  $\tilde{X}_0$ , then, as already was noted above in formula (8'), the summing must begin with  $j = 0$ . The weight function we find according to formula

$$\tilde{P}_j = C_1 e^{-d_1 j} + D_1 \sigma(j),$$

where  $d_1$  as before is determined from equation (27);  $C_1$  and  $D_1$  can be found by solving system of equations:

$$\left. \begin{aligned} \frac{C_1}{1 - e^{-(d_1 - \alpha)}} + D_1 &= 1, \\ \frac{C_1}{1 - e^{-(d_1 - \beta)}} + D_1 &= 0. \end{aligned} \right\} \quad (29)$$

Hence it follows that the difference in weight functions of interpolation and smoothing is only because of coefficients  $C$  and  $D$ .

The index of damping of weight function  $d$  can be found by solving equation (27)

$$e^d = \frac{(e^{\alpha} - 1)(e^{\beta} - 1) - \lambda(e^{\alpha} - 1)(1 + e^{\beta})}{2(e^{\alpha} - 1)e^{\beta} + \lambda(e^{\alpha} - 1)e^{\beta}} + \frac{1 - (1 - e^{-\alpha})e^{\beta} - 1 + \lambda(e^{\alpha} - 1)(1 - e^{\beta})}{2(e^{\alpha} - 1)e^{\beta} - \lambda(e^{\alpha} - 1)e^{\beta}} \quad (30)$$

It is accepted that  $\beta = \pi\alpha$  and, as noted above,  $\beta > \alpha$ , so that  $m > 1$ .

Figures 5 and 6 show changes of  $e^d$  depending on  $\lambda$  at  $m = 2$ ,  $m = 3$  for the dew point and wind. For large  $\lambda$  the quantity  $d$  tends to asymptotically to  $\alpha$ . The difference between  $\alpha$  and  $d$  becomes unimportant beginning with  $\lambda = 25$  and more for different  $m$ . Thus again we see that the index of damping of the weight function is more than for the correlation function, and only at large  $\lambda$  do these indexes differ little from one another.

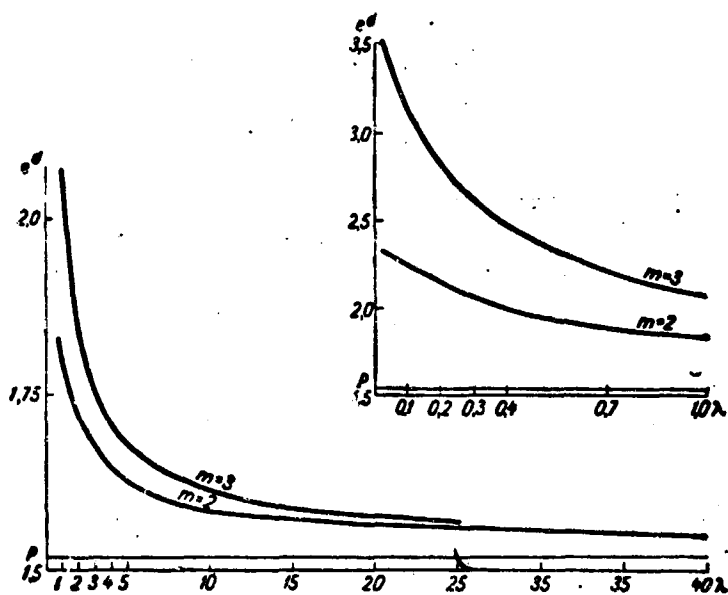


Fig. 5. Change of  $e^d$  depending on  $\lambda$  for wind at different  $m$ .

From system (28) we find coefficients  $C$  and  $D$  for optimum interpolation, and from system (29)  $C_1$  and  $D_1$  for smoothing. Simple formulas are obtained:

$$C = \frac{(e^d - e^a)(e^d - e^b)}{e^a(e^a - e^b)}, \quad D = \frac{e^d - e^a}{e^a(e^b - e^a)}; \quad (31)$$

$$C_1 = \frac{(e^d - e^a)(e^d - e^b)}{e^d(e^a - e^b)}, \quad D_1 = \frac{e^d - e^a}{e^b - e^a}. \quad (32)$$

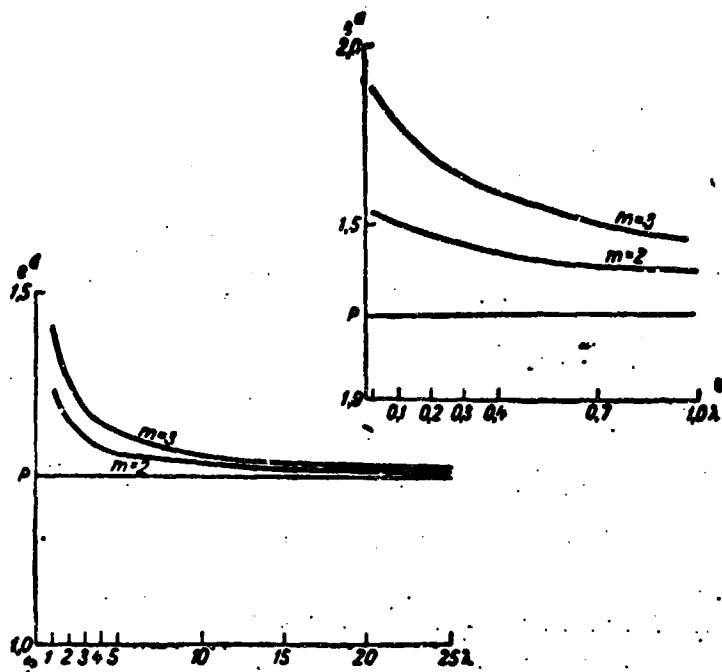


Fig. 6. Change of  $e^d$  depending on  $\lambda$  for dew point at different  $m$ .

### III. Solution of Integral Equation for Weight Function

Let us turn again to the case when the amount of meteorological element is given for continuous values of argument  $x$ . Finding the weight function of smoothing  $f(y)$  led to solving integral equation (14). Among various means of solving this equation, let us again examine the means of indeterminate coefficients, which was used in the second section.

We set again:

$$r_2(\tau) = e^{-M\tau}, \quad r_1(\tau) = e^{-N\tau},$$

and the solution we look for in the form

$$f(\tau) = A_2 e^{-M\tau} + A_1 \delta(\tau),$$

where  $\delta(\tau)$  - designates the Dirac delta-function.

Let us substitute the above quantities into integral equation (14). After this it is possible to write:

$$\int_0^x [e^{-\alpha(x-y)} + \lambda e^{-\lambda(x-y)}] [A_2 e^{-\beta y} + A_3 \delta(y)] dy + \int_x^N [e^{-\alpha(y-x)} + \lambda e^{-\lambda(y-x)}] [A_2 e^{-\beta y} + A_3 \delta(y)] dy = e^{-\alpha x}. \quad (33)$$

Carrying out the calculations, we compare coefficients of  $e^{-Sx}$ ,  $e^{-\alpha x}$ ,  $e^{-\beta x}$ . We obtain a system for determination of  $S$ ,  $A_2$ ,  $A_3$ .

$$\frac{\alpha}{S-\alpha} + \frac{\lambda\beta}{S-\beta} = 0, \quad (34)$$

$$\left. \begin{aligned} \frac{A_2}{S-\alpha} + \frac{A_3}{2} &= 1, \\ \frac{A_2}{S-\beta} + \frac{A_3}{2} &= 0. \end{aligned} \right\} \quad (35)$$

From system of equations (34) and (35) let us find  $S$ ,  $A_2$ ,  $A_3$  and write the formulas for the weight function:

$$\left. \begin{aligned} S &= \sqrt{\frac{\alpha\lambda(\beta + \lambda\alpha)}{\alpha + \lambda\beta}}, \\ A_2 &= \frac{\alpha - \beta}{(S-\alpha)(S-\beta)}, \\ A_3 &= 2 - \frac{2(\alpha - \beta)}{(S-\alpha)(S-\beta)}. \end{aligned} \right\} \quad (36)$$

Let us examine certain limiting cases. We set  $\sigma_\epsilon$  to be small in comparison with  $\sigma_g$ , i.e.,  $\lambda$  turns into zero. Then the index of damping of weight function  $S$  coincides with the index of damping of the correlation function of errors  $\beta$ . If  $\sigma_\epsilon^2/\sigma_g^2$  grows without limit ( $\lambda \rightarrow \infty$ ), then  $S$  approaches  $\alpha$ . Obviously, with finite  $\lambda$  we have the following inequality:  $\alpha < S < \beta$ .

Let us examine now the particular case of integral equation (14), when errors of observation bear the character of white noise, and the upper limit has a finite value, rather large and equal to  $N$ . Then integral equation (14) will pass into a Fredholm equation of

the 2nd order.<sup>1</sup>

$$\int_0^N r_g(x-y)f(y)dy + \lambda f(x) = r_g(x). \quad (37)$$

We assume as before  $r_g(\tau) = e^{-\alpha|\tau|}$ ; then equation (37) is rewritten in the form:

$$\int_0^N e^{-\alpha(x-y)} f(y)dy + \lambda f(x) = e^{-\alpha x}$$

or

$$\int_0^x e^{-\alpha(x-y)} f(y)dy + \int_x^N e^{-\alpha(y-x)} f(y)dy + \lambda f(x) = e^{-\alpha x}. \quad (38)$$

The solution of the equations (31) we reduce to the solution of a differential equation with constant coefficients. For this let us differentiate twice both sides of (31) with respect to variable  $x$ . We write the result of the first and second derivatives:

$$\begin{aligned} -\alpha \int_0^x e^{-\alpha(x-y)} f(y)dy + \alpha \int_x^N e^{-\alpha(y-x)} f(y)dy + \lambda f'(x) &= -\alpha e^{-\alpha x}, \\ \alpha^2 \int_0^x e^{-\alpha(x-y)} f(y)dy - 2\alpha f(x) + \lambda f''(x) &= \alpha^2 e^{-\alpha x}. \end{aligned} \quad (39)$$

If we substitute in the last formula (39) the magnitude of the integral for  $e^{-\alpha x} - \lambda f(x)$  in accordance with (38), then we obtain

$$\lambda f''(x) - \alpha(2 + \lambda \alpha) f(x) = 0.$$

whence we find the solution of the differential equation<sup>2</sup>

<sup>1</sup>Equation (37) can be reached if in the original formula (10) we smooth over a finite segment of changes  $x$ , which is more natural. In other words, let us take  $g_0 \approx \int_0^{N-x} u(x)f(x)dx$ . On the other hand, the assumptions that the upper limit corresponds to the fact that weight function  $f(y)$  turns into zero when  $y \geq N$ .

<sup>2</sup>Such a form of the solution was accepted by us for the discrete case [see formula (18)].

$$f(x) = Le^{-s_1 x} + Me^{s_1 x}, \quad (40)$$

where  $S_1 = \sqrt{\frac{s(\lambda s - 2)}{\lambda}}$ . Arbitrary constants  $L$  and  $M$  will be defined below from boundary conditions.<sup>1</sup>

Let us designate

$$\int_0^N e^{-sy} f(y) dy = G \text{ and } \int_0^N e^{sy} f(y) dy = Q.$$

We set in formula (38)  $x = 0$  and  $x = N$ ; we have correspondingly:

$$\begin{aligned} \int_0^N e^{-sy} f(y) dy + \lambda f(0) &= 1, \\ e^{-sN} \int_0^N e^{sy} f(y) dy + \lambda f(N) &= e^{-sN} \end{aligned}$$

or

$$\left. \begin{aligned} G + \lambda f(0) &= 1, \\ Qe^{-sN} + \lambda f(N) &= e^{-sN}. \end{aligned} \right\} \quad (41)$$

Accurately also, setting  $x = 0$  and  $x = N$  in formula (39), for the first derivative we obtain system of equations:

$$\left. \begin{aligned} 2G + \lambda f'(0) &= -2s, \\ -2e^{-sN}Q + \lambda f'(N) &= -2se^{-sN}. \end{aligned} \right\} \quad (42)$$

We exclude from system (41) and (42) the introduced quantities  $G$ ,  $Q$ , we write the system for the boundary conditions:

$$\left. \begin{aligned} \lambda f(0) - \lambda 2f(0) &= -2s, \\ \lambda f(N) + 2f(N) &= 0. \end{aligned} \right\} \quad (43)$$

We substitute in equations (43) the values of  $f(0)$ ,  $f(N)$ ,  $f'(0)$ , and  $f'(N)$  from formula (40). Then we go to a system of equation for determination  $L$  and  $M$ :

<sup>1</sup>In [8] is examined a more general case of the solution of the Fredholm equation of the 2nd kind with a symmetric nucleus.

$$\left. \begin{aligned} -(\gamma + a)L + (\gamma - a)M &= -\frac{2a}{k}, \\ e^{-\gamma N}(a - \gamma)L + Me^{-N(\gamma + a)} &= 0, \\ i &\neq 0. \end{aligned} \right\} \quad (44)$$

Since  $L$  and  $M$  have been found from system (44), it is simple to write the formula for the weight function

$$f(y) = \frac{2a(\gamma + a)e^{2\gamma N}}{i|e^{2\gamma N}(\gamma + a)^2 - (\gamma - a)^2|} e^{-iy} + \frac{2a(\gamma - a)}{i|e^{2\gamma N}(\gamma + a)^2 - (a - \gamma)^2|} e^{iy}. \quad (45)$$

From this formula it is evident that  $f(N)$  at large enough  $N$  approaches zero. For small values of  $y$  (at large  $N$ ) the second term of (45) is smaller than the first.

### Bibliography

1. Andreyev N. I. Korrelyatsionnaya teoriya statisticheskikh optimal'nykh sistem (Correlation theory of statistically optimum systems). Izd-vo "Nauka," m., 1966.
2. Gandin L. S. Ob'yektivnyy analiz meteorologicheskikh poley (Objective analysis of meteorological fields). Gidrometeoizdat, L., 1963.
3. Gel'fand I. M. i Fomin S. V. Variatsionnoye ischisleniye (Calculus of variations). GIFML, M., 1961.
4. Krichak M. O. Opyt ob'yektivnogo analiza polya vetra metodom optimal'noy interpolatsii (Experience in objective analysis field of the wind by the method of optimum interpolation). Tr. MMTs, vyp. 4, 1964.
5. Krut'ko P. D. Statisticheskaya dinamika impul'snykh sistem (Statistical dynamics of pulse systems). Izd-vo "Sovetskoye radio," M., 1963.
6. Levin B. R. Teoreticheskiye osnovy statisticheskoy radiotekhniki (Theoretical bases of statistical radio mechanics). Izd-vo "Sovetskoye radio," M., 1966.
7. Lening Dzh. Kh. i Bettin R. G. Sluchaynyye protsessy v zadachakh avtomaticheskogo upravleniya (Random processes in automatic control). IIL. M., 1958.
8. Pravalov I. I. Integral'nyye uravneniya (Integral equations). Nauchno-tekhnicheskoye izd-vo NKTP SSSR, M.-L., 1935.

9. Thompson F. D. Optimal'noye sglazhivaniye dvumernykh poley. Chislennyye metody prognoza pogody (Optimum smoothing of two-dimensional fields. Numerical methods of forecasting of weather). Collection perevodnykh statey, Edited by L. S. Gandina, A. S. Dubova. Gidrometeoizdat, L., 1960.

10. Yudin M. I. Novyye metody i problemy kratkosrochnogo prognoza pogody (New methods and problems of short-range forecasting of weather). Gidrometeoizdat, L., 1963.

11. Wiener N., Extrapolation, interpolation and smoothing of stationary time series, New York, 1949.

ON THE FILTRATION OF FIELDS OBTAINED AS A RESULT  
OF NONLINEAR TRANSFORMATIONS OF THE INITIAL  
VALUES OF METEOROLOGICAL FACTORS

L. N. Strizhevskiy

On the basis of the theory of optimum linear filtration of two-dimensional fields we calculate filtration operators for fields of the nonlinear part of vortex advection and the nonlinear part of the individual wind derivative. It is shown that applying results of calculations to a simple scheme of wind forecasting obtains stability before an unstable system.

Introduction

As is known original meteorological information always contains errors connected with the measurement and treatment of weather data and conditioned by the superposition of a whole series of errors: errors of the measuring devices; errors of the observers; errors which appear during encoding, decoding, transmission and analysis of meteorological information etc.

These errors (for analyzed maps) are characterized first of all by a radius of correlation which is considerably less than the correlation radius of the "true" fields of meteorological elements, which allows their partial division. The theoretical basis of such a division is the theory of optimum linear filtration, an account of which can be found in the survey article of A. M. Yaglom [7].

For the first time this theory was applied to a meteorological problem in a work of F. Thompson [4]. In [2] the operator of optimum smoothing of the geopotential  $\Phi_{500}$  for the practical correlation function of the observed field was calculated. This work indicated that during linear transformations of the original field of the optimum filtration operator does not change.

Otherwise we deal with the acquisition of nonlinear operators for initial fields. Meanwhile the most important transformations of meteorological fields used in the process of numerical forecasting and weather diagnosis are nonlinear.

This work is dedicated to finding formulas for optimum smoothing of fields obtained as a result of certain widespread nonlinear transformations of original fields.

In future calculations it is supposed that original fields are isotropic, uniform, distributed normally, and the mathematical expectations are equal to zero. We will also use a relationship given in [6], enabling us to express the moment of the fourth order of a normally distributed random quantity through its second moments.

#### Filtration of a Vortex Advection Field

As was shown in [6], the spectral density of the nonlinear part of the vortex advection can be recorded as

$$S_{\eta}(k_1, k_2) = \frac{1}{2\pi^2} \int_{-\infty}^{\infty} \int_{-\infty}^{\infty} (i_1 k_2 - i_2 k_1) \mathcal{P}(k^2 - \mathcal{D}_1 k_1 - \mathcal{D}_2 k_2) \mathcal{P} S_0(i_1, i_2) S_0^*(k_1 - i_1, k_2 - i_2) d i_1 d i_2. \quad (1)$$

For further calculations we must give the form of spectral density functions of the observed geopotential field  $S_{\Phi}(\lambda)$  and noise field  $S_{\eta}(\lambda)$ . In accordance with results of work [6] we take

$$S_0(\lambda) = B_0(0) \frac{\mathcal{P}}{2\pi(\lambda^2 + \mathcal{P})^{\frac{3}{2}}}. \quad (2)$$

where the parameters take values:  $B_{\Phi}(0) = 230 \text{ dkm}^2$ ;  $\beta = 10^{-3} \text{ km}^{-1}$ .

Spectral density noise we give as in [2] in the form

$$S_d(\lambda) = \frac{B_d(0)}{4\pi^2} e^{-\frac{\lambda^2}{4\beta^2}}. \quad (3)$$

Setting signal and noise as uncorrelated, we write

$$S_f(\lambda) = S_s(\lambda) + S_d(\lambda). \quad (4)$$

Substituting relationships (2), (4) in formula (3) and introducing (used in [6]) a change of variables:

$$\lambda_1 = \frac{\lambda}{2} + v \cos(\theta + \alpha), \quad \lambda_2 = \frac{\lambda}{2} + v \sin(\theta + \alpha), \quad (5)$$

where

$$\lambda^2 = \lambda_1^2 + \lambda_2^2$$

and the polar coordinates in plane  $\vec{k}$ :

$$\begin{aligned} k_1 &= k \cos \alpha, \\ k_2 &= k \sin \alpha, \end{aligned}$$

We obtain the expression for spectral density of the "true" component of field  $J(x, y)$ :

$$\begin{aligned} S_{J_s}(k) &= \frac{3\beta^2 B_s^2(0)}{2\pi^2 k} \int_0^{2\pi} \int_0^{2\pi} \sin^2 \theta \cos^2 \theta \frac{v dv d\theta}{\left[\left(\frac{k}{2} + v\right)^2 - 4v^2 \cos^2 \theta\right]^{\frac{3}{2}}} + \\ &+ \frac{3\beta^2 B_s^2(0)}{8\pi^2 k \beta^2} \int_0^{2\pi} \int_0^{2\pi} \sin^2 \theta \cos^2 \theta v e^{-\frac{v^2}{4\beta^2}} dv d\theta - \\ &\frac{3\beta^2 B_s^2(0) B_d(0)}{8\pi^2 k \beta^2} \int_0^{2\pi} \int_0^{2\pi} \sin^2 \theta \cos^2 \theta \frac{v e^{-\frac{v^2 + 4\beta^2 \cos^2 \theta}{4\beta^2}} dv d\theta}{\left(\frac{k}{2} + k \cos \theta - v + \beta\right)^{\frac{3}{2}}} - \\ &\frac{3\beta^2 B_s^2(0) B_d(0)}{8\pi^2 k \beta^2} \int_0^{2\pi} \int_0^{2\pi} \sin^2 \theta \cos^2 \theta \frac{v e^{-\frac{v^2 + 4\beta^2 \sin^2 \theta}{4\beta^2}} dv d\theta}{\left(\frac{k}{2} - k \cos \theta + v + \beta\right)^{\frac{3}{2}}}. \quad (6) \end{aligned}$$

The first integral is equal to the right side of formula (1) and expresses the spectral density of the field  $J(x, y)$ , calculated according to observed values of  $\Phi(x, y)$ , and is found in [6]:

$$\frac{6\pi B_0^2(0)}{\pi k} \left[ \frac{8\pi^2 + k^2}{4(4\pi^2 + k^2)^2} - 1 \right].$$

Finding the second integral also is not difficult:

$$\int_0^{\pi} \sin^2 \theta \cos^2 \theta d\theta \int_0^{\infty} e^{-\frac{v}{2a}} dv = \frac{\pi}{4} 8a^2 = 2\pi a^2.$$

The third and fourth integrals in expression (6) were found numerically. The formula for calculating the smoothing operator we write in the form

$$K(\rho) = \frac{1}{2\pi} \int_0^{\infty} \frac{S_j(h)}{S_{j'}(h)} J_0(K\rho) h dh. \quad (7)$$

where  $J_0(K\rho)$  - Bessel function of the 1st kind of zero order.

During numerical calculation of operator  $K(\rho)$  the selection of the upper boundary of integration was dictated by the following considerations.

In solving forecast problems the usual assignment of meteorological fields which take part in the process of precomputation in the form of a discrete sequence of their values limits from above the frequency range in spectral decompositions of these fields. In accordance with the theorem of Kotel'nikov [5] maximum wave numbers for a right-angled grid in the  $x, y$  directions are determined from

$$k_{1\max} = \frac{\pi}{h_1} \text{ and } k_{2\max} = \frac{\pi}{h_2}.$$

where  $h_1, h_2$  are the grid intervals in the  $x, y$  directions. For a square grid it is apparent that

$$k_{\max} = \frac{\pi}{h} \sqrt{2}.$$

For  $h = 300 \text{ km}$   $\lambda_{\text{max}} = 1.5 \cdot 10^{-2} \text{ km}^{-1}$

Results of calculations according to formula (7) at various values of parameters  $\alpha$  and  $B_n(0)$ , characterizing the average scale of the noise field and the mean-square value of this field are in Fig. 1.

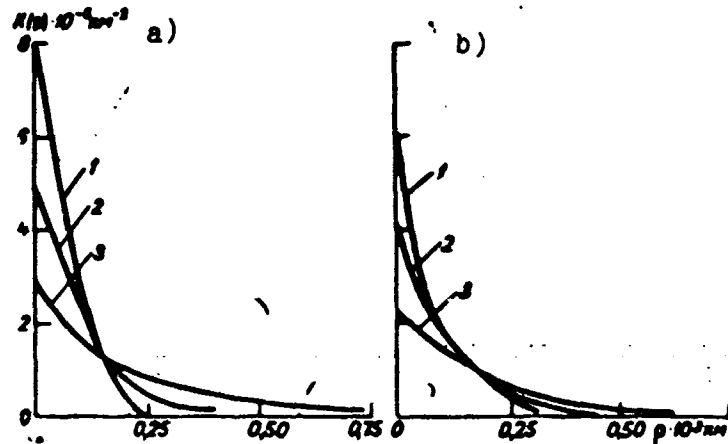


Fig. 1. Weight functions for smoothing the nonlinear part of vortex advection  $B_n(0)/B_\phi(0) = 0.02$  (a), when  $B_n(0)/B_\phi(0) = 0.1$  (b).  $1 - \alpha = 3 \cdot 10^{-3} \text{ km}^{-1}$ ,  $2 - \alpha = 1.1 \cdot 10^{-3} \text{ km}^{-1}$ ,  $3 - \alpha = 0.7 \cdot 10^{-3} \text{ km}^{-1}$ .

In order to use the obtained function  $K(\rho)$  we found integrals of form:

$$K_{0-a_1} = \int_0^{2\pi} \int_0^{a_1} K(\rho) \rho d\rho d\theta.$$

$$K_{a_1-a_2} = \int_0^{2\pi} \int_{a_1}^{a_2} K(\rho) \rho d\rho d\theta.$$

Replacing values of the neutralized function  $f(x, y)$  in a circle of radius  $a_1$  and in rings  $a_1 - a_2$  etc. by the universal means in these ranges  $\overline{f_{0-a_1}(x, y)}$ ,  $\overline{f_{a_1-a_2}(x, y)}$ , ... we obtain the working formula for smoothing of the form

$$\overline{f(x, y)} = K_{0-a_1} \overline{f_{0-a_1}(x, y)} + K_{a_1-a_2} \overline{f_{a_1-a_2}(x, y)} + \dots \quad (8)$$

The system accepted in this work for smoothing is seen in Fig. 2.  
The following working formulas for smoothing were used:

$$\begin{aligned}
 & \text{I. } \frac{B_n(0)}{B_0(0)} = 0,02 \\
 & a = 3,0 \cdot 10^{-3} \text{ км}^{-1}, \\
 & \bar{J} = 0,95\bar{J}_{0-200} + 0,05\bar{J}_{200-450}; \\
 & a = 1,1 \cdot 10^{-3} \text{ км}^{-1}, \\
 & \bar{J} = 0,87\bar{J}_{0-200} + 0,11\bar{J}_{200-450} + 0,02\bar{J}_{450-800}; \\
 & a = 0,7 \cdot 10^{-3} \text{ км}^{-1}, \\
 & \bar{J} = 0,65\bar{J}_{0-200} + 0,27\bar{J}_{200-450} + 0,08\bar{J}_{450-800}.
 \end{aligned}$$

$$\begin{aligned}
 & \text{II. } \frac{B_n(0)}{B_0(0)} = 0,1 \\
 & a = 3,0 \cdot 10^{-3} \text{ км}^{-1}, \\
 & \bar{J} = 0,91\bar{J}_{0-200} + 0,09\bar{J}_{200-450}; \\
 & a = 1,1 \cdot 10^{-3} \text{ км}^{-1}, \\
 & \bar{J} = 0,79\bar{J}_{0-200} + 0,19\bar{J}_{200-450} + 0,02\bar{J}_{450-800}; \\
 & a = 0,7 \cdot 10^{-3} \text{ км}^{-1}, \\
 & \bar{J} = 0,62\bar{J}_{0-200} + 0,29\bar{J}_{200-450} + 0,09\bar{J}_{450-800}.
 \end{aligned}$$

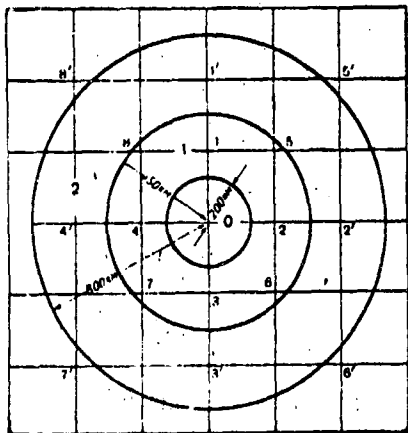


Fig. 2. Partition of area during the smoothing and numeration of points.

### Filtration of the Nonlinear Part of the Individual Wind Derivative

Let us find now the operator of optimum smoothing for an expression widespread in meteorological applications

$$F(x, y) = u \frac{\partial u}{\partial x} + v \frac{\partial u}{\partial y},$$

where  $u, v$  - components of wind velocity.

Let us present  $F, u, v$  in the form of stochastic integrals:

$$\begin{aligned} F(x, y) &= \iint_{-\infty}^{\infty} e^{i(k_1 x + k_2 y)} dZ(k_1, k_2), \\ u(x, y) &= \iint_{-\infty}^{\infty} e^{i(\lambda_1 x + \lambda_2 y)} dZ_u(\lambda_1, \lambda_2), \\ v(x, y) &= \iint_{-\infty}^{\infty} e^{i(\lambda_1 x + \lambda_2 y)} dZ_v(\lambda_1, \lambda_2). \end{aligned} \quad (9)$$

Differentiating, we write

$$F = - \iiint_{-\infty}^{\infty} e^{i(\lambda_1 - \nu_1)x + i(\lambda_2 - \nu_2)y} dZ_u^*(\lambda_1, \lambda_2) [\lambda_1 dZ_u(\nu_1, \nu_2) + \lambda_2 dZ_v(\nu_1, \nu_2)].$$

Substituting the components of wave vector  $\vec{\nu}$  with the aid of relationships

$$\nu_1 = \lambda_1 - k_1 \text{ and } \nu_2 = \lambda_2 - k_2.$$

Setting  $u$  and  $v$  as independent and in accordance with the results of [1] spectral densities  $u$  and  $v$  identical, we obtain the following expression for spectral density  $F(x, y)$ :

$$S_F(k_1, k_2) = \iint_{-\infty}^{\infty} [(2\lambda_1 - k_1)^2 + (\lambda_2 - k_2)^2] S_u(\lambda_1, \lambda_2) S_u^*(k_1 - \lambda_1, k_2 - \lambda_2) d\lambda_1 d\lambda_2. \quad (10)$$

As the wind correlation function we took an expression obtained in [1]

$$B_u(\rho) = B_u(0) J_0(l\rho) e^{-\gamma\rho^2}, \quad (11)$$

where

$$\begin{aligned} B_u(0) &= 250 \text{ m}^2 \text{ s}^{-2}, \quad \alpha = 0,797, \\ \gamma &= 0,684, \quad l = 1,28. \end{aligned}$$

<sup>1</sup>For the operator  $F'(x, y) = u \frac{\partial v}{\partial x} + v \frac{\partial u}{\partial y}$ , obviously, it is possible to write

$$S_{F'}(k_1, k_2) = \iint_{-\infty}^{\infty} [(\lambda_1 - k_1)^2 + (2\lambda_2 - k_2)^2] S_u(\lambda_1, \lambda_2) S_u^*(k_1 - \lambda_1, k_2 - \lambda_2) d\lambda_1 d\lambda_2.$$

The function of spectral density of noises was assigned in the form

$$S_n(\lambda) = \frac{B_n(0)}{2\pi a^2} e^{-\frac{(b-\lambda)^2}{a^2}}, \quad (12)$$

where the parameter  $b$  characterizes the position of maximum spectral density.

Considering relationships (4) and (10), we write the expression for spectral density of the "true" component of the field  $F(x, y)$

$$\begin{aligned} S_F(k_1, k_2) = & \int_{-\infty}^{\infty} \int_{-\infty}^{\infty} [(2\lambda_1 - k_1)^2 + (\lambda_2 - k_2)^2] S_u(\lambda_1, \lambda_2) S_u^*(k_1 - \lambda_1, k_2 - \lambda_2) d\lambda_1 d\lambda_2 - \\ & - \int_{-\infty}^{\infty} \int_{-\infty}^{\infty} [(2\lambda_1 - k_1)^2 + (\lambda_2 - k_2)^2] S_u(\lambda_1, \lambda_2) S_u^*(k_1 - \lambda_1, k_2 - \lambda_2) d\lambda_1 d\lambda_2 - \\ & - \int_{-\infty}^{\infty} \int_{-\infty}^{\infty} [(2\lambda_1 - k_1)^2 + (\lambda_2 - k_2)^2] S_u(\lambda_1, \lambda_2) S_u^*(k_1 - \lambda_1, k_2 - \lambda_2) d\lambda_1 d\lambda_2 + \\ & + \int_{-\infty}^{\infty} \int_{-\infty}^{\infty} [(2\lambda_1 - k_1)^2 + (\lambda_2 - k_2)^2] S_u(\lambda_1, \lambda_2) S_u^*(k_1 - \lambda_1, k_2 - \lambda_2) d\lambda_1 d\lambda_2, \end{aligned} \quad (13)$$

where

$$S_u(\lambda_1, \lambda_2) \text{ and } S_u^*(\lambda_1, \lambda_2)$$

are determined by formulas (11) and (12).

The first integral in the right side of (13) expresses the spectral density of field  $F(x, y)$ , calculated in terms of observed values of  $u, v$ .

Obtained as a result of numerical integration, functions  $S_F(k_1, k_2)$  and  $S_F^*(k_1, k_2)$  were, as one would expect, even. Considering this, and likewise the anisotropism of these functions, let us write down the expression for optimum smoothing of field  $F$

$$K(x, y) = \frac{1}{4\pi^2} \int_{-\infty}^{\infty} \int_{-\infty}^{\infty} \cos(k_1 x + k_2 y) \frac{S_F(k_1, k_2)}{S_F^*(k_1, k_2)} dk_1 dk_2. \quad (14)$$

The contour lines of function  $K(x, y)$  for some values of  $a$  and  $b$  are given in Fig. 3 (the picture obviously is symmetric with respect to the axes of coordinates).

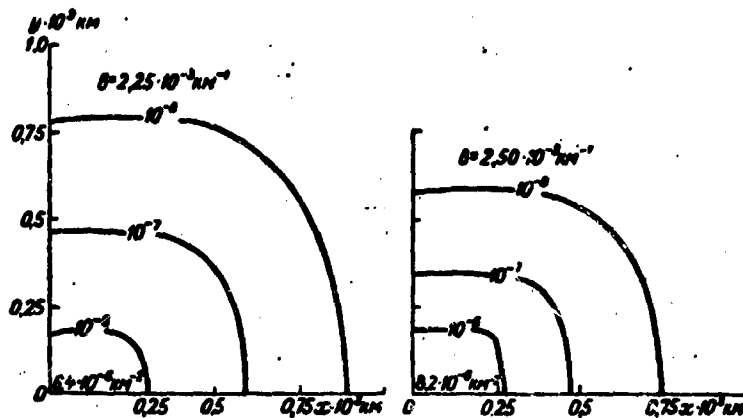


Fig. 3. Weight functions  $K(x, y)$  for the smoothing of field  $F$  when  $B_n(0)/B_u(0) = 0.04$  and  $a = 0.7 \cdot 10^{-3} \text{ km}^{-1}$ .

The most interesting result in this case is an anisotropism of the smoothing operator, which is explained by the different character of change in spectral densities of signal and noise (different degree of anisotropism) during the transformation (12). We must note that from the anisotropism of conversion (10) follows immutable anisotropism of  $K(x, y)$ : any linear anisotropic conversion, for example, differentiation according to one of the variables, retains the isotropism of the smoothing operator.

The degree of averaging in the direction of the  $X$  axis with certain characteristics of noises is almost one and a half times greater than the degree of averaging along the  $Y$  axis near the point to which the value of the neutralized field belongs. With distance from the origin of coordinates function  $K(x, y)$  becomes more isotropic.

Smoothing formulas were obtained by means analogous to those described in the previous section. Let us give the results of

calculations for certain values of noise parameters (the arrangement of points is given in Fig. 1):

$$\frac{B_n(0)}{B_s(0)} = 0,04;$$

I.  $b = 2,5 \cdot 10^{-3} \text{ км}^{-1}$   
 1)  $a = 0,7 \cdot 10^{-3} \text{ км}^{-1}$ ,  
 $\bar{F} = 0,72F_0 + 0,06(F_2 + F_1) + 0,02(F_1 + F_3 + F_5 + F_6 + F_7 + F_8 + F_2 + F_4)$ ;  
 2)  $a = 0,4 \cdot 10^{-3} \text{ км}^{-1}$ ,  
 $\bar{F} = 0,77F_0 + 0,05(F_2 + F_1) + 0,016(F_1 + F_3 + F_5 + F_6 + F_7 + F_8 + F_2 + F_4)$ ;

II.  $b = 2,25 \cdot 10^{-3} \text{ км}^{-1}$   
 1)  $a = 0,7 \cdot 10^{-3} \text{ км}^{-1}$ ,  
 $\bar{F} = 0,51F_0 + 0,125(F_2 + F_1) + 0,022(F_1 + F_3 + F_5 + F_6 + F_7 + F_8 + F_2 + F_4) + 0,01(F_1 + F_3 + F_5 + F_6 + F_7 + F_8)$ ;  
 2)  $a = 0,4 \cdot 10^{-3} \text{ км}^{-1}$ ,  
 $\bar{F} = 0,55F_0 + 0,11(F_2 + F_1) + 0,02(F_1 + F_3 + F_5 + F_6 + F_7 + F_8 + F_2 + F_4) + 0,01(F_1 + F_3 + F_5 + F_6 + F_7 + F_8)$ . (15)

Smoothing formulas (15) show that the degree of smoothing depends mainly on the magnitude of parameter  $b$  or, in other words, on the degree of overlap of the spectras of signal and noise. With an increase in the overlap naturally, it increases.

#### Using Filtration in the System of Wind Forecasting

Results obtained in the previous section were used in the one-level system of wind forecasting described in [3].

Here briefly is its variant, using as raw data the fields of actual wind.

Motion equations are written in the form:

$$\frac{du}{dt} = lv'; \quad \frac{dv}{dt} = -lu', \quad (16)$$

where  $u'$ ,  $v'$  are the components of the deviation of wind from geostrophic;

$$\frac{du}{dt} = \frac{\partial u}{\partial t} + u \frac{\partial u}{\partial x} + v \frac{\partial u}{\partial y},$$

$$\frac{dv}{dt} = \frac{\partial v}{\partial t} + u \frac{\partial v}{\partial x} + v \frac{\partial v}{\partial y}.$$

The remaining designations are generally accepted. The Ageostrophic part of the stream function is connected to  $u'$ ,  $v'$  by the relationships:

$$u' = -\frac{\partial \psi'}{\partial y}; \quad v' = \frac{\partial \psi'}{\partial x}. \quad (17)$$

Values of  $\psi'$  can be determined according to the field of practical wind from the balance equation

$$\Delta \psi' = \left(\frac{\partial u}{\partial x}\right)^2 + \left(\frac{\partial v}{\partial y}\right)^2 + 2 \frac{\partial u}{\partial y} \frac{\partial v}{\partial x} - v \frac{\partial u}{\partial x} + u \frac{\partial v}{\partial y}.$$

Further, with the aid of relationships (17) we find  $u'$  and  $v'$  and integrate equations (16) over time. The integration was in Lagrangian coordinates, which was connected with interpolation of the values of wind components every grid interval in the inside areas of the grid squares. The latter led to noticeable leveling of results.

Attempts to integrate these equations in Euler coordinates with the aid of relationships:

$$u^{(n+1)} = u^{(n)} + \delta t \left( v^{(n)} - u^{(n)} \frac{\partial u^{(n)}}{\partial x} - v^{(n)} \frac{\partial u^{(n)}}{\partial y} \right),$$

$$v^{(n+1)} = v^{(n)} - \delta t \left( u^{(n)} \frac{\partial v^{(n)}}{\partial x} + v^{(n)} \frac{\partial v^{(n)}}{\partial y} \right). \quad (18)$$

where  $n$  is the number of the time interval, were unsuccessful - in the absence of smoothing the system was unstable. Its stability was achieved after a number of experiments by smoothing in accordance with the above results. On every time step the smoothing was carried out twice: the sums of the nonlinear terms in the right side of equations (18) by formula (15), while the most successful results were obtained with the following values of parameters:

$$\frac{B_n(0)}{B_n(0)} = 0.04, \quad b = 2.5 \cdot 10^{-3} \text{ km}^{-1}.$$

and weak smoothing of wind components according to formula

$$\bar{u} = 0.94u_0 + 0.015 \sum_{i=1}^4 u_i.$$

where  $u$  is the wind component.

Results of the estimation of forecast quality are in Table 1, where  $|\bar{C}_0 - \bar{C}_d|$  - mean absolute error of wind prognostication,  $|\Delta \bar{C}_0|$  - mean modulus of vectorial wind variability for twenty-four hours.

Integration of forecast equations for formulas (18) using precalculated smoothing somewhat improved results in comparison with the earlier variant systems, which is connected in our opinion basically with obtaining more practical values of the absolute values of wind velocity. Furthermore, utilization of formulas (18) considerably simplified the computer program and shortened calculation time in comparison with the previous variant.

Table 1.

Date	Bilinear interpolation (Langrangian coordinates)		Optimum filtration (Euler coordinates)	
	$ \bar{C}_0 - \bar{C}_d $ (m/s)	$\frac{ \bar{C}_0 - \bar{C}_d }{ \Delta \bar{C}_0 }$	$ \bar{C}_0 - \bar{C}_d $ (m/s)	$\frac{ \bar{C}_0 - \bar{C}_d }{ \Delta \bar{C}_0 }$
Level 700 mbar				
0300 2 Mar 1960	5.7	0.64	5.6	0.64
0300 3 Mar 1960	6.4	0.75	6.3	0.73
0300 4 Mar 1960	7.0	0.77	4.6	0.82
0300 5 Mar 1960	7.2	0.86	6.5	0.78
0300 28 Feb 1961	9.4	0.68	8.9	0.66
1500 28 Feb 1961	12.6	0.75	12.0	0.74
Level 750 mbar				
0300 3 Mar 1960	3.4	0.83	3.3	0.84
0300 4 Mar 1960	6.0	1.10	5.8	1.04
0300 5 Mar 1960	3.7	0.79	3.2	0.80
0300 28 Mar 1961	6.3	0.82	6.0	0.91
1500 28 Feb 1961	6.6	0.97	6.5	0.86
Average.....	6.70	0.83	6.23	0.77

## Bibliography

1. Gandin L. S., Kuznetsova T. I. O strukture poley davleniya i vetra v sredney troposfere pri razlinnykh formakh tsirkulyatsii (The structure of pressure and wind fields in the middle troposphere with various forms of circulation). Tr. GGO, vyp. 121, 1961.
2. Strikhevskiy L. N. Ob optimal'noy fil'tratsii meteorologicheskikh poley (Optimum filtration of meteorological fields). Tr. TsIP, vyp. 146, 1965.
3. Strizhevskiy L. N. O chislennom metode prognoza vetra na urovnyakh 700 i 850 mb (Numerical method of wind prediction at 700 and 850 mbar). Tr. TsIP, vyp. 144, 1965.
4. Thompson F. Optimal'noye sglazhivaniye dvukhmernykh poley. "Chislennyye metody prognoza pogody" (Optimum smoothing of two-dimensional fields. "Numerical methods of weather forecasting"). Gidrometeoizdat, L., 1960 (Translated from Eng.).
5. Kharkevich A. A. Teoreticheskiye osnovy radiosvyazi (Theoretical bases of radio communication). Gostekhteorizdat, M., 1957.
6. Yudin M. I. Novyye metody i problemy kratkosrochnogo prognoza pogody (New methods and problems of short-range weather forecasting). Gidrometeoizdat, L., 1963.
7. Yaglom A. M. Vvedeniye v teoriyu statsionarnykh sluchaynykh funktsiy (Introduction to the theory of stationary random functions). UMN, t. I, vyp. 5, 1952.

OBJECTIVE ANALYSIS OF THE GEOPOTENTIAL FIELD USING  
SUPPLEMENTAL INFORMATION

V. D. Sovetova

Two methods of objective analysis are described. The first method is dedicated to the analysis of the isobaric surfaces of the troposphere over the northern hemisphere, and the second to analysis of stratospheric levels over Eurasia. To improve the quality of analysis over incompletely treated regions and at high altitudes additional information is used.

Numerical analysis and forecasting the baric field over the northern hemisphere is hampered in regions incompletely covered by meteorological information. The quality then drops off [7] over water surfaces of the Pacific, Atlantic, Indian Oceans, and over Africa, where there are few points of radiosounding of the atmosphere. On the other hand, for example, the territory of Eurasia on the whole is well covered by the data of observations in the troposphere and unsatisfactorily in the stratosphere. Therefore for improvement of analysis in such cases it is expedient to use additional information. Two methods of restoration and analysis of the geopotential field are considered: the first is developed for the troposphere, and the second for the stratosphere.

The first problem is solved for the northern hemisphere (grid of 1545 points, intervals at 470 km) and for four levels of the

troposphere - 1000, 850, 500 and 300 mbar. At the surface of the earth there were sufficient data for a successful analysis in almost all regions of the northern hemisphere. The quantity of information sharply falls upon transition to the higher-lying isobaric surfaces (850, 500, 300 mbar), where there are data only for the points of atmospheric sounding. To supplement information at these levels one could use the data of measurements of the surface field of pressure. For this purpose for interpolation onto points of a regular grid, except radiosonde stations ( $n = 589$ ), station of making only ground observations ( $n = 290$ ) have been used. Over the oceans sources of additional information are observations of 48 ships of the merchant marine.

The quantity of information on 100 and 850 mbar was substantially different, therefore before objective analysis were reconstructed absent measurements of the geopotential at 850 mbar according to available data of surface pressure; the absent information for 300 mbar was reconstructed according to data for 500 mbar.

Reconstruction of unavailable information was conducted by the method of spatial optimum interpolation [3] using mutual correlation functions of the geopotential [8] for 1000 and 850 mbar, 500 and 300 mbar. Reconstruction could have used simultaneously the data of the lower and original levels. However, because information at the original level as a rule is absent in those points around which at a distance of the radius of correlation there are no data of observations, for its reconstruction the information of five stations of one lower level better covered by meteorological information was used. One of these five stations had to lie on one vertical line with the station of the original level, and the remaining four were selected such that each of them covered one of the four quadrants arranged around the reference station. When in the circle with the correlation radius it was not possible to find four symmetric stations in which there would be data of measurements, any four stations were selected, independently of their arrangement around a point. But even if this condition could not be made, reconstruction used the information of only one lower point.

As a result of the reconstruction, subsequently in the interpolation onto regular grid points of the geopotential of 1000 and 850 mbar 879 stations can take part; objective analysis of the baric field of 500 and 300 mbar is carried out from the data of 589 radiosonde stations.

To estimate the quality of the reconstruction by the above means a numerical experiment was conducted by means of the artificial exclusion of the entire information on 850 mbar. The mean square error of reconstruction of the geopotential of 850 mbar from the data of 0300 21 January 1964 was 4.6 dam over all the northern hemisphere, 3.3. dam over North America and 4.3 dam over western Europe. The geopotential of 500 mbar was reconstructed analogously from data for 850 mbar with a mean square error of 5.0 dam; data for 300 mbar was reconstructed from data for 500 mbar with a mean square error of 7.6 dam. Taking into account that under practical conditions reconstruction of information is necessary only in the inadequately covered regions and the obtained errors are somewhat less than the corresponding deviations from climatic standards which must be used here, the results of the reconstruction can be considered satisfactory.

Comparison of standardized autocorrelation functions of the geopotential showed the proximity of functions for 1000 and 850 mbar and also the proximity of the functions of 500 and 300 mbar. The difference of correlation functions between the first and second pairs of surfaces is rather substantial. In connection with this the objective analysis of the reconstructed fields was carried out in two stages: is from the beginning for isobaric surfaces of 1000 and 850 mbar, after that for another pair of surfaces - 500 and 300 mbar.

The objective analysis was conducted by the method of optimum interpolation [4]. Not describing all units of the program, let us stop only on its separate parts, determining the distinction of our methodologies from the methodology accepted at the Hydrometeorological Center of the USSR [6].

1. For the characteristic features of the average climatic fields of the geopotential (of standards) on 1000 and 500 mbar were assigned fields, calculated in NIIAK [1]. Standards for two other surfaces (850 and 300 mbar) were calculated by the formula:

$$\begin{aligned} Z_{850} &= Z_{1000} + \overline{\Delta Z}_{1000}^{850}, \\ Z_{300} &= Z_{1000} + \overline{\Delta Z}_{1000}^{300}, \end{aligned}$$

where  $\overline{\Delta Z}$  - average climatic value of the thickness of the layer between the corresponding isobaric surfaces, figured according to the formulas:

for winter

$$\begin{aligned} \overline{\Delta Z}_{1000}^{850} &= -32.5(\sin \varphi)^2 + 7.5 \sin \varphi + 140, \\ \overline{\Delta Z}_{1000}^{300} &= -48.0(\sin \varphi)^2 + 380, \end{aligned}$$

for summer

$$\begin{aligned} \overline{\Delta Z}_{1000}^{850} &= -38.5(\sin \varphi)^2 + 27.5 \sin \varphi + 140, \\ \overline{\Delta Z}_{1000}^{300} &= -34.5(\sin \varphi)^2 + 7.5 \sin \varphi + 385. \end{aligned}$$

Comparison of actual standards of the geopotential for 850 and 300 mbar with calculated standards showed their close correspondence.

2. The stations were situated in such a way that their ordinal numbers increased along the band and from one band to another. The first station of every band took on the feature by which the bands were estimated. During interpolation onto the point with coordinates  $x, y$  the number of bands was calculated beginning from the first, and the sum was equated with  $y - 3$ . The comparison determined in which half of the bands (right or left) the point is located. Only those stations which were located in the same half as the point and which were located in the band between  $(y - 3)$  and  $(y + 3)$  were tested to see if they belonged to the neighborhood of the considered point. As soon as they began to follow stations with coordinates more than  $(y + 3)$ , the search ceased.

3. The interpolation onto regular grid points was conducted in the following manner. From the beginning an attempt was made to select the eight nearest stations, two stations in each quadrant. If this requirement was not fulfilled, eight asymmetrical stations were used. If in the whole square of  $6 \times 6$  grid intervals there were not eight stations with data from observations, the choice went to four stations satisfying the requirement of symmetry. If four asymmetrical stations were lacking, only two stations were used. To calculate the weight coefficients a system of equations of the eighth, fourth or second order was made up, depending on how many stations with measurement data were found.

On the edges of the map frequently it was not possible to find in a given square even two stations. In this instance in points on 1000 and 850 mbar the corresponding climatic values were used. Usually these points were in the southern latitudes, where the dispersions were small, and that is why the absolute errors of calculation were small.

On 500 and 300 mbar the interpolation onto points was done from eight or four stations. With fewer stations interpolation was replaced by extrapolation from the lower surface analogously the reconstruction of lacking information. The only difference is that in the first case the information was reconstructed for a station, and in the second case for a regular grid point according to data for a point located on the underlying surface (850 mbar). After this procedure the value of the geopotential in a point at 300 mbar was calculated by means of extrapolation to the upper level of the value in the same point of 500 mbar. In these cases spatial extrapolation of deviations from standard along one lower point was conducted.

Comparison of results of objective and synoptic analyses obtained mean square errors of comparison for two types of points. The first type includes points to which interpolation was produced according to the data of the considered level; the second type

includes points to the values of geopotentials which showed the effect of extrapolation from below or these values are equal to the middle climatic value. Errors in decameters are presented in Table 1.

Table 1.

Surface, mbar.....	1000	850	500	300
$\sigma$ dam:				
first type.....	1.7	2.8	2.9	6.5
second type.....	2.1	2.9	6.0	8.9

As can be seen from the tables, using standards on the edges of the map instead of interpolated values increases the error of comparison by 0.4 dam on 1000 mbar; the increase of error (by 0.1 dam) on 850 mbar is entirely insignificant. On 500 and 300 mbar the error of comparison substantially increases for cases of extrapolation from below (to 3.1 and 2.4 dam, respectively). This increase can be explained uniquely, because it is conditioned not only by the difference of methods of calculation, but also by the considerable drop in quality of synoptic analysis at these levels.

Comparison of the amounts of deviations (Table 1) with standard deviation, which is given in a work of S. A. Mashkovich and S. I. Gubanova [7], indicates the better quality of objective analysis of 1000 mbar geopotential surfaces for our method. Here, obviously, we see the effect both the using the additional information, and using the autocorrelation function of the considered level in calculations instead of the function of the geopotential at 500 mbar for all levels.

To estimate the effect on numerical analysis of the additional information over sea water surfaces the following experiment was conducted. The data of ships of the merchant marine were artificially excluded and the obtained analysis was equated with the analysis of the usual variant. Mean square errors  $\sigma$ , obtained during

the comparison of these two analyses, are given in Table 2. Here is shown the number of points  $n$  in which was discovered the difference in these analyses.

Table 2.

Surface, mbar....	1000	850	500	300
$\sigma$ dam.....	9.2	9.2	10.6	12.9
$n$ .....	214	207	211	211

As can be seen from this table, measurements of pressures on 48 ships show the effect on values of the geopotential in large quantities of regular grid points, and the difference in analyses is rather considerable. For 1000 mbar, where the oceans are covered considerably better by the information than at heights and, consequently, synoptic analysis is more reliable, the objective analysis in the absence of data from additional ships was compared with synoptic analysis. It turned out that the absence of additional ships increases the mean square error of objective analysis over oceans in comparison with synoptic analysis by 8.6 dam, i.e., it can be considered that the effect of additional information on the results of numerical analysis is rather considerable.

During the analysis of calculated fields of pressure over all the northern hemisphere it was explained that in the inadequately covered water surfaces of the oceans during extrapolation from lower levels to 500 and 300 mbar deeper cyclones than noted on the operational constant-pressure charts are obtained. The authenticity of the calculated values is difficult to verify, because synoptic analysis in these regions is accomplished according to the data of the observations of one or two stations. However, the wind data allow proposing the presence here of gradients greater than noted on the map. For example, 21 January 1964 in the center of a cyclone over the Atlantic Ocean ( $42^\circ$  north lat. and  $37^\circ$  west long.) our calculations obtain a value of the geopotential for 500 mbar of 512 dam. On a constant-pressure map prepared by the forecasters at

GMTs SSSR [Hydrometeorological Center USSR] in the center of this cyclone a height of 517 dam is noted; on the map of another forecasting institution in the center of the cyclone a height of 530 dam is noted. Thus, our data differ in the first case by 5 dam, and in the second by 18 dam. The actual depth of the cyclone and its accurate location are unknown inasmuch as in the range of the cyclone there are observations of only individual stations.

The second problem was solved for levels of the stratosphere over the territory of Europe and Asia ( $29 \times 22$  grid, interval 450 km). The primary surface whose data (geopotential  $Z$  and temperature  $t$ ) were used for the reconstruction of information on higher levels was 200 mbar. Selecting this surface avoids the effect of tropopause; losses of information at this level in comparison with 300 mbar are insignificant (2-3%).

Analysis of our autocorrelation functions of the geopotential for stratospheric levels showed a substantial difference between functions for 100 mbar and for 300 and 200 mbar. Therefore analysis at 100 mbar was conducted using the autocorrelation functions corresponding to this level.

After monitoring the original  $Z$  and  $t$  data [5], the missing  $Z$  and  $t$  information was reconstructed at the primary 200 mbar level by the method of optimum interpolation [4] according to the observations of eight stations. Values at stations located on the edges of the maps were reconstructed in some other way. For these stations ( $n = 60$ ) separately from the general field the field of pressure and temperature was assigned according to a previous map (radiosonde data if available, or values taken from isohypses). In the absence of information after a similar period, the values of pressure and temperatures at the regional stations their values in a previous period of observations were taken. As a result of reconstruction on 200 mbar we had data about geopotential and temperature in 439 points.

Using further the mutual correlation functions of temperature [2], by the method of spatial interpolation [3] the missing temperature was reconstructed on 100 mbar (note that the missing information at this level comprises 15-20% of the relative surface at 300 mbar, not including erroneous data). Then according to the average temperature of the layer the height of the surface at 100 mbar was resolved in the points where there was no or rejected information.

Before objective analysis all available information was again monitored. Rejected data were reconstructed by the method of optimum interpolation on a fixed level. Because the accepted methodology of reconstruction of information allows having at all levels always the same number of data, it is possible to attach at every regular grid point the very best located stations according to the data of which the interpolation will be carried out. In the first place objective analysis was conducted for the central rectangle (24 × 16 points), then for surrounding rectangles using already calculated values in certain points lying on the contour of the central rectangle.

#### Bibliography

1. Aeroklimaticheskiy atlas severnogo polushariya (Aeroclimatic atlas of the northern hemisphere). t. 1, 2, NIIAK, 1961.
2. Boltenkov V. P. Issledovaniye statisticheskoy makrostruktury temperatury vozdukha (Investigation of the statistical macrostructure of air temperature). Tr. GGO, vyp. 165, 1964.
3. Boltenkov V. P. O trekhmernom ob'yektivnom analize polya temperatury vozdukha (Three-dimensional objective analysis of the temperature field of air). Tr. GGO, vyp. 191, 1966.
4. Gandin L. S. Ob'yektivnyy analiz meteorologicheskikh poley (Objective analysis of meteorological fields). Gidrometeoizdat, L., 1963.
5. Krichak M. O. Opyt ob'yektivnogo kontrolya iskhodnykh dannykh pri operativnom prognoze polya geopotentsiala (Experiment in objective control of raw data in operational forecasting of the geopotential field). Collection "Ob'yektivnyy analiz i prognoz meteorologicheskikh elementov," Izd. AN SSSR, M., 1963.

6. Mashkovich S. A. Ob ob'yektivnom analize kart baricheskoy topografii severnogo polushariya (Objective analysis of constant-pressure maps of the northern hemisphere). Tr. MMTs, vyp. 4, 1964.

7. Mashkovich S. A., Gubanova S. I. Opyt primeneniya metodiki ob'yektivnogo analiza kart baricheskoy topografii severnogo polushariya (Experiment in using the methodology of objective analysis of constant-pressure maps of the northern hemisphere). Tr. MMTs, vyp. 10, 1965.

8. Fortus M. I. Trekhmernaya prostranstvennaya struktura polya geopotentsiala (Three-dimensional spatial structure of the geopotential field). Tr. GGO, vyp. 165, 1964.

Improving the Methodology of Forecasting Baric  
Field to Several Days

Mashkovich S. A., Transactions GMTs, 1968,  
No. 19, pp. 3-9

A generalization is made of a prediction system proposed earlier by S. A. Mashkovich and Ya. M. Kheyfets (Transactions TsIP, No. 93). The generalization consists of recording the effect of horizontal turbulent mixing in the vortex equation and the effect of surface friction. The latter is introduced when the boundary condition at sea level for the vertical component of velocity is recorded. The original equations are vortex and heat influx equations, linearized relative to the zone of motion. A three-level model of the atmosphere is considered. Motion is assumed to be quasi-solenoidal. The solution for the stream function is looked for in the form of a series in spherical functions. The problem was solved by computer. Seventeen series of forecast maps for a period up to four days were calculated. The quality of the forecasts for four days is estimated. Thanks to the generalization of the system it was possible to diminish the absolute forecast error on the average by 15-20%. In July 1966, the composition of forecasts of ground pressure by this system became operational.

Table 1, Ill. 1, Bibl. 3.

One Finite-Difference Algorithm for the Solution of  
the Vortex Equation for the Middle Troposphere  
Over the Northern Hemisphere

Isayev N. V. and Fuks-Rabinovich M. S., Transactions  
GMTs, 1968, No. 19, pp. 10-21

A system for forecasting the geopotential at the middle troposphere over the northern hemisphere is examined. To prevent non-linear instability a finite-difference approximation of nonlinear terms was used, proposed by A. Arakava. With such an approximation there is conservation of the quadratic integral features, i.e., conservation on the forecast range of the integrals of the vorticity rate, its square and kinetic energy. Integration in time was conducted using several methods, among which most suitable was the Adams method.

The system was used to execute calculations over a long period in order to steady the character of change in kinetic energy of forecast fields  $H_{500}$  in time. It turned out that the finite-difference algorithm allows calculation of a forecast over long periods, moreover the kinetic energy of forecast fields during calculation remains practically constant. Results of testing the system over a period of up to three days are presented, and a quantitative and qualitative analysis of the obtained forecast fields are given.

Table 3, Ill. 5, Bibl. 14.

Experiment in the Numerical Solution of Balance Equations  
Within the Framework of a Quasi-Solenoidal System of  
Forecasting the Geopotential on the  
Northern Hemisphere

Sitnikov I. G. and Krichak S. O., Transactions  
GMTs, 1968, No. 19, pp. 22-30

A finite-difference system for solving the balance equation on the northern hemisphere is given, and a number of characteristic features found with the solution of this equation within the framework of the quasi-solenoidal system of forecasting the geopotential at the middle troposphere.

For solving the balance equation the method of successive approximations is used, and the balance equation is reduced to a Poisson equation relative to the stream function and values of the right side are determined from the previous approximation. One feature of the solution of the balance equation is the reduction of the rate of convergence of the iteration process in the low latitudes.

Obtained as a result of solving the balance equation, the field of the stream function is used as the original for the quasi-solenoidal forecast based on a barotropic model. At the end of each forecast period, i.e., after 24, 48 and 72 hours, the geopotential field is located by inversion of the balance equation, i.e., solving it relative to the geopotential according to the known distribution of the stream function.

An example of calculating a forecast from the quasi-solenoidal model is presented, and it is compared with a quasi-geostrophic forecast.

Ill. 6, Bibl. 9.

About Research on Warming Trends in the Stratosphere  
Using Numerical Experiments

Barg B., Mashkovich S. A., Transactions GMTs,  
1968, No. 19, pp. 31-43

The evolution of a narrow band of temperature perturbation in the stratosphere is studied. The starting equations are those proposed by A. S. Dubov (Transactions GGO, No. 124). The investigation is conducted according to stylized initial conditions: it assumes that the original temperature perturbation has a circular form and occupies a limited range. An initial disturbance of the baric field is absent. Finite-difference approximation of equations is described, a numerical method of solution is formulated, the calculating stability of the solution is investigated.

Preliminary results are given on the basis of which the following basic conclusions are made:

1) the range of temperature perturbation used in the calculations does not substantially affect circulation in the stratosphere, specifically, the polar vortex does not break down;

2) perturbation in the temperature field also causes a perturbation of the baric field, the range of which grows in the considered period of time (4-6 days), while the range of the temperature perturbation diminishes;

3) maximum pressure perturbation remains during the first 48 hours at the same latitude on which the temperature perturbation lay, then the geopotential perturbation shifts to the north, while the temperature perturbation remains at the original latitude.

Table 1, Ill. 4, Bibl. 10.

Application of the Theory of Filtration of Random Processes to Certain Problems in Objective Analysis

Ovchinskiy B. V., Transactions GMTs, 1968,  
No. 19, pp. 44-57

Formulas are set for calculating weight functions of optimum interpolation and smoothing meteorological elements when correlation function of the true magnitude (signal) and observation errors (noise) are known.

During optimum interpolation one must take into account that the data of observations contain random errors, and an attempt is made to achieve a magnitude of the meteorological element in a regular grid point free from these random errors. If the examination includes small-scale fluctuations, then it is necessary to reject the assumption of noncorrelatability of the random errors. This circumstance was pointed out by Thompson, who used the theory of filtration of random processes for optimum smoothing of meteorological fields.

The structure and features of weight functions were studied both for discrete and continuous data of observations. The problem of determining weight functions reduces to solving the integral Wiener-Hopf equation (or a discrete model of the Wiener-Hopf equation). Of the various ways of solving this equation the method of indeterminate coefficients was used; in this case the correlation function is approximated by the sum of the model functions.

Cases of a solution when errors of observation are "white noise" or when the number of stations increases without limit are examined also.

Ill. 6, Bibl. 11.

Filtration of Fields Obtained as a Result of Nonlinear  
Transformations of the Original Values of  
Meteorological Elements

Strizhevskiy L. N., Transactions GMTs, 1968,  
No. 19, pp. 58-66

It is assumed that observable values of meteorological elements are the sum of their actual values and measurement errors. The statistical characteristics of such summary fields are known from the results of treatment of the data of observations, and statistical characteristics of the error fields were assigned on the strength of certain general considerations about the relationships of scales and intensities of fields of true values and noises.

On the basis of the theory of optimum linear filtration of two-dimensional fields filtration operators are calculated for two nonlinear transformations of original fields widespread in meteorology: the nonlinear part of vortex advection and the nonlinear part of the individual wind derivative. In obtaining the corresponding formulas the assumption of statistical isotropism and homogeneity of the original fields is used. Furthermore, it is assumed that the investigated meteorological elements are distributed normally. Calculations are conducted for various values of scales and intensities of the error field corresponding to the various degrees of complete treatment and the accuracy of measurements over the different regions. The theoretically obtained filtration operator for the nonlinear part of the individual wind derivative is used in a one-level diagram of wind forecasting, which achieved definite improvements in comparison with the variant of the system which did not use smoothing.

Table 1, Bibl. 7.

Objective Analysis of the Geopotential Field Using  
Supplemental Information

Sovetova V. D., Transactions GMTs, 1968,  
No. 19, pp. 72-77

Two methods of objective analysis of a baric field are described, and results of calculations based on one of them are given.

The first method is developed for the geopotential field of isobaric surfaces of the troposphere (1000, 850, 500 and 300 mbar) over the northern hemisphere. In poorly treated information of regions of the northern hemisphere apart from data of radiosonde stations additional information in the form of results of the measurement of pressure over the surface of the earth was used: over the oceans observations of ships of the merchant marine were used. Using mutual correlation functions of the geopotential [7], the method of spatial optimum interpolation [2] reconstructed missing

information on 850 mbar from the data of measurements of the pressure field over the surface of the earth; at 300 mbar data from 500 mbar was used. Objective analysis of the geopotential by the method of optimum interpolation [3] was conducted at first for one after that for another pair of surfaces with corresponding levels by the mean autocorrelation functions. Results of calculations showed a substantial improvement of the quality of objective analysis, especially over oceans.

The second method was developed for levels of the stratosphere over Europe and Asia. The problem of reconstruction of missing information at high altitudes and subsequent objective analysis of the baric field according to more complete raw data of observations was solved. As the basic isobaric surface according to the data of which the information was reconstructed 200 mbar was used. The additional information in this instance air temperature was used. During the first stage of solving the problem by the method of spatial optimum interpolation the missing temperature measurements were reconstructed on 100 mbar. Then based on the average temperature of the layer and the height of the underlying surface the height of the 100 mbar surface was figured. Objective analysis was carried out always for the same number of stations, which made it possible to attach preliminarily to each point the eight best located stations and to interpolate to grid point according to their information.

Table 2, Bibl. 7.

UNCLASSIFIED

Security Classification

DOCUMENT CONTROL DATA - R & D		
<i>(Security classification of title, body of abstract and indexing annotation must be entered when the overall report is classified)</i>		
1. ORIGINATING ACTIVITY (Corporate author) Foreign Technology Division Air Force Systems Command U. S. Air Force		2a. REPORT SECURITY CLASSIFICATION UNCLASSIFIED
		2b. GROUP
3. REPORT TITLE IMPROVEMENT OF THE METHODOLOGY OF FORECASTING THE BARIC FIELD FOR SEVERAL DAYS		
4. DESCRIPTIVE NOTES (Type of report and inclusive dates) TRANSLATION		
5. AUTHOR(S) (First name, middle initial, last name) Mashkovich, S. A.		
6. REPORT DATE 1968	7a. TOTAL NO. OF PAGES 9	7b. NO. OF REFS 3
8a. CONTRACT OR GRANT NO.	8b. ORIGINATOR'S REPORT NUMBER(S) FTD-MT-24-174-70	
8c. PROJECT NO. 60103		
8d. DIA TASK T69-01-69	9b. OTHER REPORT NO(S) (Any other numbers that may be assigned this report)	
10. DISTRIBUTION STATEMENT Distribution of this document is unlimited. It may be released to the Clearinghouse, Department of Commerce, for sale to the general public.		
11. SUPPLEMENTARY NOTES		12. SPONSORING MILITARY ACTIVITY Foreign Technology Division Wright-Patterson AFB, Ohio
13. ABSTRACT A generalization is given of an earlier proposed linear three-level forecast model. The effect of horizontal turbulent mixing in the vorticity equation and effects of surface friction are considered additionally. The system is computerized. An evaluation of the forecasts is given.		

DD FORM 1473  
1 NOV 65

UNCLASSIFIED

Security Classification

UNCLASSIFIED

Security Classification

14. KEY WORDS	LINK A		LINK B		LINK C	
	ROLE	WT	ROLE	WT	ROLE	WT
Weather forecasting Baric field Legendre polynomial						

UNCLASSIFIED

Security Classification

UNCLASSIFIED

Security Classification

DOCUMENT CONTROL DATA - R & D		
<i>(Security classification of title, body of abstract and indexing annotation must be entered when the overall report is classified)</i>		
1. ORIGINATING ACTIVITY (Corporate author) Foreign Technology Division Air Force Systems Command U. S. Air Force		2a. REPORT SECURITY CLASSIFICATION UNCLASSIFIED
		2b. GROUP
3. REPORT TITLE FINITE-DIFFERENCE ALGORITHM OF A SOLUTION OF THE VORTICITY EQUATION FOR THE MIDDLE TROPOSPHERE OVER THE NORTHERN HEMISPHERE		
4. DESCRIPTIVE NOTES (Type of report and inclusive dates) Translation		
5. AUTHOR(S) (First name, middle initial, last name) Isayev, N. V.; Fuks-Rabinovich, M. S.		
6. REPORT DATE 1968	7a. TOTAL NO. OF PAGES 17	7b. NO. OF REFS 14
8a. CONTRACT OR GRANT NO.	8b. ORIGINATOR'S REPORT NUMBER(S) FTD-MT-24-174-70	
a. PROJECT NO. 60103		
c.	9b. OTHER REPORT NO(S) (Any other numbers that may be assigned this report)	
d. DIA TASK T69-01-69		
10. DISTRIBUTION STATEMENT Distribution of this document is unlimited. It may be released to the Clearinghouse, Department of Commerce, for sale to the general public.		
11. SUPPLEMENTARY NOTES	12. SPONSORING MILITARY ACTIVITY Foreign Technology Division Wright-Patterson AFB, Ohio	
13. ABSTRACT A system for forecasting the geopotential at the middle troposphere using a space (in coordinates x, y) finite-difference approximation, which provided conservation of the quadratic integral features is considered (i.e., vorticity, its square and kinetic energy); integration in time follows the method of Adams. Charts of the change in average kinetic energy of forecast fields $H_{subscript 500}$ , in time are constructed. Results are given for the calculation of long-range forecasting of a brief length of time before forecast phenomenon occurrence according to the given system. (AT8025207)		

DD FORM 1 NOV 68 1473

UNCLASSIFIED

Security Classification

UNCLASSIFIED

Security Classification

14. KEY WORDS	LINK A		LINK B		LINK C	
	ROLE	WT	ROLE	WT	ROLE	WT
Long range weather forecasting Troposphere Laplace transform Atmospheric geopotential Jacobi polynomial						

UNCLASSIFIED

Security Classification

UNCLASSIFIED

Security Classification

DOCUMENT CONTROL DATA - R & D		
<i>(Security classification of title, body of abstract and indexing annotation must be entered when the overall report is classified)</i>		
1. ORIGINATING ACTIVITY (Corporate author) Foreign Technology Division Air Force Systems Command U. S. Air Force		2a. REPORT SECURITY CLASSIFICATION UNCLASSIFIED
		2b. GROUP
3. REPORT TITLE NUMERICAL SOLUTION OF THE BALANCE EQUATION IN THE FRAMEWORK OF A QUASI-SOLENOIDAL FORECAST DIAGRAM OF THE GEOPOTENTIAL FOR THE NORTHERN HEMISPHERE		
4. DESCRIPTIVE NOTES (Type of report and inclusive dates) Translation		
5. AUTHOR(S) (First name, middle initial, last name) Sitnikov, I. G.; Krichak, S. O.		
6. REPORT DATE 1968	7a. TOTAL NO. OF PAGES 13	7b. NO. OF REFS 9
8a. CONTRACT OR GRANT NO.	8b. ORIGINATOR'S REPORT NUMBER(S) FTD-MT-24-174-70	
b. PROJECT NO. 60103		
c.	8c. OTHER REPORT NO(S) (Any other numbers that may be assigned this report)	
d. DIA TASK T69-01-69		
10. DISTRIBUTION STATEMENT Distribution of this document is unlimited. It may be released to the Clearinghouse, Department of Commerce, for sale to the general public.		
11. SUPPLEMENTARY NOTES		12. SPONSORING MILITARY ACTIVITY Foreign Technology Division Wright-Patterson AFB, Ohio
13. ABSTRACT A finite-difference model for the solution of the balance equation for the northern hemisphere is described. The balance equation, rendered initially in a local isobaric system of coordinates (x, y, p) for polar stereographic projection, belongs to the family of Monge-Ampere equations. One of the requirements to it is that it must be elliptic at all points of the projection grid. The balance equation was reduced to a Poisson equation with respect to the function of flux and solved by the method of successive approximations. An interesting characteristic of the solution is the decrease of the convergence rate of the iteration processes at low latitudes. The field of the flux function, obtained from the solution of the balance equation was used as the initial field for a quasisolenoidal forecast, i.e., for a barotropic model. At the end of each forecast, i.e., every 24, 48 and 72 hours, the field of the geopotential is found by inversion of the balance equation, i.e., by solving it for the geopotential, using the known distribution of the flux function. The suggested method is close to fast method described by K. Mikoyada (Numerical Solution of the Balance Equation, Collected Meteorological Papers, Vol. X, No. 1-2, Tokyo, 1960) and by F. Schuman (Numerical Methods in Weather Prediction; The Balance Equation. Monthly Weather Review, Vol. 85, No. 10, 1957. (AT 8025208)		

DD FORM 1473  
1 NOV 65

UNCLASSIFIED

Security Classification

UNCLASSIFIED

Security Classification

14. KEY WORDS	LINK A		LINK B		LINK C	
	ROLE	WT	ROLE	WT	ROLE	WT
Atmospheric geopotential Weather map Geopotential forecasting Poisson equation Successive approximation						

UNCLASSIFIED

Security Classification

UNCLASSIFIED

Security Classification

DOCUMENT CONTROL DATA - R & D		
<i>(Security classification of title, body of abstract and indexing annotation must be entered when the overall report is classified)</i>		
1. ORIGINATING ACTIVITY (Corporate author) Foreign Technology Division Air Force Systems Command U. S. Air Force		2a. REPORT SECURITY CLASSIFICATION UNCLASSIFIED
		2b. GROUP
3. REPORT TITLE THE INVESTIGATION OF HEATING IN THE STRATOSPHERE USING NUMERICAL EXPERIMENTS		
4. DESCRIPTIVE NOTES (Type of report and inclusive dates) TRANSLATION		
5. AUTHOR(S) (First name, middle initial, last name) Barg, B.; Mashkovich, S. A.		
6. REPORT DATE 1968	7a. TOTAL NO. OF PAGES 30	7b. NO. OF REFS 10
8a. CONTRACT OR GRANT NO.	8b. ORIGINATOR'S REPORT NUMBER(S) FTD-MT-24-174-70	
b. PROJECT NO. 60103		
c.	8d. OTHER REPORT NO(S) (Any other numbers that may be assigned this report)	
d. DIA TASK T69-01-69		
10. DISTRIBUTION STATEMENT Distribution of this document is unlimited. It may be released to the Clearinghouse, Department of Commerce, for sale to the general public.		
11. SUPPLEMENTARY NOTES	12. SPONSORING MILITARY ACTIVITY Foreign Technology Division Wright-Patterson AFB, Ohio	
13. ABSTRACT The evolution of sudden thermal perturbations, which occur in the stratosphere at the end of winter and at the beginning of the spring and are known as the Berlin Phenomenon, was investigated. It was assumed that the initial disturbance of the temperature has a spherical shape and occupies a limited domain, and that there is no initial perturbation of the baric field. Finite-difference equations were approximated, leading to a numerical solution, and the solution stability was tested. The resulting preliminary data suggest the following tentative conclusions: 1) The thermal perturbations (at maximum zonal wind velocities of 10 and 30 m/sec) appear to have no substantial influence upon the atmospheric circulation, and consequently, do not destroy the polar vortex. 2) A perturbation in the temperature field also causes a perturbation of the baric field whose amplitude grows during the considered period of time (4 to 6 days) whereas the amplitude of the temperature perturbation decreases. 3) Within the first 48 hours, the perturbation maximum of the geopotential remains at the same latitude at which the temperature perturbation was initially located. Thereupon, the perturbation of the geopotential shifts northward, whereas the temperature perturbation remains at the initial latitude. This differs considerably from processes that are observed in nature. (AT 8025209)		

DD FORM 1 NOV 65 1473

UNCLASSIFIED

Security Classification

UNCLASSIFIED

Security Classification

14. KEY WORDS	LINK A		LINK B		LINK C	
	ROLE	WT	ROLE	WT	ROLE	WT
Stratosphere Atmospheric temperature gradient Atmospheric ozone Atmospheric circulation Atmospheric geopotential Geostrophic wind						

UNCLASSIFIED

Security Classification

UNCLASSIFIED

Security Classification

DOCUMENT CONTROL DATA - R & D		
<i>(Security classification of title, body of abstract and indexing annotation must be entered when the overall report is classified)</i>		
1. ORIGINATING ACTIVITY (Corporate author) Foreign Technology Division Air Force Systems Command U. S. Air Force		2a. REPORT SECURITY CLASSIFICATION UNCLASSIFIED
		2b. GROUP
3. REPORT TITLE ON THE APPLICATION OF THE FILTRATION THEORY OF RANDOM PROCESSES TO SOME PROBLEMS OF OBJECTIVE ANALYSIS		
4. DESCRIPTIVE NOTES (Type of report and inclusive dates) TRANSLATION		
5. AUTHOR(S) (First name, middle initial, last name) Ovchinskiy, B. V.		
6. REPORT DATE 1968	7a. TOTAL NO. OF PAGES 21	7b. NO. OF REFS 11
8a. CONTRACT OR GRANT NO.	8b. ORIGINATOR'S REPORT NUMBER(S) FTD-MT-24-174-70	
b. PROJECT NO. 60103		
c.	8c. OTHER REPORT NO(S) (Any other numbers that may be assigned this report)	
d. DIA TASK T69-01-69		
10. DISTRIBUTION STATEMENT Distribution of this document is unlimited. It may be released to the Clearinghouse, Department of Commerce, for sale to the general public.		
11. SUPPLEMENTARY NOTES	12. SPONSORING MILITARY ACTIVITY Foreign Technology Division Wright-Patterson AFB, Ohio	
13. ABSTRACT Formulas are derived for the computation of the weighting functions for optimal interpolation and smoothing of meteorological elements for the case when the correlation functions of the true (or discrete) magnitude (signal) and of the observation errors (noise) are known. For optimum interpolation, it is mandatory to take into account that the observational data contain random errors, and hence it becomes necessary to obtain a magnitude expressing the meteorological element, that is free of such errors. If, however, the errors are presumed to include also certain small-scale fluctuations, the assumption on the uncorrelatability of random errors would no longer be valid. Using the F. Thompson technique for the filtration of random processes, meteorological fields can be optimally smoothed. The structure and the properties of the weighting functions are examined using discrete as well as continuous data. Ultimately, the problem of determination of a weighting function is reduced to the solution of a Wiener-Hopf integral equation, or to the solution of a discrete analog of the W-H equation. The W-H equation was solved using the method of indeterminate coefficients, approximating the correlation function by a sum of power functions. Several alternate random solutions are considered, e.g. when the errors are white noise, or when the number of stations is increasing without restrictions. Orig. art. has: 6 figures, 45 formulas. (AT8025210)		

DD FORM 1473  
1 NOV 68

UNCLASSIFIED

Security Classification

UNCLASSIFIED

Security Classification

14. KEY WORDS	LINK A		LINK B		LINK C	
	ROLE	WT	ROLE	WT	ROLE	WT
Meteorologic observation Error statistics Signal correlation Signal to noise ratio Random process						

UNCLASSIFIED

Security Classification

UNCLASSIFIED

Security Classification

DOCUMENT CONTROL DATA - R & D

(Security classification of title, body of abstract and indexing annotation must be entered when the overall report is classified)

1. ORIGINATING ACTIVITY (Corporate author) Foreign Technology Division Air Force Systems Command U. S. Air Force		2a. REPORT SECURITY CLASSIFICATION UNCLASSIFIED	
		2b. GROUP	
3. REPORT TITLE ON THE FILTRATION OF FIELDS OBTAINED AS A RESULT ON NONLINEAR TRANSFORMATIONS OF THE INITIAL VALUES OF METEOROLOGICAL FACTORS			
4. DESCRIPTIVE NOTES (Type of report and inclusive dates) TRANSLATION			
5. AUTHOR(S) (First name, middle initial, last name) Strizhevskiy, L. N.			
6. REPORT DATE 1968		7a. TOTAL NO. OF PAGES 13	7b. NO. OF REFS 7
8a. CONTRACT OR GRANT NO.		8b. ORIGINATOR'S REPORT NUMBER(S) FTD-MT-24-174-70	
b. PROJECT NO. 60103			
c.		8c. OTHER REPORT NO(S) (Any other numbers that may be assigned this report)	
d. DIA TASK T69-01-69			
10. DISTRIBUTION STATEMENT Distribution of this document is unlimited. It may be released to the Clearinghouse, Department of Commerce, for sale to the general public.			
11. SUPPLEMENTARY NOTES		12. SPONSORING MILITARY ACTIVITY Foreign Technology Division Wright-Patterson AFB, Ohio	
13. ABSTRACT An attempt was made to derive formulas for the optimum smoothing of fields obtained from certain nonlinear transformations of the initial fields. The initial fields were assumed to be isotropic and uniform, with a normal distribution and a mathematical expectancy of zero. The statistical characteristics of summary fields were derived from the evaluation of empirical data, whereas the statistical characteristics of the error fields were derived from certain general considerations, regarding the ratios of the scales and intensities of the fields of the true values, and of the noise. The filtration operators were computed for two nonlinear transforms of the initial fields, i.e., for the nonlinear advection component of the vortex, and for the nonlinear component of the individual derivative of the wind. The calculations were performed for different values of the scales and intensities of the field of errors that corresponded to different degrees of exposure and measurement precision over different areas. The theoretically obtained filtration operator for the nonlinear component of the wind's derivative was used in a one-level diagram of the wind forecast. It is believed that this approach brings somewhat better results, as compared to the previously used variant, essentially because of the more realistic values of the wind velocity modules. The computer program was also simplified and computer time was reduced. Orig art. has: 3 figures, 18 formulas, 1 table. (AT8025211)			

DD FORM 1473  
1 NOV 65

UNCLASSIFIED

Security Classification

UNCLASSIFIED

Security Classification

14. KEY WORDS	LINK A		LINK B		LINK C	
	ROLE	WT	ROLE	WT	ROLE	WT
Geostrophic wind Filtration Geopotential forecasting Wind profile Correlation statistics						

UNCLASSIFIED

Security Classification

UNCLASSIFIED

Security Classification

DOCUMENT CONTROL DATA - R & D		
<i>(Security classification of title, body of abstract and indexing annotation must be entered when the overall report is classified)</i>		
1. ORIGINATING ACTIVITY (Corporate author) Foreign Technology Division Air Force System Command U. S. Air Force		2a. REPORT SECURITY CLASSIFICATION UNCLASSIFIED
2b. GROUP		
3. REPORT TITLE OBJECTIVE ANALYSIS OF THE GEOPOTENTIAL FIELD USING SUPPLEMENTAL INFORMATION		
4. DESCRIPTIVE NOTES (Type of report and inclusive dates) TRANSLATION		
5. AUTHOR(S) (First name, middle initial, last name) Sovetova, V. D.		
6. REPORT DATE 1968	7a. TOTAL NO. OF PAGES 10	7b. NO. OF REFS 3
8a. CONTRACT OR GRANT NO.	8b. ORIGINATOR'S REPORT NUMBER(S) FTD-MT-24-174-70	
a. PROJECT NO. 60103	8c. OTHER REPORT NO(S) (Any other numbers that may be assigned this report)	
c.		
d. DIA TASK T69-01-69		
10. DISTRIBUTION STATEMENT Distribution of this document is unlimited. It may be released to the Clearinghouse, Department of Commerce, for sale to the general public.		
11. SUPPLEMENTARY NOTES	12. SPONSORING MILITARY ACTIVITY Foreign Technology Division Wright-Patterson AFB, Ohio	
13. ABSTRACT Two methods of objective analysis of the baric field are described. The first method is applicalbe to the field of the geopotential of isobaric surfaces, i.e., for four levels of the troposphere over the northers hemisphere. In addition to the data collected by radiosonde stations in areas of the northern hemisphere, that have a low exposure, additional information was used: Pressure measurements at the surface of the earth and data collected by merchant marine vessels. Using the cross-correlation functions of the geopotential, the information lacking at the 850mb isobaric level was reconstructed from data obtained from the measurement of the pressure field at the earth's surface. The data lacking at the 300 mb level were reconstructed from measurements performed at the 500 mb level. Using the method of optimal interpolation, the geopotential was analyzed objectively first for one and then for the other pair of surfaces, using the applicable autocorrelation functions. The computations indicate a considerable qualitative improvement of the objective analysis, especially for the water areas. The second method was developed specifically for the stratospheric levels of Europe and Asia. The problem involved the reduction of information that was not available for higher levels, and a subsequent objective analysis of the baric field from more complete initial observation data. (AT8025213)		

DD FORM 1473

UNCLASSIFIED

Security Classification

UNCLASSIFIED

Security Classification

14. KEY WORDS	LINK A		LINK B		LINK C	
	ROLE	WT	ROLE	WT	ROLE	WT
Atmospheric geopotential Weather station Troposphere Stratosphere Interpolation						

UNCLASSIFIED

Security Classification